

On R-matrix approaches to knot invariants

A. Anokhina*

Abstract

We present an elementary introduction to one of the most important today knot theory approaches [79], which gives rise to a representation for a class of knot polynomials in terms of quantum groups. Historically, the approach was at the same time developed from the state model approach [53] and from the braid group approach [52], and we consider the both approaches and their relation to each other and to the \mathcal{R} -matrix approach in details with help of the simple explicit examples. We also discuss various kind of motivation for referring to the above approaches as to the *physical* approaches in knot theory [54]. For instance, we concern a highly inspiring QFT interpretation for a knot polynomial [95].

Contents

1	Introduction	3
2	Knots and knot polynomials	4
3	Examples of physical problems reduced to topological problems	6
3.1	Adiabatic transformations theory	7
3.1.1	Adiabatic transformations of a physical pendulum	7
3.1.2	Idea of an adiabatic transformation	7
3.1.3	Adiabatic transformations and discrete degrees of freedom	8
3.1.4	Adiabatic transformations of quantum systems	9
3.1.5	Adiabatic transformations in statistical physics	9
3.2	Analytic continuation approach	9
3.2.1	Geometric sense of the analytic continuation	9
3.2.2	Semiclassical wave function as integral of a meromorphic form over a Riemann surface and geometric sense of the Bohr-Sommerfeld rule.	10
3.3	Ward identities giving rise to a topological quantum field theory	11
4	Towards QFT interpretation of knot invariants	12
4.1	Knot invariants as observables in Wess-Zumino-Witten theory and as axiomatically defined exact Wilson averages	12
4.1.1	Visual presentation of the construction	13
4.1.2	Knot polynomials as invariants of the conformal blocks	14
4.1.3	Wess-Zumino-Witten conformal blocks and classical Chern-Simons fields	14
4.1.4	Towards relating the knot invariants to the perturbatively computed Wilson averages in the Lagrangian Chern-Simons theory	15
4.2	Wilson averages in the Chern-Simons theory	15
4.2.1	Basic definitions	15
4.2.2	Simplest examples of Chern-Simons fields and Wilson averages	17
4.2.3	Gauging out of the cubic term in the non-abelian Chern-Simons theory.	20
4.3	Linking number as a contribution to abelian Wilson average	21

*ITEP, Moscow, Russia; anokhina@itep.ru

4.4	Properties of the knot invariants as general properties of the ordered exponential and of the Gaussian average.	21
4.4.1	Relevant properties of the ordered exponential	21
4.4.2	Relevant properties of the Gaussian average	22
4.4.3	Green functions giving rise to contour independent integrals	24
4.5	Knot invariants as link invariants: framing of knot from the Chern-Simons theory standpoint	24
4.5.1	Second order framing contribution	24
4.5.2	Higher orders framing contributions	25
4.5.3	Framing in non-abelian theory.	26
4.6	Kontsevich integral for the Vassiliev invariants as the perturbative expansion for the Chern-Simons Wilson average in the holomorphic gauge	26
4.6.1	HOMFLY polynomial as a generating function for the Vassiliev invariants	26
4.6.2	Structure of the Kontsevich integral	27
4.6.3	Kernels of Vassiliev invariants as propagators of the complexified Chern-Simons theory	28
4.6.4	Second order contribution to the Wilson average in the holomorphic gauge	28
5	Knot polynomial as an observable in a state model	30
5.1	Formulating the approach	30
5.2	Definition of average	30
5.3	Operator identities	30
5.4	Jones polynomial for the trefoil knot as an average in the state model	31
5.4.1	Ward identities	31
5.4.2	Explicit form of the crossing operators	32
5.4.3	Turn-over operators instead of average	33
5.4.4	Explicit definition of average	34
5.4.5	Character expansion	35
6	Knot polynomial as an averaged trace of a braid group element	37
6.1	Properties of braids and braid closures	37
6.1.1	The braid group an extension of the permutation group	38
6.1.2	Braids closures and knots	40
6.1.3	Unlinked knots and multiplication property	40
6.2	Algorithm of constructing a knot invariant	41
6.3	Explicit calculating of the knot invariant in particular cases	42
6.3.1	Two-strand braids	42
6.3.2	Three-strand braids	43
6.3.3	Four-strand braids	49
6.4	Weight coefficients as $SU(N)$ characters	56
7	Constructing a knot polynomial from \mathcal{R}-matrices	57
7.1	The notion of \mathcal{R} -matrix	57
7.2	A contraction of \mathcal{R} -matrices as a cut knot diagram invariant	58
7.2.1	The general part of the state model approach adopted to the \mathcal{R} -matrix approach	58
7.2.2	The \mathcal{R} -matrices as crossing operators.	59
7.3	Explicit verifying the topological invariance constraints for the simplest \mathcal{R} -matrix	60
7.3.1	Yang-Baxter equation	60
7.3.2	Inverse crossings	62
7.4	First Reidemeister move and turn-over operators	63
7.4.1	RI invariance as a condition on the \mathcal{R} -matrix contraction	63
7.4.2	Turn-over operators	63

7.4.3	Topological normalization of the turn-over operators and framing of a knot . . .	65
7.4.4	Turn-over operators and loop version of the RII move.	67
7.4.5	Commutation of the turn-over operators with the R -matrices	67
7.4.6	Conventional non-covariant approach: the extremum point operators	69
7.4.7	Examples of using the covariant approach	69
7.5	Explicit evaluation of the invariant for the trefoil knot	72
7.5.1	Mirror symmetry	73
7.6	From \mathcal{R} -matrices approach to the braid group approach	74
7.6.1	Reduction of four-indices operators to matrices. Twisted R -matrices	74
7.6.2	Eigenvectors of regular and twisted crossing operators in a two-strand braid . .	74
7.6.3	Turn-over operators in a two-stand braid and character decomposition	75
7.6.4	Common eigenspaces of twisted crossing operators in a three-stand braid . . .	76
8	Conclusion	80
9	Acknowledgements	81
A	Obtaining of a non-trivial solution of classical equations for the $SU(2)$ Chern-Simons	85
B	On the form of the Green functions for the abelian Chern-Simons theory in Lorenz and holomorphic gauges.	86
C	Plat representation of knot and presenting Kontsevich integral as a contraction of the “elementary contribution” operators	87
D	Examples of calculating the elementary non-trivial contributions to the Kontsevich integral	88

1 Introduction

The text is a **review** of various question concerning the \mathcal{R} -matrix approaches to the knot invariants. We hope that the text may be useful both for the first acquaintance with the notions and methods we discuss and for clarifying certain subtle points, the simplest examples we study through the text providing good illustrations to the ones. The text is also addressed to anyone who wanders what do the knots to do with the physics. This question definitely desires asking since, as a matter of the fact, up to day knot theory is considered as a chapter of physics at the same extend as a chapter of mathematics. Referring to [54] for a much broader presentation of the subject, we discuss here some points, which are especially close to the main questions we consider.

Our main task is to provide a pedagogical introduction to the \mathcal{R} -matrix representation for the HOMFLY polynomials [79], in the version developed and used in [71, 17, 18, 43, 44, 16, 9, 11, 10, 45, 13]. Trying to keep a rather elementary level of presentation and mostly restricting ourselves by the simplest examples, we go in each presented examples into various details and subtleties, which are usually omit in literature. We intentionally do not start from presenting a completed construction, doing what a naive person would do and indicating one pitfall after another instead. As a preface, we discuss in details the representation of the (uncolored) HOMFLY polynomial in term of the matrix representation of the braid group, or, more precisely, of the Hecke algebra [54]. Although literally replicating the \mathcal{R} -matrix representation for the same polynomials, this Hecke algebra representation was known even before [52], and we find it instructive to derive this representation in particular cases from the first principles. Apart from that, the braid group approach to the knot polynomials is the most simple and common way of relating them to observables in various physical models, since the braid group is

an extension of the permutation group [94, 54]. This is the content of sec.6, and we pass to the very \mathcal{R} -matrix approach in following sec.7.

As a related subject, we would like to discuss a highly intriguing problem of correspondence between the HOMFLY polynomial and Chern-Simons Wilson average [95], which naturally arises in the context of the \mathcal{R} -matrix representation for the former ones [70, 71]. Although the very correspondence is considered as a matter of fact, many problems concerning it remain unresolved [54, 48, 70, 71, 8, 21]. For instance, a problem of deriving the \mathcal{R} -matrix formalism from the perturbative Chern-Simons theory in the temporal gauge [70, 71] is especially interesting in the context of our discussion. Although the very problem is left beyond the scope of our present text, we do what seems to us the only way of approaching to this problem, as well as to numerous other problems of the same kind. Namely, we take the standpoint of skeptics and try to answer the question why the above correspondence is believed to be true. The discussion on this subject is presented in sec.4. We also try to give some sort of physical intuition about the simplest properties of the very Chern-Simons theory in the same section.

The construction, which serves a kind of bridge between the \mathcal{R} -matrix representation for knot invariants and quantum field theory, is referred to a *state model* representation of the knot polynomials, first mentioned under this name by L.Kauffman [53]. A knot polynomial is in fact presented with help of this construction as an observable in a *topological quantum field theory* [23], although the theory is defined in rather abstract terms. We outline this construction in sec.5, illustrating how several different versions of the construction enable calculating a knot polynomial in a simple particular case. Our aim here is two-fold. First, we wish to illuminate the formalism, which might be treated as a rigorous definition of a topological quantum field theory, a knot polynomial as an observable. Second, we explain here the first part of the \mathcal{R} -approach, which is in fact a particular case of the state model approach.

As an introduction, we say a few general words on the knot invariants of our interest in sec.2. Then, before addressing to the main presentation, we discuss (in sec.3) some simple examples the pure topological problems arising in various fields of physics, the “non realistic” topological theories might turning out to be a useful tool for studying the ones.

2 Knots and knot polynomials

This section is a brief review of the knot theory quantities the following presentation refers to. We also try to formulate what kind of questions is asked about these quantities.

A knot theory is one of the most ancient fields of mathematics. Naively speaking, this science tries to answer the question how to describe all embeddings of a circle in the three-dimensional space that can not be continuously transformed into each other. In a wide sense, this is still an open problem, although huge knot tables with various built in computer interfaces [1, 2, 3, 4] are available now. In particular, [1], which provides the detailed description of about 800 in a sense the simplest knots, is often referred to as *a knot Zoo*.

First of all, to determine the table item relevant to a given curve in the three-dimension space is a separate, generally involved problem. But it may be even more important to set and to study various questions going beyond the plane enumeration, like how complicated is a given knot, or how alike or different are two distinct knots, or how to describe *discontinuous* transformations acting of various knots, or whether one can split the set of all knots into subsets of in some sense similar knots, or whether is there a natural way to select an infinite series of knots with the members being enumerated by a single increasing parameter, etc.

A powerful tool in studying this kind of questions is a notion of a *knot invariant*. By definition, it is a quantity which coincides for any pair of the closed three-dimensional curves that are continuously transformed into each other. Note that the inverse is generally wrong. Moreover, a single knot invariant which enables one to distinguish all invariants is unknown yet. Values of many different invariants calculated for a vast amount of knots can be found in [1, 2, 3, 4].

Hence, each knot is associated with a number of quantities, which are various knot invariants, which may be thought of as coordinates on the set of knots and used to compare different knots in one or another sense. On the other hand, most of the known invariants can be explicitly evaluated for an arbitrary three-dimensional curve, and one can at least conclude that two curves are *not* continuously transformed one into the other if they have a different value of the same invariant.

Name of the polynomial	Group	Representation	Formal variables	Knot		Polynomial
				Name	Rolfsen notation	
Jones	$SU(2)$	\square	q	Trefoil, fig.12	3_1	$-q^{-8} + q^{-6} + q^{-2}$
				Figure-eight	4_1	$q^4 - q^2 + 1 - q^{-2} + q^{-4}$
HOMFLY	$SU(N)$	\square	A, q		3_1	$-A^{-4} + A^{-2} (q^2 + q^{-2})$
					4_1	$1 + q^2 (A + A^{-1}) - (q^2 + q^{-2})$
Alexander	$SU(0)$	\square	q		3_1	$q^2 - 1 + q^{-2}$
					4_1	$q^2 + 1 - q^{-2}$
Kauffman	$SO(N)$	\square	a, q		3_1	$a^2 (q^2 + q^{-2}) - a^4 (q^2 - 1 + q^{-2}) + (-a^3 + a^5) (q - q^{-1})$
Colored Jones	$SU(2)$	$\square\square$	q		3_1	$q^{-4} + q^{-10} - q^{-14} + q^{-16} - q^{-18} - q^{-20} + q^{-22}$

Especially interesting examples of knot invariants present themselves *knot polynomials*, which are not just numbers but (Laurent) polynomials in some formal variable(s). The first discovered knot polynomial is *Alexander polynomial*, which was already known in 1928 [15]. Today this invariant is thought of as a very rude one. Nevertheless, Alexander polynomials of all the prime knots (i.e., the knots not reduced to “simpler” knots, see [94] for the exact definition) with the crossing number (the minimum number of self-crossings in a knot planar projection) no more than 8, 36 knots altogether including the unknot, are all different [27], and these knots hence can be enumerated by their Alexander polynomials.

The next polynomial invariant, the *Jones polynomial*, was introduced only in 1984 [50]. Jones polynomials enables one to distinguish already all prime knots with no more than 9 crossings [14]. E.g., the Jones polynomial for the prime knot 6_1 in the Rolfsen table (with 6 crossings) differs from the Jones polynomial of the knot 9_{146} (with 9 crossings), which has the same Alexander polynomial. Unlike that, the knot 10_{132} with 10 crossings has the same Jones polynomial as the knot 5_1 with 5 crossings.

A short time after the Jones polynomial was introduced, in 1985, several groups of researchers, namely, P.Freyd and D.Yetter, J. Hoste, W. B. R. Lickorish and K. Millet, A. Ocneany [40], J. H. Przytycki and P. Traczyk [76], independently discovered a *HOMFLY polynomial*, which is a generalization both of the Jones and Alexander polynomials (the full name of the invariant, *HOMFLY-PT*, is an abbreviation of the eight enumerated names). Although the HOMFLY polynomial sometimes enables to distinguish the knots that are knot distinguished by the Jones polynomial, e.g., the prime knot 8_9 and the composite knot $4_1 \# 4_1$ (see [94] for the definition) [63], the two polynomials have alike “distinguishable” powers; in particular, the first pair of knots with the same Jones polynomial, 5_1 and 10_{132} , has the same HOMFLY polynomial as well. The real interest to the HOMFLY polynomial was caused by completely different reasons, the present text may be considered as a review of such ones.

Finally, the invariant which was afterwards called a *Kauffman polynomial* was first mentioned in 1987 [53], and was noticed in the same paper that all the above enumerated knot polynomials can be defined in a similar way, which we discuss in details in sec.5.

The next development of the subject consisted in introducing of the *colored* first Jones and then HOMFLY and Kauffman polynomials. In the first papers (for instance, in [72]), the colored poly-

mials are introduced with help of the *satellite* knots, which are obtained from the original knot by substituting the original curve with a braid. For braids with a given number of strands, such braids form a finite-dimensional linear space, the dimension being small for a small number of strands. E.g., there are just 2 linearly independent HOMFLY polynomials among those for the various satellites with 2-strands braids (if the linear combinations with coefficients depending on the variable q but not on the variable A are considered), 3 ones for 3-strand braids, 5 ones for 4-strand braids, and 7 ones for 5-strand braids (however, the dimensions grow then faster and faster). The colored polynomials can be introduced as a certain distinguished basis in the space of the satellite knot polynomials, but they were the spaces themselves, which we treated in the early papers. Probably the most remarkable result in studying the colored polynomials from this standpoint is due to Morton, who demonstrated [72] that the simplest pair of the *Mutant knots*, the so called *Kinoshita-Terasaka* knot (11n42 in the *Hoste-Thistlethwaite* table) and the Conway knot (11n34) [1], are *not* distinguished by all colored Jones polynomials, as well as by the colored HOMFLY polynomials for the two-strand satellites, but *are* distinguished by the colored HOMFLY polynomials for the three-strand satellites. The result of Morton was recently confirmed by an explicit calculation of the colored HOMFLY polynomials [83], with help of on the R -matrix approach [79], which is just the main subject of the present text.

However, the sense and properties of the colored polynomials become much more transparent from the standpoint of their other definition. The one relies on the construction of our main interest. Although we discuss this construction in details for plain (uncolored) HOMFLY polynomials only, this is sufficient to present the very idea, the color entering just as one of the parameters in the construction.

Examples of the various knot polynomials mentioned above are presented in table2.1. The second and third columns announce the sense of these polynomials from the standpoint of the construction we discuss starting from sec.5.

However, a description of knots with help of their invariants does not go beyond a formal enumeration, unless some underlying structures in knot invariants are studied. Although very different such structures were fruitfully researched for a long time [94], a nice description of the “space of all knots”, which the scientists dream about since ancient times, still lacks for.

A fresh wind came in theory of knot invariants in late 80-s, when it was noticed that some knot invariants can be introduced in terms and explicitly calculated with tools, which was originally developed in quantum physics. This observation inspired some new approaches to knot invariants, which are now referred to as “physical” approaches.

These approaches turned out to be extremely fruitful themselves, but even more inspiring is the idea of relating a knot to a state of a physical system, the set of various knots could be described that as the Hilbert space the system [14]. The approaches to knot invariants discussed in the present text are just of this kind.

3 Examples of physical problems reduced to topological problems

The knot theory approach, which we are mostly interested in and discuss in details in sec.6 and 7, refers to a class of the so called *physical* approaches in knot theory. We briefly review some ideas underlining this name in sec.4 and 5. However, the very idea of studying the topological questions, i.e., of identifying any two objects related by a continuous transformation at the first glance seems rather exotic from the physical standpoint. By this reason, we start from recalling several natural ways of pure topological questions arising in various physical problems.

One may enumerate several bright examples of physical phenomena known as topological effects. The list starts from the *Aharonov-Bohm effect* [64], proceeds with the *monopole* solution in the Weinberg-Salam model [73], *instantonic solutions* of the Yang-Mills equations [7] and the Polyakov conjecture on these solutions being responsible for the *confinement* [74], and includes various experimentally observed topological quasiparticles in a solid matter, among them *Abrikosov vortices*, which

are responsible for the high temperature superconductivity and *anyons* in graphene [96], which probably explain the fractional quantum Hall effect [89] and might enable us with a quantum computer [59]. Discovering of these phenomena gave rise to a separate subject that studies topological effects in gauge theories [81]. Denied that, we intentionally concentrate on another kind of examples, in which topological problems arise in much more regular ways.

3.1 Adiabatic transformations theory

3.1.1 Adiabatic transformations of a physical pendulum

Topology studies a question whether two objects (curves, surfaces, etc.) can be transformed one into the other by a continuous transformation. A similar kind of questions arises in physics, namely in theory of adiabatic transformations [22, 64], where one studies a question whether two states of a physical system with variable parameters can be turned into each other by an *adiabatic*, i.e., in a sense infinitely slow (see further), variation of the system parameters. A closely related question is whether one of the states can be considered as a perturbation over the other one.

3.1.2 Idea of an adiabatic transformation

Consider a physical system with variable parameters. The equations of motion of the system depend then these parameters. A solution of these equations depends then on the same parameters, as well as their solutions. If one interests just in motion of the system for given values of the parameters, one should just substitute these values in the solution. However, if one wanders for a motion of the system as the parameters *vary* in time, one must solve different *differential* equation, with the coefficients that were constant now vary, and generally obtain the completely different function as a solution. Yet, if parameters vary “enough slow” (see the explicit example below), the solution is obtained from a similar one for unvarying system by plain substitution of the constant parameters with the corresponding functions. Such “enough slow” transformations of a physical system are referred to as *adiabatic* transformations.

Example E.g., the equation of motion of a frequency alternating oscillator

$$\ddot{x} + \omega(t)x^2 = 0, \quad \omega(t) = \omega_0(1 + \lambda \cos(\Omega t)), \quad (3.1)$$

has a frequency modulated oscillation

$$x(t) = A \cos(\omega(t)t + \phi) \quad (3.2)$$

as a general solution if the modulation frequency is negligibly small compared to the natural frequency of the system,

$$\ddot{x}(t) = \frac{d}{dt} \left\{ -(\omega(t) + \dot{\omega}(t)t) A \sin(\omega(t)t + \phi) \right\} \xrightarrow{\Omega/\omega \rightarrow 0} -\omega^2(t)x(t), \quad (3.3)$$

even if the modulation depth λ is not small.

The basic ideas of the adiabatic transformation theory, as well as their relation to the topology questions is well illustrated by the following simple example.

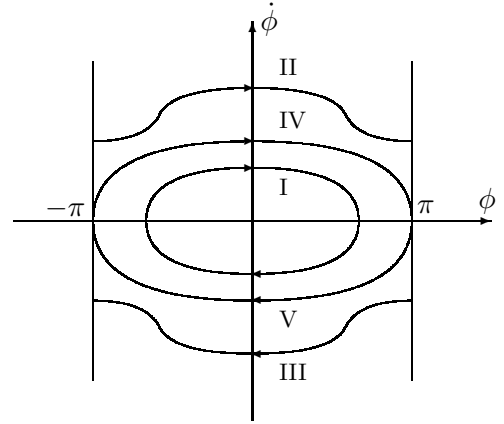


Figure 1: Various kinds of phase trajectories for a physical pendulum.

A motion of a physical pendulum is described by the second order equation

$$\ddot{\phi} + \omega^2 \sin \phi = 0, \quad (3.4)$$

which, one time integrated, gives the energy conserving law

$$\dot{\phi}^2 - 2\omega^2 \cos \phi = \frac{2E}{ml^2} = \text{const.} \quad (3.5)$$

Constraint (3.5), in turn, can be considered as equation of the pendulum phase trajectory in the phase plane $(\phi, p \equiv m\dot{\phi})$ (fig.1). There are then five different kinds of phase trajectories, corresponding to the five kinds of the pendulum motion. Namely, phase trajectory *I* corresponds to the pendulum swinging, never performing a complete turnover, while phase trajectory *II* corresponds to the pendulum turning over in the counter-clock-wise direction, its mirror image w.r.t. the ϕ axis *III* corresponds to the turning over in the clock-wise direction. There are infinitely many phase trajectories of all the three kinds, and the two phase trajectories corresponding to the limiting cases, *IV* and its mirror image *V*, represent, respectively, a counter-clock and a clock-wise turn-overs, performed by the pendulum for infinite time.

A pendulum motion of one kind can not be turned in a *finite time* into a motion of another kind by an *adiabatic* transformation, i.e., by an infinitely slow variation of the pendulum energy or period. E.g., if a pendulum performs small oscillations and one pulls the wire in, slowly enough for the pendulum motion being approximated at each time point by oscillation of the pendulum with a constant frequency, the pendulum energy increases (as may be shown [22]), and naively may be turned arbitrarily large. However, the period decreases at the same time, running at the infinity as the pendulum approaches to the critical trajectory with $E = 2mgl$, as one can see from the explicit formula

$$T = 2\tau \left| \int_{-\phi_{max}}^{\phi_{max}} \frac{d\phi}{1 + \lambda \cos \phi} \right|, \quad \cos \phi_{max} = -\lambda^{-1} \leq \cos \phi \leq 1, \quad (3.6)$$

$$|\lambda| > 1 \Leftrightarrow E < mgl, \quad \lambda = \frac{mgl}{2E}, \quad \tau = \sqrt{\frac{ml^2}{2E}},$$

which follows from (3.5) straightforwardly. The energy being enough for a turn-over, the dependence of the period on the energy takes different form,

$$T = \tau \int_0^{2\pi} \frac{d\phi}{1 + \lambda \cos \phi}, \quad |\lambda| > 1 \Leftrightarrow E > mgl. \quad (3.7)$$

This property of the two described pendulum motions matches the corresponding phase trajectories (fig.1-I and II, respectively) can not being turned one into the other by a continuous transformation. Consequently, a turn-over of a pendulum can *not* be obtained as a perturbation over harmonic oscillation, because as long as a polynomial in a perturbation parameter reasonably approximates form of the trajectory, the trajectory continuously depends on the parameter.

3.1.3 Adiabatic transformations and discrete degrees of freedom

In other words, one can associate each motion of the pendulum (except for the two limiting cases) with a number +1, 0, or -1, which equals the divided by 2π phase increment for the period. This number can be considered as a *discrete degree of freedom*, which can not be changed by continuous transformations of the system parameters. Note that this approach is valid only in the adiabatic limit, where the phase trajectories at each time point are the same to those of the system with parameters kept constant.

Note that coinciding of the discrete parameter value is not sufficient for two motions of the system being related by an adiabatic transformation. For instance, two for two pendulum motions in the considered example being related in such a way, the quantity that equals the energy times the period must be the same for these motions [22]. However, coincidence of all discrete degrees of freedom is necessary for two motions being related by an adiabatic transformation.

3.1.4 Adiabatic transformations of quantum systems

This above approach is widely applied in wave and quantum mechanics, when one often deals with the discrete specters. For instance, one can *not* obtain a wave function of a particle in the delta potential $V(x) = \frac{\hbar^2}{2mb}\delta(x)$ from such one in the double-delta potential $V(x) = \frac{\hbar^2}{2mb}(\delta(x) + \delta(x - a))$ by an adiabatic transformation that sends the parameter a to infinity, since there is just one discrete energy level $E_0 = -\frac{\hbar^2}{2mb^2}$ in the former case, while there are the two ones, $E_{s,a} = E_0 \mp \frac{\Delta}{2}$ with $\Delta = \frac{e^{-\frac{a}{b}}}{mb^2}$ (for $\frac{a}{b} \gg 1$), in the latter case. The wave functions of the corresponding confined states are given by the symmetric and antisymmetric functions, respectively,

$$\psi_{s,a}(x) = const \cdot \begin{cases} e^{-\kappa x}, & x < -a, \\ e^{\kappa(x-2a)} + \pm e^{\kappa(-x-2a)}, & -a < x < a, \\ \pm e^{\kappa x}, & x > a \end{cases}, \quad \kappa = \sqrt{-2mE}. \quad (3.8)$$

The linear combination of this functions

$$\psi(t) = const \cdot e^{-i\frac{E_0}{\hbar}t} \left(e^{-i\frac{\Delta}{\hbar}t}\psi_s + e^{i\frac{\Delta}{\hbar}t}\psi_a \right) \quad (3.9)$$

describes the particle passing from the one delta-hole to the other, since

$$\psi(0) = const \cdot \begin{cases} e^{-\kappa x}, & x < -a, \\ e^{\kappa(x-2a)}, & -a < x < a \\ 0, & x > a \end{cases} \approx const \cdot e^{-\kappa|x+a|}, \quad \psi\left(\frac{\pi}{2\Delta}\right) \approx const \cdot e^{-\kappa|x-a|}. \quad (3.10)$$

This example also illustrates the close relation between obtaining an effect as a result of an adiabatic transformation and studying the effect in perturbation theory. In this particular case, neither the separation of the energy levels, nor the tunneling solution can be obtained in perturbation theory, since the distance between the levels 2Δ is proportional to $e^{-\kappa a}$ so that its perturbation series in $\frac{1}{a}$ identically vanishes. By this reason a particle tunneling from one hole to the other is often referred to as a *non-perturbative* effect.

3.1.5 Adiabatic transformations in statistical physics

The notion of an adiabatic transformation is of grate invariance in statistical physics [65], where energies of discrete levels but not the filling numbers are changed in adiabatic processes. Adiabatic condition consists then in the characteristic time of the process being much bigger than the inverse smallest distance between the energy levels.

3.2 Analytic continuation approach

Another source of the topological questions in physics is a common method, applied in many chapters of physics and mathematics [64, 65, 77, 25, 93, 73, 85, 28].

3.2.1 Geometric sense of the analytic continuation

The technique we mean consists in the *analytic continuation* of a function $f(x)$ from real values of the argument x to the complex plane z [85]. The resulting function $f(z)$ by definition satisfies the Cauchy-Riemann condition $\partial_{\bar{z}}f(z) = 0$ everywhere but the special points. If the function $f(x)$ is a rational function of x , then the function $f(z)$ is defined on the *Riemann sphere* (a complex plain coupled to the point $z = \infty$) without the points where the function $f(z)$ has the poles. A basic fact of the complex analysis is that an integral $\int dz f(z)$ depends in this case not on the particular form of the

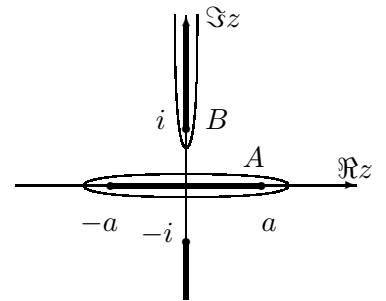


Figure 2: Integration contours in (3.13) winding over A and B cycles on the torus ($a = \sqrt{\frac{1-\lambda}{1+\lambda}}$).

contour but on the winding numbers of the contour on the poles. A case of an algebraic function $f(x)$ is more complicated. The function $f(z)$ is determined then on the several sheets of the complex plain with cuts, or, equivalently, on a non-trivial *Riemann surface*. The value of the same integral this time depends also on whether the contour encircles a cut, or, equivalently, on whether the contour contains a non-contractible cycle on a Riemann surface (see the explicit example below). Other words, the value of the integral is in the both cases conserved as the contour is transformed continuously never passing through the special points. Hence, a physical quantity, which was originally given by the integral $\int dx f(x)$ is now presented, in the above sense, as a topological invariant. Evaluation of these kind of integrals and studying of their properties is often performed with help of topology methods [28].

3.2.2 Semiclassical wave function as integral of a meromorphic form over a Riemann surface and geometric sense of the Bohr-Sommerfeld rule.

A good and rather simple illustration of the very approaches and of the topological terms it refers to is provided by the semiclassical approximation in quantum mechanics.

A semiclassical wave function of an energy E stationary state of a quantum particle in the potential $V(x)$ is expressed (in the lowest approximation) as

$$\psi_{sc}(a) = \psi(0) \exp \left(\int_0^a p(x) dx \right), \quad p = \sqrt{2m(E - V(x))}. \quad (3.11)$$

The obtained integral can be treated as an integral of the complex function $p(z)$ analytically continued to the corresponding Riemann surface, the integration contour being selected properly.

In particular, if the potential has the form $V(x) = \frac{\hbar^2}{2mb^2} \cos^2(\frac{x}{b})$, phase of the wave function can be expressed as

$$-i \log \phi_{cs} = \frac{b\sqrt{2mE}}{\hbar} \left(1 + \lambda \frac{\partial}{\partial \lambda} \right) J(\lambda), \quad \lambda = \frac{\hbar^2}{2mEb^2}, \quad (3.12)$$

with the integral

$$J(\lambda) \equiv \int \frac{d\xi}{\sqrt{1 - \lambda \cos^2 \xi}}, \quad (3.13)$$

the integral being brought to an integral of the algebraic function

$$J(\lambda) = \int \frac{dz}{\sqrt{(1+z^2)((1+\lambda)z^2 - (1-\lambda))}} \quad (3.14)$$

by introducing the variable $z = \tan \frac{\xi}{2}$. The integrand can be analytically continued to the two sheets of the complex plane glued along the two cuts, the segment of the real axis $\left(-\sqrt{\frac{1-\lambda}{1+\lambda}}, \sqrt{\frac{1-\lambda}{1+\lambda}}\right)$ and the part of the imaginary axis composed of the segments $(-i\infty, -i)$ and $(i, i\infty)$ can be chosen as the ones (we suppose that $\lambda > 1$), see fig.2. Integral (3.13) taken over the classically forbidden area, which coincides with one of the selected cuts selects, equals then the half of integral (3.14) over closed contour A in fig2, which encircles the first cut. This integral gives the phase increment of the quantum particle as it passes along a closed contour, so that the semiclassical wave function is defined unambiguously provided the value of the integral being an integer multiple of $2\pi i$. This requirement constraints the energy of a stationary state and is known as the Bohr-Sommerfeld quantization rule ¹.

On the other hand, integral (3.14) can be equivalently considered as an integral over the torus (which is the Riemann surface for the analytically continued integrand) of a meromorphic one-form.

¹However, the semiclassical approximation to the wave function of a *non-stationary* state is not generally a single-valued complex function; the phenomenon is known as *Stocks phenomenon* [77].

The corresponding contour integral is non-vanishing if the integration contour winds over a torus cycle, yielding then the corresponding period of the torus. Such presentation is useful for deriving the differential equations (Ward identities) for this integral, since there is just a three-dimensional linear space of meromorphic one-forms on a torus. In addition, since the considered contour integral enters the Bohr-Sommerfeld quantization rule, the energy of the stationary state can be expressed this way via certain geometric quantities, such as *theta functions* [28]. Being rather a textbook subject [64, 25, 93], this approach is still rather popular in QCD phenomenology [88].

Dispersion relations method. The above outlined analytic continuation approach is a basis for the widely used method of *dispersion relations* (see, e.g., [64],[65] and [25] for quantum mechanics, statistical physics and QFT examples, respectively). Roughly speaking, the method consists in relating an average of some function to a sum of the function values in certain points, putting the integral of the function over the real axis is equal to a proper sum over residues of the analytically continued function. In other version of the approach, a value of a function in a certain point is treated as the corresponding residue, $f(w) = \frac{1}{2\pi i} \oint \frac{f(z)dz}{z-w}$, and then the integration contour is pulled to the area of the w plain where the function $f(w)$ admits a perturbative expansion in w . The value of a function $f(w)$ for a w having a physical sense is then approximated by a perturbation series in a non-physical area, provided that one adds to the series the certain terms accounting the contour passing through the special points, when being deformed.

3.3 Ward identities giving rise to a topological quantum field theory

One more way of associating physical quantities with topological invariants come from the following widely used approach [94]. First, a smooth object (a curve, a surface, etc.) is associated with a certain graph. By construction, the graph remains one and the same as the object is subjected to transformations that form a large subclass of arbitrary continuous transformations. The remaining transformation correspond to certain operations with the graph, each operation being presented as a composition of several elementary ones.

In particular, various topological invariants are in the most cases calculated not with help of the smooth object itself, but with help of the associated graph. It is then necessary and sufficient to care that two graphs related by each of elementary operations give one and the same value of the invariant.

One the other hand, various correlating functions in a quantum field theory are often associated with the Feynman diagrams. Constraints on these functions, which are referred to as *Ward identities*, can be formulated then as equalities of correlators for the Feynman diagrams related by a certain operation, or, more generally, as conditions of vanishing of proper linear combinations of such diagrams.

Coinciding of values of a topological invariant calculated with help of two graphs related by an elementary operation (and thus corresponding to the objects that can be continuously deformed one onto the other) may be then looked at as a Ward identity in a quantum field theory. A topological invariant may be, in turn, considered as value of the correlating function in this model. Hence, any construction that enables to calculate values of some topological invariant for all objects of a given kind, i.e., for all knots, may be considered as a definition of a quantum field theory, with topological invariance constraints as Ward identities. Constructions of this kind are referred to as *topological quantum field theories* (TQFT) [23].

Surprisingly or not, Ward identities of this kind are not exotic but may arise rather naturally. In particular, one of elementary equivalence relations of the knot diagrams, the most important one in the approach we study, gives rise to the constraint known as the *Yang-Baxter equation*, which coincides with one of the constraints on the permutation group generators [94] (see sec.6 as well). The operators satisfying Yang-Baxter equation were first applied to the inverse scattering problem in quantum mechanics [91], and they arise in a large class of physical models, including spin chains and ice-type models in statistical physics [24] and two-dimensional conformal field theory [39].

4 Towards QFT interpretation of knot invariants

In the above section, we outlined how a topological invariant may be considered as a quantity related to a Feynman diagram of some abstract quantum field theory. For instance, a class of knot invariants possess various representations of this kind (see sec.5), and the main content of the present text is devoted to one of them. However, connection between knot invariants and quantum observables is not exhausted by this point. In this section, we discuss a highly inspiring interpretation, or rather two different interpretations *a la* [95, 55, 80, 75, 78, 56, 32] and [37, 38, 67, 41, 49, 48], respectively, of knot invariants as exactly computable observables in a quantum field theory.

Structure of the section. We start from formulating the precise statement about the relation of knot polynomials and observables in a topological quantum field theory in sec.4.1. We outline then the idea of the reasoning, which was presented in [95] as a derivation of this statement and developed in the subsequent works [55, 80, 75, 78, 98, 86, 56, 46, 68, 69, 32] into a new representation for a class of knot polynomials. We complete the section with formulating an essential question, which arise as the result. Sec.4.2-4.6 are devoted to the discussion of this question.

In sec.4.2, we write out the basic notions of the particular TQFT the statement under discussion refers to. We also attempt to give some geometrical and physical intuition about this theory properties. Sec.4.3 contains the detailed presentation of the simplest explicit example of the discussed correspondence between the knot (more precisely, link) invariant and the TQFT observable. In fact, this example was well known (although rare mentioned in the published papers; one may cite [84] as an exception) even before [95] and essentially motivated the presented there conjecture. In the following sections we address to a more general case of the knot polynomial — TQFT observable correspondence. A significant argument in the sake of the correspondence is that properties of the certain knot invariants match the properties of the two important in QFT quantities. The first them is *ordered exponential*, with help of which an *evolution operator* in QFT is introduced [73]. The second quantity is the *Gaussian average* of the operator product, on which, for instance, the perturbative definition of the path integral relies on [73]. By this reason, we start the discussion from sec.4.4, where we recall the needed definitions and formulate the properties of the ordered exponential and gaussian average referring to the question under discussion. Next comes sec.4.5, in which we discuss the regularization problem for the particular TQFT quantity corresponding to the knot polynomial, which can be cured by the *framing procedure* [37]. We start from providing the simplest illustration to the framing procedure, briefly discussing some subtleties concerning a general case afterwards. We also comment (in sec.4.5) a part of the framing procedure as of the argument in the *sake* of the knot invariant-TQFT observable correspondence under discussion. Finally, sec.4.6 contains the main part of the discussion. In the section, we discuss the particular properties of the certain knot invariants, which motivate identifying them with the perturbative contributions to a Gaussian average of an ordered exponential, thus interpreting them as TQFT observables. One of the subtleties arising here is that the original observation referred to the knot invariants are *other* knot invariants than [95] refers to. The relation of them two is also known [27] and discussed in the same section.

4.1 Knot invariants as observables in Wess-Zumino-Witten theory and as axiomatically defined exact Wilson averages

A modern sight on the QFT sense of knot invariants is concentrated in the statement that

- A HOMFLY polynomial is a Wilson average in the Chern-Simons theory.

A HOMFLY polynomial [94] is the particular case of knot polynomial mentioned in sec.2 and sec.5.4.1. This is the knot polynomial of our main interest. The above statement was literally presented and considered in details in famous paper by Witten [95]. However, various considerations underlying this statement were already widely discussed by that time (unfortunately, these discussions mostly

remained unpublished; see, e.g., [84] and [23]), and the paper itself did not put the end in the subject but rather gave rise to numerous studies of the question [55, 80, 75, 78, 56, 37, 38, 41, 67, 49, 48, 70, 71, 21] which continue up to day (one more highly intriguing story is presented in [5]). The discussed correspondence of the knot polynomials to the QFT observables thus do not reduce to a single once proved theorem, rather being an entire subject including many different and highly intertwined ideas.

4.1.1 Visual presentation of the construction

In the present section, we briefly discuss a QFT interpretation of the knot invariants, as it is presented in [95]. The there established correspondence of the knot polynomials relies on the statement

- Skein relations for HOMFLY polynomials coincide with the known relations between Wess-Zumino-Witten conformal blocks.

However, the presented in the paper reasoning can be presented rather visually, what may be instructive both for extending the established correspondence to the case of the colored HOMFLY polynomials and for developing the presented construction explicit computational procedure. We sketch this visual presentation below.

Encircled crossing on a knot diagram as a projection of the four-punctured sphere. The idea of the construction is presented in [95] rather visually. Namely, an encircled crossing on a knot planar projection may be looked at as projection of the sphere, two arcs of the original curve inside. These arcs can be continuously transformed, never intersecting, into two lines on the sphere, pairwise connecting the four intersection points of the sphere with the curve. One may treat the obtained configuration as a Riemann sphere with the four selected points and two cuts. Such sphere is a domain of analytic in certain regions, but generally multi-valued complex functions, like $\log \frac{(z-a)(z-b)}{(z-c)(z-d)}$, the cuts connecting the point a with the points c , and the point b with the d [85]. A certain matrix-valued generalization of such functions is known as *Wess-Zumino-Witten conformal block* [61], and this is the quantity, which is associated with described sphere in the construction under discussion.

Inverting a crossing as continuous move of the punctures Relating the WZW conformal blocks to the knot invariants (namely, to the HOMFLY polynomials) relies then on the both quantities satisfying the same system of the defining equations. More precisely, the WZW blocks on the sphere with the given four selected points form a three-dimensional linear space, in analogy with the meromorphic functions with the poles in the given points. In particular, three WZW conformal blocks related to variously made cuts satisfy the linear relation, which, when projected on a plain, reproduces the defining constraint on the Jones polynomials (see sec.5 for details)

$$\begin{aligned}
 (q - q^{-1}) \times \begin{array}{c} \text{C} \quad \text{A} \\ \text{D} \quad \text{B} \end{array} &= q^{-2} \times \begin{array}{c} \text{A} \quad \text{C} \\ \text{D} \quad \text{B} \end{array} - q^2 \times \begin{array}{c} \text{A} \quad \text{C} \\ \text{D} \quad \text{B} \end{array} \\
 \mathbb{1} &\quad \hat{\Omega}_{AB} \quad \hat{\Omega}_{AB}^{-1}
 \end{aligned} \tag{4.1}$$

Skein relations for the Jones polynomial as the projection of a three-dimensional figure.

The operator Ω_{AB} moves the points A and B continuously on the each other positions in the selected direction, the cuts attached.

The Jones polynomial is argued then to be a “contraction” of the WZW conformal blocks. The precise definition of this contraction, as well as the explicit formulas for the conformal blocks are not involved in the approach discussed.

4.1.2 Knot polynomials as invariants of the conformal blocks

Presented in [95] construction, although being implicit itself, gave rise to a new approach to calculating knot polynomials [55, 80, 75, 78, 56, 32]. We briefly outline this approach below.

Cutting of the knot with punctured spheres. A knot is composed of “elementary pieces”, each piece being constraint by a topological sphere with $2k$ punctures pairwise connected by k segments of the original curve. The punctures of the spheres are matched by the parallel lines in the external space area. It is know then that a knot can be obtained from the unknot with help of certain “elementary transformations” of the “elementary pieces”, which consist in intertwining of the curve segments inside the spheres (see the above papers and references therein for the corresponding theorems).

Relating a punctured sphere to a linear operator. The k line segments composing each “elementary piece” can be continuously transformed into k cuts, pairwise connecting the $2k$ punctures on the constraining this piece sphere. Intertwining the segments corresponds then to moving the punctures continuously on the positions of each other, together with the attached cuts. A sphere with punctures and cuts corresponding to a WZW conformal block, such interchangings of the punctures positions correspond to certain transformations of the WZW conformal blocks. Unlike the conformal blocks themselves, operators of these transformations can be calculated explicitly and rather effectively, the corresponding technology being developed in [55, 80, 75, 78, 98, 86, 56, 46, 68, 69, 32]. If the unknot corresponds to the unity operator, then a knot corresponds to an operator product, and a knot polynomial is obtained in this approach as a matrix element of the operator product.

Case of the colored HOMFLY polynomials. A more general WZW conformal block is related to a punctured topological sphere (or to a higher genus curve), a Lie group representation being associated with each puncture. In particular, the conformal blocks related to the HOMFLY polynomials are in the fundamental representation of the $SU(N)$ group; in particular, for $N = 2$ the Jones polynomial is obtained. The next conjecture was that the colored HOMFLY polynomials (see sec.2) are related to the WZW conformal blocks for higher representations of the same group in a similar way (although the reasoning of [95] can not by straightforwardly extended to the case since the colored polynomials do not possess an implicit definition generalizing the skein relations definition of the plain polynomials).

The conformal blocks approach as the state model approach. The approach outlined above provides a representation of a knot invariant of the same kind as the representation we consider (see sec.5), and as the representation that arises in the Kontsevich integral method (see sec.4.6), which is closely related to interpretation of knot invariants from the standpoint of the perturbative Chern-Simons theory. Moreover, all three approaches use the so called R -matrix (see sec.7) as one of the elementary operators. For instance, R -matrix in the WZW approach arises as, roughly speaking, a square root of the conformal block monodromy operator.

4.1.3 Wess-Zumino-Witten conformal blocks and classical Chern-Simons fields

Finally, a knot polynomial represented as sketched above, is related in [95] to an observable (precisely, to Wilson averages, see sec.4.1.4) in a three-dimensional gauge theory by means of one more implicit step. Namely,

- Wess-Zumino-Witten *conformal blocks* are in a one-to-one correspondence with the curvature free three dimensional fields inside the sphere, the fields being singular along the curve arcs.

Such fields may be considered as solutions of the classical equations of motions (with the field sources along the arcs) for a certain three-dimensional action, which is called *Chern-Simons action* [26, 36] (see also sec.4.1.4). This correspondence is one of inspiration sources for associating knot invariants with observables in a topological quantum field theory. We briefly discuss some points of the subject in the next section.

4.1.4 Towards relating the knot invariants to the perturbatively computed Wilson averages in the Lagrangian Chern-Simons theory

As we briefly discussed in the last section, it is the *implicit* correspondence between the HOMFLY polynomials and Wilson averages, which is suggested in [95]. A problem of obtaining the knot polynomial as an observable in the Lagrangian Chern-Simons theory remains then open, being intensively studied by other researches soon afterwards [67, 37, 38, 41, 49, 48]. These studies came to the same relation between the knot polynomials and the Chern-Simons Wilson averages as the one stated in [95], approaching it from a completely different direction. The correspondence of the two quantities is now established *explicitly*, but only *perturbatively*. Namely, a perturbation series for the Chern-Simons Wilson average is compared term-wise with the expansion for the HOMFLY polynomial in the logarithm of a formal variable. Apart from that, a variant of this approach also gives rise to an operator-contraction presentation for the knot invariants, similarly to the WZW approach and to the approach we follow.

4.2 Wilson averages in the Chern-Simons theory

In this section, we recall the form of the Chern-Simons action and the definition of the Wilson average, giving some comments about a physical sense of these quantities as well.

4.2.1 Basic definitions

Chern-Simons action In the Lagrangian approach, the three-dimensional Chern-Simons theory is defined by the cubic action

$$\int d^3x \text{Tr}_{\text{adj}} \left\{ \epsilon^{ijk} \left(A_i \partial_j A_k + \frac{2gi}{3} A_i A_j A_k \right) \right\} \equiv S_{CS}, \quad (4.2)$$

where $A_\mu(x)$ is a three-dimensional gauge field. Action (4.3) arises, for instance, from the topological term in the four-dimensional Yang-Mills theory,

$$S_{CS} = \int dx^4 \text{Tr} \epsilon^{\mu\nu\rho\sigma} F_{\mu\nu} F_{\rho\sigma}, \quad (4.3)$$

where the Wick rotation $t \equiv i\tau$ was performed, and the integral in the r.h.s. is taken over the infinity sphere, the Chern-Simons field being the projection of the Yang-Mills field on the sphere. The Chern-Simons action S_{CS} being independent of the metric approves referring it to as a *topological theory* [26, 37].

Although is not included in the standard classical Yang-Mills action, the topological term might be created by non-perturbative corrections [81]. On the other hand, the value of the classical Yang-Mills action in the Euclidian space, when being finite², is restricted from below by the value of S_{CS} evaluated for a Yang-Mills field from the same topological class. As a result, self-dual fields, which satisfy the first-order equation $F_{\mu\nu} = \epsilon_{\mu\nu\rho\sigma} F^{\rho\sigma}$ so that S_{YM} equals S_{CS} , are particular solutions of the Euclidian Yang-Mills equations [7]. The corresponding solutions in the Minkowski space are referred to as Yang-Mills *instantons*, the interest to these solutions being inspired by Polyakov result [74],

²For this to take place the Yang-Mills field must be locally the pure gauge in the infinity sphere, the Chern-Simons action giving then the number of covers of an $SU(2)$ subgroup of the gauge group by the infinite sphere [7, 81].

which consisted in demonstrating the solutions of a similar kind being responsible for the confinement in a toy model (lattice two-dimensional electrodynamics).

The classical equations of motion for the Chern-Simons action

$$\epsilon^{ijk}(\partial_j A_k + A_j A_k) = \epsilon^{ijk} F_{jk} = 0 \quad (4.4)$$

require for vanishing of the field tensor F_{jk} . However, the corresponding potential is not necessarily a pure gauge. Particular examples of the non-trivial classical Chern-Simons potentials are given by projecting the already mentioned instantonic solutions of the Yang-Mills equations [7] on the infinity sphere.

One can also consider the Chern-Simons action in Minkowski signature (there is no factor if i in (4.3) then). As usual, the two variants of the theory are related by the Wick rotation [73] $t \rightarrow it$, or, equivalently, $A_0 \rightarrow iA_0$. We start from considering the more intuitively clear Euclidian version in sec.4.2.2,4.3, and 4.5, switching to the Minkowski version in sec.4.6, since the statement discussed there refers to the light-cone gauge, which can be selected in the Minkowski signature (see [48] and sec.4.2.3).

Wilson lines and loops A Wilson line is an observable introduced in a field gauge theory [73]. The Wilson line in an abelian gauge theory by definition equals

$$W^{ab}[A(x), \gamma] \equiv \exp \int_{\gamma} dx^{\mu} A_{\mu}(x^{\mu}). \quad (4.5)$$

This quantity gives the phase increment of a wave function as the particle subjected to the field A passes the line γ .

The Wilson line in a non-abelian gauge theory is defined with help of a notion of the path exponential. The path exponential of a non-abelian gauge field $\vec{A}(t)$ over a curve γ , a parameter t is selected on the curve, is an operator that by definition satisfies

$$W(t + \delta t) = W(t)(1 + \vec{A}(t) \cdot \vec{n}(t)\delta t), \quad (4.6)$$

with $\vec{n}(t)$ being the tangent vector to the curve. One writes

$$W[A(x), \gamma] \equiv \text{Pexp} \left(\int_{0[\gamma]}^t \vec{A}(s) \cdot \vec{n}(s) ds \right) \equiv \text{Pexp} \left(\int_{\gamma} \vec{A} \cdot dl \right). \quad (4.7)$$

This quantity represents the finite gauge transformation responsible for mixing of the matter fields in a multiplet as they pass the line γ .

A Wilson line for the closed contour γ is called a Wilson loop. The trace of this quantity over the gauge group is a gauge invariant and independent of the reference point on the contour quantity. The quantity can be observed intermediately in the phenomena like Aharonov-Bohm effect.

Wilson averages. In quantum field theory, one introduces the notion of the Wilson average as well. This quantity is defined in perturbation theory as an average of the formal series for the path exponential,

$$\langle W_{\gamma}(A) \rangle \equiv \sum_{k=0}^{\infty} g^k \int_{\tilde{x}}^{\tilde{x}} dx_k^{i_1} \int_{\tilde{x}}^{x_1} dx_k^{i_2} \dots \int_{\tilde{x}}^{x_{k-1}} dx_k^{i_1} \langle A_{i_k}(x_k) \dots A_{i_2}(x_2) A_{i_1}(x_1) \rangle,$$

where all integrals are taken over the arcs of contour γ .

Wilson averages in Chern-Simons theory. A remarkable property of the Chern-Simons theory is that it can be reduced to an abelian theory by the proper gauge fixing (see [37] and sec.4.6). As a result, the Chern-Simons Wilson average is in fact equal to the Wilson line evaluated on the proper solution of the classical equations of motion in the corresponding gauge. Because the classical Chern-Simons equations are the curvature vanishing equations, the Wilson loop contains then a contour integral of a closed one-form, being thus unaffected by the smooth deformations of the contour and giving a topological invariant.

In case of an everywhere regular Chern-Simons field, which satisfies the classical equations of motion in the *entire* space, all Wilson loops will take the same and trivial value. Unlike that, the Chern-Simons field having a line-like singularity gives results in appearing of topologically distinct Wilson loops, the contours variously intertwined with the line of the field singularity. The value of the Wilson loop depends then only on the topological class of the contour.

The singular locus of the Chern-Simons field can be accounted for by putting the corresponding delta-function in the r.h.s. of classical equations of motion, or, equivalently, by adding the source term to the Chern-Simons action. Roughly speaking, such a term in turn can be obtained by inserting the second Wilson line under the average sign, joining then the exponent to the action as an interaction term of the Chern-Simons field with a line-like field source. Hence, a correlator of the two Wilson averages is in this sense similar to a one Wilson loop evaluated over a classical Chern-Simons field, generated by the source placed along the other loop. This is in fact the idea of perturbative evaluation of the Wilson averages in an abelian gauge [48, 49, 35, 71] (see sec.4.5 for details).

4.2.2 Simplest examples of Chern-Simons fields and Wilson averages

To better illustrate what kind of theory is under discussion, we write down explicitly the Chern-Simons actions for the simplest gauge groups, considering them from the standpoint of some physical and geometrical analogies. A more broad and detailed discussion of the Chern-Simons theory from the physical standpoint can be found in [36].

Gauge group $U(1)$. In this simplest case, the Chern-Simons field is an abelian gauge field, which may be considered as a static magnetic field satisfying the Maxwell equations

$$\text{rot}\vec{H}(\vec{x}) = 4\pi\vec{j}(\vec{x}), \quad \text{div}\vec{H} = 0. \quad (4.8)$$

The first equation can be obtained by variation of the effective action

$$S_{CS}^{ab}[A_0 = H_z, A_x = H_x, A_y = H_y] = \frac{\kappa}{4\pi} \int d^3x \epsilon^{ijk} A_i \partial_j A_k \stackrel{\kappa=1}{=} \frac{1}{4\pi} \int dV \vec{H} \cdot \text{rot}\vec{H} + \int dV \vec{H} \cdot \vec{j} \quad (4.9)$$

which coincides with the abelian Chern-Simons action, the magnetic *field* standing for the Chern-Simons *potential*. The second equation may be considered then as the gauge fixing condition $\partial_k A_k = 0$, a gauge transformation of the Chern-Simons field $A_k \rightarrow A_k + \partial_k f$ corresponding to adding a rotor-free magnetic field, which satisfies the homogeneous Maxwell equations.

An abelian Wilson loop is then an exponentiated circulation of the Chern-Simons field over a closed circuit

$$W(\gamma)[A_0 = H_z, A_x = H_x, A_y = H_y] \equiv \exp\left(\oint_{\gamma} \vec{dl} \vec{H}\right). \quad (4.10)$$

When evaluated on a Maxwell equations solution, this quantity is equal to the circulation of a circuit magnetic field over the circuit. This quantity is not well defined for an infinitely thin circuit. However, if there are two intertwined circuits, the quantity contains a well defined contribution, which is the circulation of the one circuits magnetic field over the other circuit. Due to the integral form of the corresponding Maxwell equation, such a cross term is proportional to the linking number of the contours.

Gauge group $SU(2)$. The simplest case of a non-abelian Chern-Simons theory contains the triple of gauge fields $(\vec{A}_1, \vec{A}_2, \vec{A}_3)$ entering the action

$$S = \int d^3x \left(\sum_{a=1}^3 \vec{A}_a \cdot \text{rot} \vec{A} + (\vec{A}_1, \vec{A}_2, \vec{A}_3) \right), \quad (4.11)$$

where a dot stands for scalar product and the parentheses stand for a mixed product of the vectors, $(\vec{a}, \vec{b}, \vec{c}) \equiv \vec{a} \cdot [\vec{b} \times \vec{c}] = \vec{b} \cdot [\vec{c} \times \vec{a}] = \vec{c} \cdot [\vec{a} \times \vec{b}]$. The same action can be presented in the form The same action can be presented in the more standard form

$$S = \int d^3x \text{Tr} \left\{ \epsilon^{ijk} \left(\hat{A}_i \partial_j \hat{A}_k + \frac{2i}{3} \hat{A}_i \hat{A}_j \hat{A}_k \right) \right\}, \quad (4.12)$$

with \hat{A} being an anti-hermitian matrix,

$$W = \begin{pmatrix} iA_3 & iA_1 + A_2 \\ iA_1 - A_2 & -iA_3 \end{pmatrix} = i \sum_{a=1}^3 A^a b_a, \quad (4.13)$$

which is expanded over the Pauli matrices

$$b_1 = \begin{pmatrix} 0 & 1 \\ 1 & 0 \end{pmatrix}, \quad b_2 = \begin{pmatrix} 0 & -i \\ i & 0 \end{pmatrix}, \quad b_3 = \begin{pmatrix} 1 & 0 \\ 0 & -1 \end{pmatrix},$$

$$b_a b_b = \frac{1}{2} [b_a, b_b] = \epsilon_{abc} b_c. \quad (4.14)$$

The action being presented as (4.12), it is easier to demonstrate its invariance under a transformation generated by an arbitrary unitary matrix with the unit determinant and generally with the coordinate dependent entries,

$$A_k \rightarrow \Omega^{-1} A_k \Omega + \Omega^{-1} \partial_k \Omega, \quad \Omega = \begin{pmatrix} a(x, y, z) & b(x, y, z) \\ -\bar{b}(x, y, z) & \bar{a}(x, y, z) \end{pmatrix} \in SU(2), \quad (4.15)$$

where the bar stands for the complex conjugate. Transformation (4.15) is called an $SU(2)$ *gauge transformation* of the theory, which is thus by definition an $SU(2)$ *gauge theory*.

Classical equations the $SU(2)$ theory Variation of action (4.11) in the fields $\vec{A}_1, \vec{A}_2, \vec{A}_3$ gives rise to the classical equations of motion,

$$\text{rot} \vec{A}_1 = [\vec{A}_2, \vec{A}_3], \quad \text{rot} \vec{A}_2 = [\vec{A}_3, \vec{A}_1], \quad \text{rot} \vec{A}_3 = [\vec{A}_1, \vec{A}_2], \quad (4.16)$$

respectively. Alternatively, one can vary the action in form (4.11) w.r.t. the matrix-valued field \hat{A} , obtaining the same equations, this time presented as the curvature vanishing equations,

$$\partial_i \hat{A}_j - \partial_j \hat{A}_i + [\hat{A}_i, \hat{A}_j] = 0. \quad (4.17)$$

Solutions of the classical equations through the scalar potential. The classical equations of motion being the curvature-vanishing equations, a solution is locally expressed as

$$A_\mu = \Omega^{-1} \partial_\mu \Omega, \quad (4.18)$$

where $\Omega \in SU(2)$ is a gauge group element, namely, a 2×2 special ($\det \Omega = 1$) unitary ($\Omega \Omega^\dagger = \mathbf{1}$) matrix. One can straightforwardly verify that (4.18) satisfies (4.17), using that $\partial_\mu (\Omega \Omega^{-1}) = 0$ to express $\partial_\mu \Omega^{-1}$, namely,

$$\partial_\mu A_\nu - \partial_\nu A_\mu = \partial_\nu \Omega^{-1} \partial_\mu \Omega + \Omega^{-1} \partial_\nu^2 \Omega - (\mu \leftrightarrow \nu) = \Omega^{-1} \partial_\nu \Omega \cdot \Omega^{-1} \partial_\mu \Omega - (\mu \leftrightarrow \nu) = -[A_\mu, A_\nu] \quad (4.19)$$

If the scalar potential Ω is everywhere regular, then the Chern-Simons field A_μ is everywhere vanishing up to gauge transformation (4.15) generated by Ω . Unlike that, Ω having at least one special point can not be used as a matrix of a gauge transformation in the entire space, and the corresponding solution for A can be highly non-trivial.

“Abelian” solution with a line-like source In the context of the knot theory, the solutions of the classical equations with a line-like singularity are especially interesting (see discussion in sec.4.2). The simplest of such solutions is obtained from the above presented solution by ignoring z dependence of the scalar potential and by setting the parameter a to be zero,

$$\tilde{\Omega}(x, y, z = 0, a = 0) = \Omega(x, y, z = 0, a = 0) = \frac{1}{r} \begin{pmatrix} 0 & ix + y \\ ix - y & 0 \end{pmatrix}. \quad (4.20)$$

The corresponding components of the field A ,

$$\tilde{A}_x = A_x(x, y, z = 0, a = 0) = -\frac{y}{r^2} \begin{pmatrix} i & 0 \\ 0 & -i \end{pmatrix}, \quad \tilde{A}_y = A_y(x, y, z = 0, a = 0) = \frac{x}{r^2} \begin{pmatrix} i & 0 \\ 0 & -i \end{pmatrix}, \quad (4.21)$$

$$\tilde{A}_z = 0,$$

are regular everywhere but the line $x = y = 0$. In fact, this case reduces to the abelian case, both the non-vanishing field components being proportional to one and the same matrix everywhere in the space. However, it is already instructive to examine the various Wilson lines in this case.

Wilson loops for the “abelian” solution The phase increment of a minimally coupled to the field (with the charge g) particle passing an infinitely small segment of the circle $x^2 + y^2 = 1$ is given in this case by the diagonal matrix

$$\omega \equiv A_x \frac{dx}{d\varphi} + A_y \frac{dy}{d\varphi} = -y dA_x + x dA_y = \frac{1}{r^2 + a^2} \begin{pmatrix} i & 0 \\ 0 & -i \end{pmatrix}. \quad (4.22)$$

All the matrices on the particle path commuting, the path exponential in expression for Wilson line (4.6) reducing to the plain matrix exponential, which yields

$$W[\gamma(\psi)] = \begin{pmatrix} e^{ig\psi} & 0 \\ 0 & e^{-ig\psi} \end{pmatrix}. \quad (4.23)$$

In turn, the Wilson loop

$$\text{Tr } W[\gamma(2\pi)] = 2 \cos(2\pi g) \quad (4.24)$$

is a gauge invariant quantity that measures the phase increment of the particle passed along the closed contour. It can be shown that the phase shift corresponding to a closed contour is given by a non-unity matrix only for the contours winded over the line $x = y = 0$ of Ω singularity.

The presented solution in fact an example of the *abelian* Chern-Simons field, since the non-vanishing components of the vector potential commute at each point, as well as operators of the various Wilson lines.

“Non-abelian” solution with a line-like source Now we present an example of an “essentially non-abelian” classical Chern-Simons field (see Appendix A for how the corresponding expression may be obtained and presented visually) Namely, one should take the scalar potential

$$\Omega(x, y, z) = \Omega(x, y) = \frac{1}{\sqrt{(x^2 + y^2)(x^2 + y^2 + a^2)}} \begin{pmatrix} x^2 + y^2 & a(ix + y) \\ a(ix - y) & x^2 + y^2 \end{pmatrix}, \quad (4.25)$$

which gives rise to the vector potential

$$A_x = \Omega^{-1} \partial_x \Omega = \frac{a}{(x^2 + y^2)(x^2 + y^2 + a^2)} \begin{pmatrix} -iay & i(-x^2 + y^2) - 2xy \\ i(-x^2 + y^2) & iay \end{pmatrix},$$

$$A_y = \Omega^{-1} \partial_y \Omega = \frac{a}{(x^2 + y^2)(x^2 + y^2 + a^2)} \begin{pmatrix} iax & -ixy + (x^2 - y^2) \\ -ixy - (x^2 - y^2) & -iax \end{pmatrix},$$

$$A_z = \Omega^{-1} \partial_z \Omega = 0. \quad (4.26)$$

Note, that different components of the field A at the same point do not commute, e.g.,

$$\frac{1}{2}[A_y, A_x] = \frac{a^2}{(x^2 + y^2)(x^2 + y^2 + a^2)^2} \begin{pmatrix} x^2 + y^2 & a(iy - x) \\ a(iy + x) & -i(x^2 - y^2) \end{pmatrix}, \quad (4.27)$$

so that it is not just the antisymmetric derivative $\partial_x A_y - \partial_y A_x$, but the non-abelian field tensor F , which vanishes.

Wilson loops for the “non-abelian” solution. This time an infinitely small phase increment along the same line is given by the matrix

$$\omega \equiv A_x \frac{dx}{d\phi} + A_y \frac{dy}{d\phi} = -y dA_x + x A_y = \frac{a}{x^2 + y^2 + a^2} \begin{pmatrix} ia & x - iy \\ -x - iy & -ia \end{pmatrix} = \begin{pmatrix} iA & B e^{-i\phi} \\ -B e^{i\phi} & -iA \end{pmatrix} \quad (4.28)$$

$$A = \frac{a^2}{\rho^2 + a^2}, \quad B = \frac{a\rho}{\rho^2 + a^2}, \quad x = \rho \cos \phi, \quad y = \rho \sin \phi.$$

Because the phase shifts in the different points of the path do not commute, the Wilson line, which by definition equals

$$\text{Pexp} \int_{0[x=\rho \cos \phi, y=\rho \sin \phi]}^{\alpha} \omega d\phi \equiv \lim_{\substack{N \rightarrow \infty \\ q^N = \exp(i\alpha)}} \prod_{i=0}^N \left\{ \begin{pmatrix} 1 & 0 \\ 0 & 1 \end{pmatrix} + \frac{\phi}{N} \begin{pmatrix} iA & Bq^{-1} \\ -Bq & -iA \end{pmatrix} \right\}, \quad (4.29)$$

no longer reduces to the plain matrix exponential.

4.2.3 Gauging out of the cubic term in the non-abelian Chern-Simons theory.

An essential property of action (4.3) is that the cubic term vanishes in certain gauges, which are called *abelian* gauges. This property is essential for our discussion, because it is in fact a *Gaussian* average, the properties of which reproduces the discussed integral presentation for the knot invariants.

Any gauge where the three matrices A_x, A_y, A_z (in euclidian signature) or A_0, A_x, A_y (in Minkowski signature) are linearly dependent is an abelian gauge. One may verify that this indeed may be achieved by a gauge transformation; moreover, the quantum correction do not create the cubic term either [49]. In Minkowski metric, the most common abelian gauges are the temporal gauge $A_0 = 0$ [70, 71, 48] and a light-cone gauge $\vec{n} \cdot \vec{A} = 0$ with $\vec{n} \cdot \vec{n} = 0$. The light-cone gauge with $\vec{n} = (1, 1, 0)$ can be reformulated as a *holomorphic* gauge [49], by passing to the euclidian signature via the Wick rotation $A_0 \rightarrow -iA_0$, and by setting

$$A_t = A_y, \quad A_z = A_x - iA_0, \quad A_{\bar{z}} = A_x + iA_0. \quad (4.30)$$

The gauge-fixing condition then reads

$$A_{\bar{z}} = 0. \quad (4.31)$$

The Chern-Simons theory in the holomorphic gauge is the most explored the moment. For instance, the main statement about relation of the knot invariants to the perturbative Chern-Simons theory, which we formulate and discuss in sec.4.6, refers to this gauge [49, 48]. Unlike that, non much is known about the Chern-Simons theory in the temporal gauge, there being a lot more questions that answers [70, 71, 48]. To examine this gauge is a highly intriguing problem since the \mathcal{R} -matrix representation for the knot polynomials [79, 71], which is the main subject of the present text and which we discuss in details in sec.7, is conjecturally related to the perturbative expansion of the Chern-Simons Wilson average in the holomorphic gauge [70, 71].

4.3 Linking number as a contribution to abelian Wilson average

The first motivation for the QFT interpretation of the Vassiliev invariants is the integral formula for the simplest of this of this invariants, which is the linking number of two closed curves \mathcal{C}_1 and \mathcal{C}_2 [27],

$$\mathcal{L}(\mathcal{C}_1, \mathcal{C}_2) = \oint_{\mathcal{C}_1} dy^i \oint_{\mathcal{C}_2} dx^i \frac{\epsilon_{ijk} (x^k - y^k)}{|\vec{x} - \vec{y}|^3}. \quad (4.32)$$

The integration kernel may be considered as a Green function of the abelian Chern-Simons theory (see sec.4.4.2 for details), the action being

$$S_{CS}^{abelian} = \frac{\kappa}{4\pi} \int d^3x \epsilon^{kij} A_k \partial_i A_j. \quad (4.33)$$

The corresponding integral arises then as a second order contribution to abelian Wilson average (4.5). More precisely, (4.5) contains the double integral of the Green function, which is divergent. Postponing the interpretation of this phenomenon for the sec.4.5, we just notice now that presenting in case of a *link* crossing term

$$\begin{aligned} \langle W_{\text{cross}}^{(2)}(\mathcal{C}_1 \otimes \mathcal{C}_2) \rangle &= \left\langle \oint_{\mathcal{C}_2} dx^i \oint_{\mathcal{C}_1} dy^j A_i(x) A_j(y) \right\rangle = \oint_{\mathcal{C}_2} dx^i \oint_{\mathcal{C}_1} dy^j \langle A_i(x) A_j(y) \rangle = \\ &= \oint_{\mathcal{C}_2} dx^i \oint_{\mathcal{C}_1} dy^j G_{ij}(z) \end{aligned} \quad (4.34)$$

is well-defined, giving just linking number (4.32).

4.4 Properties of the knot invariants as general properties of the ordered exponential and of the Gaussian average.

As already mentioned in the introduction, an interpretation of more general knot invariants in terms of a non-abelian QFT is essentially motivated by the observation that the Vassiliev invariants possess the integral representation and can be assembled into a generating function that has the properties of the gaussian average of the ordered exponential [49, 48]. In the section, we recall the relevant properties of the ordered exponential and of the gaussian average, briefly mentioning the corresponding properties of the knot invariants.

4.4.1 Relevant properties of the ordered exponential

Composition property as the defining property of the ordered exponential. First of all, the ordered exponential by definition possess the composition property

$$\boxed{\text{Pexp} \int_a^b dt F(t) = \text{Pexp} \int_a^c dt F(t) \text{Pexp} \int_c^b dt F(t)} \quad (4.35)$$

One can demonstrate explicitly that this property holds at any order of the perturbative expansion,

$$\text{Pexp} \int_a^b dt F(t) = \mathbf{1} + \int_a^b dt F(t) + \frac{1}{2} \int \int_{a \leq s < t \leq b} dt ds F(t) F(s) + \frac{1}{2} \int \int_{a \leq t < s \leq b} dt ds F(s) F(t) + \dots \quad (4.36)$$

Splitting the last explicitly written out summand as

$$\int_a^b dt \int_a^t ds F(s) F(t) = \int_a^c dt \int_a^t ds F(s) F(t) + \int_b^c dt \int_c^t ds F(t) F(s) + \int_b^c dt \int_a^c ds F(t) F(s), \quad (4.37)$$

and taking into account that

$$\int_b^c dt \int_a^c ds F(t)F(s) = \left(\int_b^c dt F(t) \right) \left(\int_a^c ds F(s) \right), \quad (4.38)$$

one obtains the result to agree with the r.h.s. of (4.35),

$$\begin{aligned} & \text{Pexp} \int_a^c dt F(t) \text{Pexp} \int_c^b dt F(t) = \\ & = \left(\mathbb{1} + \int_a^b dt F(t) + \int_a^b dt \int_a^t ds F(s)F(t) + \dots \right) \left(\mathbb{1} + \int_c^b dt F(t) + \int_c^b dt \int_a^t ds F(s)F(t) + \dots \right) \end{aligned} \quad (4.39)$$

up to second order.

Tensor product presentation. Property (4.35) enables one to identically rewrite a path exponential in form of a tensor contraction, which is similar to the one entering the definition of knot invariants of our interest (see sec.5). Indeed,

$$\text{Tr Pexp} \oint_{\gamma} t F(t) = \text{Tr} \left\{ \text{Pexp} \int_a^b dt F(t) \text{Pexp} \int_b^c dt F(t) \text{Pexp} \int_c^d dt F(t) \text{Pexp} \int_d^a dt F(t) \right\} = S_{kl}^{ij} \bar{S}_{ji}^{kl} \quad (4.40)$$

where we introduced the operators

$$S = \text{Pexp} \int_a^b dt F(t) \otimes \text{Pexp} \int_c^d dt F(t), \quad \bar{S} = \text{Pexp} \int_b^c dt F(t) \otimes \text{Pexp} \int_d^a dt F(t), \quad (4.41)$$

and used the identity

$$L_j^i M_k^j P_l^k Q_i^l = (L \otimes P)_{jl}^{ik} (M \otimes Q)_{ki}^{jl}. \quad (4.42)$$

4.4.2 Relevant properties of the Gaussian average

Definition of the Gaussian average The next property of the generating function for the Vassiliev invariants is it having a structure of a *sum over pairings*, same to a Gaussian average. Namely, there is the formula of Gaussian integration [73]

$$\langle F_i F_j \rangle \equiv \frac{\int \prod_{i=1}^N dF_i F_k F_l \exp(-\frac{1}{2} \sum_{i,j=1}^N K_{ij} F^k F^l)}{\int \prod_{i=1}^N dF_i \exp(-\frac{1}{2} \sum_{i,j=1}^N K_{ij} F^k F^l)} = K_{ij}^{-1}, \quad (4.43)$$

which is straightforward to verify for a finite N . In analogy with the finite-dimensional case, the Gaussian average of the product of two operators $F(t)$ and $F(s)$ w.r.t. a quadratic action

$$S[F] = \int_0^T ds \int_0^T dt \mathcal{K}(t, s) F(t) F(s) \quad (4.44)$$

(the most common case is $\mathcal{K}(t, s) = \ddot{\delta}(t - s)$) by definition equals

$$\langle F(t) F(s) \rangle_S = G(t, s) \quad (4.45)$$

where the r.h.s. contains the Green function, which by definition satisfies

$$\mathcal{K}(t, u) = \int_0^T ds G(t, s) \mathcal{K}(s, u), \quad (4.46)$$

being in the sense the inverse of the kinetic operator $dt ds \mathcal{K}(t, s)$.

Any other correlator by definition either vanishes, if containing an odd number of operators,

$$\left\langle \prod_{i=1}^{2k-1} F(t_i) \right\rangle \equiv 0, \quad (4.47)$$

or is expressed via the pairwise correlators, if containing an even number of operators,

$$\left\langle \prod_{i=1}^{2k-1} F(t_i) \right\rangle \equiv \sum_{\sigma} \prod_{i=1}^{2k-1} \langle F(t_i) F(t_{\sigma(i)}) \rangle \quad (4.48)$$

The r.h.s. of (4.48) contains *the sum over all pairings* σ of the numbers from 1 to $2k$, and the equality is referred to as *Wick theorem*, which also can be derived by a straightforward computation in case of plain (not functional) Gaussian integral.

Peculiar cases when the average factorizes If one takes the Gaussian average of the both parts of composition property (4.35), the r.h.s. does **not** decompose into the product of the two averages generally. However, the decomposition takes place in the particular case when the operators $F(t)$ for $a < t < b$ do not correlate with the operators $F(s)$ for $b < t < c$. Moreover, due to the Wick theorem, it suffices to require the pairwise correlators of fields from different regions to vanish,

$$\langle F(t)F(s) \rangle = 0 \text{ for } a < t < c < s < b \Rightarrow \left\langle \text{Pexp} \int_a^b dt F(t) \right\rangle = \left\langle \text{Pexp} \int_a^c dt F(t) \right\rangle \left\langle \text{Pexp} \int_c^b dt F(t) \right\rangle \quad (4.49)$$

The simplest and rather common case where property (4.49) holds is the case

$$\langle F(t)F(s) \rangle = \delta(t - s), \quad (4.50)$$

which corresponds to averaging with the weight

$$\exp(-S) = \exp\left(-\int dt F^2(t)\right). \quad (4.51)$$

More generally, (4.49) holds for two distant regions if the correlator decreases fast enough,

$$\langle F(t)F(t + b - a) \rangle \ll \langle F(t)F(t + \epsilon) \rangle, \quad \epsilon \ll b - a, \quad (4.52)$$

e.g., for

$$\langle F(t)F(s) \rangle = \frac{1}{(t - s)^2 + T^2}, \quad T \geq b - a. \quad (4.53)$$

Property (4.49) of the Gaussian average match the factorization property of the Vassiliev invariants and HOMFLY polynomials for the disjoint union of links (see the next paragraph) [94]. Moreover, the combinatorial representation for the Kontsevich integral [27, 35] can be derived with help of this property, if one takes into account identity (4.40) for the path exponential as well.

Expansion of the averaged trace over the traces of the algebra generators products. As soon as $F(t)$ is an operator, the ordered exponential of $F(t)$ is an operator as well. Generally, an averaged trace of the operator is **not** equal to the trace of the averaged operator. In particular,

property (4.49) do not hold for the traces of the corresponding operators. However, if the operator $F(t)$ takes values in a Lie algebra, one may expand all the operators over algebra generators T_a ,

$$\begin{aligned}
\langle F(t)F(s) \rangle = 0 \text{ for } a < t < c < s < b &\Rightarrow \left\langle \text{Tr Pexp} \left(\int_a^b dt \sum_a F^a(t) T^a \right) \right\rangle = \\
&= \left\langle \text{Tr} \left\{ \text{Pexp} \left(\int_a^c dt \sum_a F^a(t) T_a \right) \text{Pexp} \left(\int_c^b dt F^a(t) T^a \right) \right\} \right\rangle = \\
&= \left\langle \text{Tr} \left\{ \sum_a \left(\text{Pexp} \int_a^c dt F(t) \right)^a T_a \sum_b \left(\text{Pexp} \int_c^b dt F(t) \right)^b T_b \right\} \right\rangle = \\
&= \sum_{a,b} \left\langle \left(\text{Pexp} \int_a^c dt F(t) \right)^a \right\rangle \left\langle \left(\text{Pexp} \int_c^b dt F(t) \right)^b \right\rangle \text{Tr } T_a T_b. \tag{4.54}
\end{aligned}$$

The product in (4.54) is substituted now with the sum, each term being a product of the *group factor* $\text{Tr } T_a T_b$ and of the *coordinate factor*, which is given by the corresponding component of the path exponential, and for which decomposition (4.49) still takes place.

A similar structure of the Kontsevich integral [27] motivates comparing it with an averaged trace of the ordered exponential [49, 48, 35].

4.4.3 Green functions giving rise to contour independent integrals

The above observations on the generating function for the Vassiliev invariants in the integral representation can be summarized into a claim, that the generating function has the structure of a Gaussian average of a path exponential. One more property of the integral representation, in turn, enables one to relate the Vassiliev invariants with the Lagrangian Chern-Simons theory. The property consists in the contour independence of the corresponding integrals. For instance, these integrals can be presented as integrals of a holomorphic functions in a complex plane.

On the other hand, if a Green function is a closed two form ($\partial_\mu G_{\mu\nu}(x-y) = 0$), or a holomorphic two-form ($\partial_z G(z-w) = 0$), then the integrals of Gaussian averages entering the perturbative series for the average of the path exponential are independent of integration contour, i.e., are topologically invariant. Hence, if one interprets the integral kernel of the Vassiliev invariants as the Green functions if pairwise correlators in a quantum field theory, the gradient vanishing or holomorphic condition should arise as the classical equations of motion in the theory. Example of a proper theory is given by an abelian Chern-Simons theory with the action (4.33) [49, 48]. Modulo the subtleties discussed in Appendix B, the Green function of the abelian Chern-Simons theory is

$$G_{ij}(x-y) = 4\pi\epsilon_{ijk}\partial^k \frac{1}{|\vec{x}-\vec{y}|}, \tag{4.55}$$

if the Lorenz gauge where $\partial_k A_k = 0$ is selected.

4.5 Knot invariants as link invariants: framing of knot from the Chern-Simons theory standpoint

Now we address to the question of the divergent contributions in perturbative expansion for the Wilson average, which we have already encountered with in sec.4.3.

4.5.1 Second order framing contribution

Second order term in perturbative expansion for the Wilson average contains, apart from well defined cross term (4.34), the diagonal terms with the both integrals being taking over the same link component. Moreover, in case of a knot, not a link, the answer includes such diagonal term only.

Yet, substituting of Green function to (B.3) to second order term (4.34) in expansion for the Wilson average, one indeed obtains a divergent integral for the coinciding integration contours $\mathcal{C}_1 = \mathcal{C}_2$.

The singularity we came across with is conventionally resolved by shifting the second integration contour relative to the first (and the original) one [41],

$$\oint_{\mathcal{C}} dy^i \longrightarrow \oint_{\mathcal{C}'} dy^i. \quad (4.56)$$

The corresponding second order contribution to the Wilson average takes then form of cross terms (4.34), with the original and shifted contours as the two integration contours. The resulting integral yields then the linking number of these contours.

Arising of a new parameter as a result of the regularization procedure is a common point in QFT. E.g., in case of UV regularization of a perturbative QFT, this new variable is associated with the considered energy scale. In turn, the maximum (or somehow averaged) distance ε between the contours \mathcal{C} and \mathcal{C}' can be considered as the regularization parameter in the problem under discussion. As usual, the answer does not have a definite limit as ε tends to 0; instead, all possible values of this limit are parameterized by a new independent variable, which in the case is the linking number of the contours \mathcal{C} and \mathcal{C}' . A possible interpretation of the observed phenomenon is that CS Wilson average is related not to a closed *contour*, but to a *closed* ribbon. The quantity thus depends not only on the shape of contour, but on the number of the ribbon intertwinings as well. On the other hand, the knot invariants we consider are also invariants of the ribbon knots in fact, what can be shown from the standpoint of completely independent definition of these invariants (see [94] and sec.7.4.3). Such a correspondence is one of the main inspiration sources for looking at the knot invariants as on the QFT observables.

4.5.2 Higher orders framing contributions

At a first glance, it seems that taking into account higher orders in the expansion for the Wilson average requires for introducing more and more new contours, \mathcal{C}'' , \mathcal{C}''' , \dots . Actually, the situation is different. As follows from the Wick theorem (see [73] and sec.4.4.2), a term in the perturbation series for the Wilson average is expressed via the second order term. In particular, the fourth order term reads

$$\begin{aligned} \left\langle \left(\oint_{\mathcal{C}} dx^i A_i(x) \right)^4 \right\rangle &= \left\langle \oint_{\mathcal{C}} dx^i \oint_{\mathcal{C}} dy^j \oint_{\mathcal{C}} du^k \oint_{\mathcal{C}} dv^l A_i(x) A_j(y) A_k(u) A_l(v) \right\rangle = \\ &= \left\langle \oint_{\mathcal{C}} dx^i \oint_{\mathcal{C}} dy^j A_i(x) A_j(y) \right\rangle \left\langle \oint_{\mathcal{C}} du^k \oint_{\mathcal{C}} dv^l A_k(u) A_l(v) \right\rangle + \\ &+ \left\langle \oint_{\mathcal{C}} dx^i \oint_{\mathcal{C}} du^k A_i(x) A_k(u) \right\rangle \left\langle \oint_{\mathcal{C}} dy^j \oint_{\mathcal{C}} dv^l A_j(y) A_l(v) \right\rangle + \\ &+ \left\langle \oint_{\mathcal{C}} dx^i \oint_{\mathcal{C}} dv^l A_i(x) A_l(v) \right\rangle \left\langle \oint_{\mathcal{C}} dy^j \oint_{\mathcal{C}} du^k A_j(y) A_k(u) \right\rangle = \\ &= \oint_{\mathcal{C}} dx^i \oint_{\mathcal{C}} dy^j G_{ij}(x-y) \oint_{\mathcal{C}} du^k \oint_{\mathcal{C}} dv^l G_{kl}(u-v) + \\ &+ \oint_{\mathcal{C}} dx^i \oint_{\mathcal{C}} du^k G_{ik}(x-u) \oint_{\mathcal{C}} dy^j \oint_{\mathcal{C}} dv^l G_{jl}(y-v) + \\ &+ \oint_{\mathcal{C}} dx^i \oint_{\mathcal{C}} dv^l G_{il}(x-v) \oint_{\mathcal{C}} dy^j \oint_{\mathcal{C}} du^k G_{jk}(y-u) = 3 \left(\oint_{\mathcal{C}} dx^i \oint_{\mathcal{C}} dy^j G_{ij}(x-y) \right)^2. \end{aligned} \quad (4.57)$$

Hence, it is enough to substitute exactly half of the contours appearing in each pairing by the contour \mathcal{C}' . After that all terms of the perturbative expansion assemble into the exponential of the linking number. Indeed, all the odd order terms vanish, and each term of order $2k$ yields the sum over

$(2k - 1)!!$ pairings, each pairing yielding the contribution n^k . In somewhat symbolic notations, that reads

$$\langle \exp(W) \rangle = \sum_{k=0}^{\infty} \hbar^k \frac{\langle W^k \rangle}{k!} = \sum_{k=0}^{\infty} (2k - 1)!! \frac{\hbar^k n^k}{(2k)!} = \sum_{k=0}^{\infty} \frac{n^k}{2^k k!} = \exp\left(\frac{nh}{2}\right). \quad (4.58)$$

4.5.3 Framing in non-abelian theory.

A similar approach is applied to the non-abelian theory, although its realization is more involved then. First of all, the Wilson line is now given by path ordered exponential (4.7), so that each integral in perturbative expansion (4.8) is taken not over the entire curve but from a selected origin point to the point associated with the inner integration variable. Hence, a shifted contour should be now introduced together with the matching rule of its points to the points of the original contour (fig.3). Equivalently, one should associate each point with of the original contour with a vector pointing out to the corresponding point of the shifted contour. The resulting construction is referred to as *framing* of a knot. Although evaluating of the framing contribution in a non-abelian theory is not as simple as the above presented calculation for the abelian case, the calculation can be carried out explicitly [49]. The result reads that the framing dependence separates of the rest perturbation series as a (4.58)-like factor. Hence, if the integration contour contains several connection component, or is artificially split into several parts, only the contribution to the Wilson average with the integration variables running over the different parts are non-trivial, while those with the variables running over the same part, after being regularized, contribute to the framing factor. By this reason, we concentrate on the well defined cross contribution in the remaining of the section, neglecting the singular contributions.

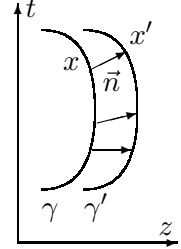


Figure 3: Framing of the knot from the non-abelian gauge theory standpoint.

In sec.4.6, we explicitly evaluate a non-abelian analog of the linking number, which has the same form as the framing factor.

4.6 Kontsevich integral for the Vassiliev invariants as the perturbative expansion for the Chern-Simons Wilson average in the holomorphic gauge

In the present section, we finally address to the main part of our discussion on relations between the knot invariants and the perturbatively formulated TQFT. The up to day view on the correspondence of the knot polynomials to the perturbative Chern-Simons theory relies on the following two statements:

- Kontsevich integral provides an integral representation for the HOMFLY polynomial.
- Kontsevich integral may be term-wise related to the perturbative expansion for the Chern-Simons Wilson average in the holomorphic gauge.

After providing some comments on the first statement, we discuss the second statement in details in the remaining part of the section.

4.6.1 HOMFLY polynomial as a generating function for the Vassiliev invariants

As we already mentioned, an essential part of interpretation of the knot polynomials in the context of the perturbative TQFT is the integral presentation for the certain knot invariants. These invariants are known in knot theory as *Vassiliev invariants* [27], the corresponding presentation for them is referred to as *Kontsevich integral* [62].

The Kontsevich integral for a separate Vassiliev invariant already has a rather specific structure, which we discuss below. But is much more important for our purposes that the integrals for *various*

Vassiliev invariants are assembled in a generating function, \hbar being the formal parameter. On the one hand, this generating function possesses the properties of the perturbative expansion for the Wilson average, as we discuss in what follows. On the other hand, one may verify the HOMFLY polynomial, when expanded in the parameter \hbar related to the formal variables entering the polynomial as $q = e^{2\pi\hbar}$, $A = e^{2\pi N\hbar}$, to reproduce the same generating function. These facts can be considered as a *perturbative* correspondence between the HOMFLY polynomials and the Chern-Simons Wilson average.

Moreover, the Kontsevich integral as entire series is known decompose into the tensor contraction of the certain elementary constituents [27, 48, 35], thus providing one more state model representation for the HOMFLY polynomial (see sec.5), which is of the same kind as the \mathcal{R} -representation [79, 71], which we discuss in details in sec.7, and as the WZW -representation [55, 80, 75, 78, 56, 32] developed on the base of [95]. Examining how these representations are related to each other hence illuminates the interference of the associated with them QFT ideas [48, 71, 35, 34].

4.6.2 Structure of the Kontsevich integral

In this section, we formulate the properties of the Kontsevich integral essential for comparing it with the perturbative expansion for the Chern-Simons Wilson average.

- The entire Kontsevich integral is an infinite series of the integrals of the increasing (even) multiplicity.
- Each multiple integral is a *t-ordered* integral, i.e., the integration variables satisfy $t_1 \leq t_2 \leq \dots \leq t_k$.
- Each multiple integral is multiplied on its own *group factor*, which is a certain contraction of a Lie algebra generators.
- All the integrals with a multiplicity $2g$, together with their group factors, are enumerated by all *pairings* of the $2g$ points.
- A kernel of each multiple integral is a product of *Green functions* of a certain differential equation.
- The entire series can be presented as a tensor contraction of certain “elementary constituents”.

For example, the series can start from 1, proceeding with the 6 double integrals of the form

$$\int_a^b dt \underbrace{\frac{\dot{z}_1(t) - \dot{z}_2(t)}{z_1(t) - z_2(t)}}_{\langle 12 \rangle} + \int_a^b dt \underbrace{\frac{\dot{z}_1(t) - \dot{z}_3(t)}{z_1(t) - z_3(t)}}_{\langle 13 \rangle} + \dots, \quad (4.59)$$

which are followed by the fourfold integrals having the structure

$$\begin{aligned} & \sum_{a,b} \text{Tr} \int_a^b dt \int_a^t ds 2 \underbrace{\frac{\dot{z}_1(t) - \dot{z}_2(t)}{z_1(t) - z_2(t)} \cdot \frac{\dot{z}_1(s) - \dot{z}_2(s)}{z_1(s) - z_2(s)} T_a T_b T_a T_b}_{\langle 12 \rangle \langle 12 \rangle} + \underbrace{\frac{\dot{z}_1(t) - \dot{z}_2(t)}{z_1(t) - z_2(t)} \cdot \frac{\dot{z}_1(s) - \dot{z}_3(s)}{z_1(s) - z_3(s)} \left(\underbrace{T_a T_b T_a T_b}_{(12)(13)} + \underbrace{T_a T_b T_b T_a}_{\langle 13 \rangle \langle 12 \rangle} \right)}_{\langle 1123 \rangle} + \\ & + \underbrace{\frac{\dot{z}_1(t) - \dot{z}_2(t)}{z_1(t) - z_2(t)} \cdot \frac{\dot{z}_3(s) - \dot{z}_4(s)}{z_3(s) - z_4(s)} T_a T_a T_b T_b}_{\langle 12 \rangle \langle 34 \rangle} + \underbrace{\frac{\dot{z}_1(t) - \dot{z}_2(t)}{z_1(t) - z_2(t)} \cdot \frac{\dot{z}_3(s) - \dot{z}_4(s)}{z_3(s) - z_4(s)} T_a T_a T_b T_b}_{\langle 1212 \rangle} + \underbrace{\frac{\dot{z}_3(s) - \dot{z}_4(s)}{z_3(s) - z_4(s)} T_a T_a T_b T_b}_{\langle 13 \rangle \langle 24 \rangle} + \underbrace{\frac{\dot{z}_1(t) - \dot{z}_2(t)}{z_1(t) - z_2(t)} \cdot \frac{\dot{z}_3(s) - \dot{z}_4(s)}{z_3(s) - z_4(s)} T_a T_a T_b T_b}_{\langle 14 \rangle \langle 23 \rangle} + \dots, \\ & \underbrace{\hspace{15em}}_{\langle 1234 \rangle} \end{aligned}$$

and so on. The structure of the series matches then the expansion of the Gaussian average

$$P \prod_{k=1}^4 \left(1 + \int dz A^a(z_k) T_a + A^a(z_k) A^b(z_k) T_a T_b + \dots \right), \quad (4.60)$$

double integrals (4.59) corresponding to the second order terms, fourfold integrals (4.60) corresponding to the fourth order terms, etc. We label each term (4.59) and (4.60) by the corresponding average (e.g., $\langle 1234 \rangle$ stands for $\langle A(z_1)A(z_2)A(z_3)A(z_4) \rangle$) and by the corresponding pairing (e.g., $\langle 12 \rangle \langle 34 \rangle$ stands for $\langle A(z_1)A(z_2) \rangle \langle A(z_3)A(z_4) \rangle$). The P sign in (4.60) means that all the multiple integrals in the expansion are ordered w.r.t. subscripts of the integration variables, e.g.,

$$P \int \int dz_1 dz_2 \equiv \int_a^b dz_2 \int_a^{z_2} dz_1. \quad (4.61)$$

One of the subtleties arising here is that the expansion of (4.60) reproduces (4.59,4.60), as well as the higher order terms in the Kontsevich integral, only up to the singular pairings like $\langle 11 \rangle \langle 22 \rangle$ coming from the correlator $\langle 1122 \rangle$. Yet ignoring of these terms has a certain sense in the framework of the *framing procedure* [27, 48], which is the standard way of regularizing the Wilson average discussed in sec.4.5.

4.6.3 Kernels of Vassiliev invariants as propagators of the complexified Chern-Simons theory

As a next step towards the Chern-Simons theory, one may observe that all the kernels (we mean the denominators, relating the numerators to the measure $\dot{z}dt = dz$) of integrals (4.59,4.60) are products of the Green functions of the equation, which is the holomorphic condition (see Appendix B for details)

$$\partial_{\bar{z}} \frac{\delta(t)}{z} = \delta(t)\delta(z)\delta(\bar{z}). \quad (4.62)$$

The holomorphic condition, in turn, may arise as the classical equations of motion in the theory with the lagrangian

$$\mathcal{L} = A_0(t, z, \bar{z})\partial_{\bar{z}}A_{\bar{z}}(t, z, \bar{z}) - A_{\bar{z}}(t, z, \bar{z})\partial_{\bar{z}}A_0(t, z, \bar{z}). \quad (4.63)$$

This the form, which the Chern-Simons lagrangian takes in the holomorphic gauge [41, 49, 48], as we discuss in sec.4.2.3.

The Lagrangian being quadratic, components of the Green function

$$G_{00} = G_{zz} = 0, \quad G_{0z} = -G_{z0} = \frac{\delta(t)}{z} \quad (4.64)$$

may be considered as the Gaussian averages

$$|A_z A_z\rangle \equiv G_{zz} = 0, \quad |A_0 A_0\rangle \equiv G_{00} = 0, \quad |A_0 A_z\rangle = -|A_z A_0\rangle \equiv G_{0z}. \quad (4.65)$$

4.6.4 Second order contribution to the Wilson average in the holomorphic gauge

To complete our discussion on the relation of the Kontsevich integral to the Chern-Simons Wilson average, we provide an illustration of how evaluating of a perturbative contribution to the Chern-Simons Wilson average can be reduced to evaluating integrals of type (4.59) in the simplest case.

We evaluate explicitly the first non-vanishing contribution to the Wilson average for the contour γ placed as in fig.4. Referring to sec.4.5, we regularize the divergent contributions to the average by introducing the shifted contour γ' , each point x' corresponding the point x of the original contour, and moving one point in each pairwise correlator to the shifted contour. For instance, the second order contribution to the Wilson average then equals

$$\oint_{\gamma} dx^{\mu} \oint_{\gamma'} dx^{\nu} \langle A_{\mu}(t, z, \bar{z}) A_{\nu}(t, z, \bar{z}) \rangle \quad (4.66)$$

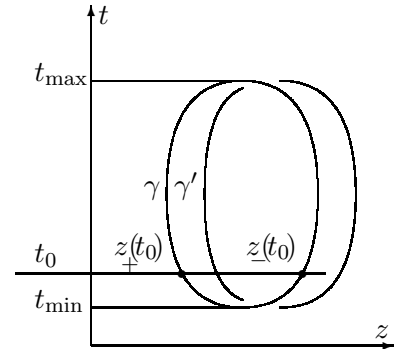


Figure 4: The original (γ) and shifted (γ') integration contours in case of unknot with one minimum and one maximal points.

Then, using definition (4.45) of the Gaussian average and explicit expression for the Green function in the holomorphic gauge (4.65), we rewrite the contribution as

$$\oint_{\gamma} dz \oint_{\gamma'} dt' \langle A_t(t, z, \bar{z}) A_z(t', z', \bar{z}') \rangle + \oint_{\gamma} dt \oint_{\gamma'} dz' \langle A_z(t, z, \bar{z}) A_t(t', z', \bar{z}') \rangle = \\ = \oint_{\gamma} \frac{dz}{z - z'} + \oint_{\gamma'} \frac{dz'}{z' - z}. \quad (4.67)$$

The next step is in passing to the integration over the selected axes. In the simplest case of the contour having two critical points (as each contour in fig.4), one should split the contour γ into two pieces, γ_+ , γ_- , given by the explicit functions $z = z_+(t)$ and $z = z_-(t)$, respectively, and one should split the contour γ' in a similar way. The integral over t is composed then of four summands,

$$\int_0^1 dt \frac{\dot{z}_+(t) - \dot{z}'_+(t)}{z_+(t) - z'_+(t)} + \int_0^1 dt \frac{\dot{z}_+(t) - \dot{z}'_-(t)}{z_+(t) - z'_-(t)} + \int_1^0 dt \frac{\dot{z}_-(t) - \dot{z}'_-(t)}{z_-(t) - z'_-(t)} + \int_1^0 dt \frac{\dot{z}_-(t) - \dot{z}'_+(t)}{z_-(t) - z'_+(t)}. \quad (4.68)$$

To proceed with, we use contour independence of the original integral to place the contours γ and γ' parallel everywhere but the region, corresponding, e.g., to the segments of contours pieces γ'_+ and γ'_- with $t_1 \leq t \leq t_2$, where the contours intertwine. The integral acquires the value only in the layer $t_1 \leq t \leq t_2$, because

$$\dot{z}_+(t) = \dot{z}_-(t) = \dot{z}'_-(t) = \dot{z}'_+(t), \quad 0 \leq t \leq t_1, \quad t_2 \leq t \leq 1, \quad (4.69)$$

so that the integrand identically vanishes in all the remaining space. To continue, we notice that the Green function in the holomorphic gauge is a decreasing function of the argument absolute value, and we use the contour independence once again to move the intertwined segments γ_+ and γ'_+ apart from the parallel segments γ_- , γ'_- in the layer $t_1 \leq t \leq t_2$ on the infinitely increasing distance,

$$|z_+(t) - z'_-(t)| \sim |z_-(t) - z'_+(t)| \rightarrow \infty. \quad (4.70)$$

The value of the integral must be independent of this distance, hence, the terms with two variables running over the different connection components vanish in this limit. Finally, we notice that the non-intertwined pieces of contours can be placed vertically so that they do not contribute to the integral as well,

$$\dot{z}_-(t) = \dot{z}'_-(t) = 0, \quad t_1 \leq t \leq t_2. \quad (4.71)$$

Finally, for the integration contours placed as in fig.4, the integral takes form

$$\mathcal{I} = \int_{t_1}^{t_2} dt \frac{\dot{z}_+(t) - \dot{z}'_+(t)}{z_+(t) - z'_+(t)}, \quad (4.72)$$

For instance, this example illustrates the Kontsevich integral decomposing into the sum of the “elementary contributions” in the considered simplest case. While these contributions are merely summed up in the lowest perturbation order, the higher orders reproduce their tensor contraction. This property of the Kontsevich integral, well known in the Vassiliev invariants theory [27], can be derived as a property of the Chern-Simons Wilson average [48], with help of the properties of the path exponential and of the Gaussian average discussed in sec.4.4.1 and sec.4.4.2, respectively (if the abelian gauge is selected, see sec.4.2.3, and the framing procedure is performed, see sec.4.5).

We outline the decomposition of the Wilson average in the holomorphic gauge into the elementary constituents of the Kontsevich integral in Appendix C, and we demonstrate the explicit evaluation of the lowest order perturbative contributions to the basic kinds of these constituents in Appendix D.

5 Knot polynomial as an observable in a state model

5.1 Formulating the approach

All the knot invariants enumerated in sec.2 can be introduced with help of the construction presented in L.Kauffman paper [53].

- A knot or a link, a direction on each connection component selected, corresponds to a directed four-valent planar graph with two kinds of vertices (fig.7), which is obtained by projecting a knot on a plane, arrangement of lines in the self-crossing w.r.t. the projection plane is kept. This graph is called *a knot (or link) diagram* (fig.5).
- The two kinds of vertices on the knot diagram correspond to two kinds of four-script operators, S_{kl}^{ij} and \tilde{S}_{kl}^{ij} , respectively, superscripts for incoming edges, subscripts for the out going once, and the left pair for the upper line. Components of the operators commute, as reads the first line of table 5.2 reads.
- An entire knot diagram corresponds then to a contraction of the operators along the edges (fig.5).

5.2 Definition of average

As we discuss below, a knot invariant can not be constructed just as an operator contraction. One more item is put then in the construction. Namely, a knot polynomial is going to be an *average* of the operator product. One may keep in mind that the operators now depend on additional parameters, averaging over the parameters yielding a knot invariant. The case is indeed like that in certain variants of the construction, for instance, in the version we discuss in details in sec.7. However, the original variant [53] introduces the average just as a formal operation, namely,

- An *average* of the operator contraction is introduced as a scalar quantity related to the contraction, the properties in tab.5.1 being satisfied.

$\langle \hat{O}_1(\lambda\hat{O}_2 + \mu\hat{O}_3)\hat{O}_4 \rangle = \lambda \langle \hat{O}_1\hat{O}_2\hat{O}_4 \rangle + \mu \langle \hat{O}_1\hat{O}_3\hat{O}_4 \rangle$	Poly-linearity	(5.1)
$\langle \text{Tr } \hat{O}_1\hat{O}_2\hat{O}_3 \rangle = \langle \text{Tr } \hat{O}_3\hat{O}_1\hat{O}_2 \rangle$	Symmetry under cyclic permutations	
$\langle \hat{O}_1 \text{Tr } \hat{O}_2 \rangle = \langle \hat{O}_1 \rangle \langle \text{Tr } \mathbf{1} \rangle \text{Tr } \hat{O}_2$	Decoupling of full contraction	

5.3 Operator identities

Similarly, instead introducing the operators of the crossing points explicitly, one requires that

- The operators satisfy the identities listed from the second to the fourth lines in tab.5.2 together with the corresponding deformations of knot diagrams.

$S_{kl}^{ij} S_{cd}^{ab} = S_{cd}^{ab} S_{kl}^{ij}$		Distant commutation
$S_{\alpha\beta}^{ij} S_{l\gamma}^{\alpha k} S_{mn}^{\beta\gamma} = S_{\gamma\alpha}^{jk} S_{n\beta}^{\beta i} S_{lm}^{\gamma\alpha}$		RII
$\tilde{S}_{\alpha\beta}^{ij} S_{kl}^{\alpha\beta} = S_{\alpha\beta}^{ij} \tilde{S}_{kl}^{\alpha\beta} = \delta_k^i \delta_l^j$		RIII
$\langle S_{\alpha j}^{i\alpha} \mathcal{O}_i^j \rangle = \langle \delta_\alpha^\alpha \rangle \langle \mathcal{O}_i^i \rangle$		RI
$(S_{\alpha\beta}^{ij} - Aq\delta_\alpha^i \delta_\beta^j) (S_{kl}^{\alpha\beta} - Aq^{-1}\delta_k^\alpha \delta_l^\beta) = 0$ $\Leftrightarrow A^{-1}S_{kl}^{ij} - A\tilde{S}_{kl}^{ij} = (q - q^{-1}) \delta_k^i \delta_l^j$		Skein relations

According to the Reidemeister theorem, two closed curves can be continuously transformed one into the other if and only if the corresponding knot diagrams are related by a sequence of three elementary transformations listed in tab.5.2 (lines 2-4), which are referred to as *Reidemeister moves*. Hence, the corresponding constraints imposed on the operators guarantee coinciding of averages associated with different diagrams representing the same knot.

As it is reflected in the table, only two out of the three Reidemeister moves (lines 2-3 of tab.5.2) can be imposed on the operators themselves. The remaining condition (line 4 of tab.5.2) turns out to be inconsistent with former two, when being treated as an operator identity, and it can hold only under the average sign [94].

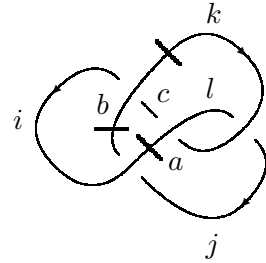


Figure 5: $S_{ab}^{ij} S_{lc}^{ak} S_{mi}^{bc} S_{kj}^{ml}$

* * *

The constraints on the operators and on the averages enumerated above turn out to be very restrictive, yet insufficient to calculate the knot invariant. One should couple these constraints with some additional data, which varies for different versions of the construction.

5.4 Jones polynomial for the trefoil knot as an average in the state model

Outlined the general construction, we proceed now with a more detailed presentation, relying on the explicit calculation of the knot polynomial for a particular knot diagram with help of several variants of the above construction.

5.4.1 Ward identities

The first way to complete the construction enables to determine plain (uncolored) HOMFLY polynomials, as well as Alexander and Jones polynomials, which are obtained from the HOMFLY polynomial

one by setting $A = 1$ and $A = q^2$, respectively, and, with some complications, for the plain Kauffman polynomial [53]. Following this way, one should additionally require that

- The operators satisfy the eigenvalue equation (line 5 of tab.5.2).

Taking into account the identity in line 2 of tab.5.2, one can rewrite the eigenvalue equation as a linear relation between the direct and inverse crossing operators (also given in line 5 of tab.5.2), which can be presented graphically (second column of line 5 of tab.5.2). The relations between the averages that follow from this form of the equation are known as *skein relations* for knot polynomials [94]. The resulting system of constraints, together with the properties of the average listed in table 5.1, then enables to evaluate a knot polynomial for arbitrary knot diagram. E.g., for knot diagram in fig.5, which is a diagram of the trefoil knot, one has

$$\begin{aligned}
\left\langle S_{ab}^{ij} S_{lc}^a S_{mi}^{bc} S_{kj}^{ml} \right\rangle &= \left\langle S_{bc}^{jk} S_{ia}^{ci} S_{lm}^{ab} S_{kj}^{ml} \right\rangle = z \left\langle S_{bc}^{jk} S_{ia}^{ci} S_{kj}^{ab} \right\rangle + \left\langle S_{kc}^{jk} S_{ij}^{ci} \right\rangle = \\
&= z^2 \left\langle S_{ia}^{ci} S_{bc}^{ab} \right\rangle + z \left\langle \delta_b^b \right\rangle \left\langle S_{ia}^{ai} \right\rangle + \left\langle S_{kc}^{jk} S_{ij}^{ci} \right\rangle = z^2 q \left\langle S_{ba}^{ab} \right\rangle + zq \left\langle \delta_b^b \right\rangle \left\langle \delta_a^a \right\rangle + q \left\langle S_{kj}^{jk} S_{ij}^{ci} \right\rangle = \\
&= z^2 q^2 \left\langle \delta_a^a \right\rangle + zq \left\langle \delta_a^a \right\rangle^2 + q^2 \left\langle \delta_a^a \right\rangle. \tag{5.3}
\end{aligned}$$

The above exercise is the standard calculation of a HOMFLY polynomial with help of the skein relations, which is usually represented graphically [94], but we intentionally keep the operator language, which is the main subject of the present text.

* * *

According to the corresponding theorem [94], an average corresponding to an arbitrary knot diagram can be calculated this way. Moreover, one obtains one and the same quantity for all ways of evaluating the average for a given knot diagram, as well as for all diagrams representing the same knot³. This approach thus provides a tool for calculating HOMFLY polynomials of, in principle, arbitrary knots, and this tool turns out to be highly effective; for instance, the numerous HOMFLY polynomial presented in [1, 2, 3] were calculated in this way.

However, the announced in [53] *state model* for the knot polynomial is not fully presented yet. Apart from that, this approach can not be straightforwardly extended to the case of *colored* HOMFLY polynomials, which cause much more interest today. These two points make one to search for a more explicit variants of the construction.

5.4.2 Explicit form of the crossing operators

An alternative way is to find an explicit expression for the crossing operator S , which would provide the operator satisfying the topological invariance constraints. There is a proper expression of a very simple form in the particular case $A = q^2$ (when the average, generally being equal to the HOMFLY polynomial, reduces to the Jones polynomial), namely,

$$S_{kl}^{ij} = q^{-1} \delta_l^j \delta_k^j - q^{-2} \epsilon^{ij} \epsilon_{kl}, \tag{5.4}$$

and

$$\langle \text{Tr} \mathbb{1} \rangle \equiv q + q^{-1}. \tag{5.5}$$

Expression (5.6) is referred to as *Kauffman matrix* [54]. Form of the operator (5.6) guarantees satisfying of the constraints in lines 1-3 and 5 of tab.5.2 (although the last one is not used explicitly in

³However, we omit here certain subtleties; see sec.7.4.3 for details.

this variant of the approach). Unlike that, the constraint in line 4 of tab.5.2, does *not* holds for (5.6), being valid only under the trace sign (where an arbitrary operator \mathcal{O}_i^l can be inserted as well),

$$\langle S_{jl}^{ij} \rangle = a \langle \delta_l^i \rangle \langle \delta_j^j \rangle - b \langle \epsilon^{ij} \epsilon_{jl} \rangle = \left(a \langle \delta_j^j \rangle - b \right) \text{Tr} \langle \mathbf{1} \rangle = \langle \delta_l^i \rangle \Rightarrow \text{Tr} \langle \mathbf{1} \rangle = \frac{1+b}{a}, \quad (5.6)$$

we denote the coefficients in (5.6) by $a \equiv q^{-1}$ and $b \equiv -q^{-2}$ to better demonstrate the structure of the answer. We see that, generally, the average is invariant under the R1 transformation only up to a factor, which equals the unity provided that the trace of the averaged unity operator takes a particular value, namely

$$\text{Tr} \langle \mathbf{1} \rangle = q + q^{-1}. \quad (5.7)$$

Since expression (5.6) reduces a general full contraction of the operators to a polynomial in $\text{Tr} \langle \mathbf{1} \rangle$, it is necessary and sufficient to fix the value of this quantity to calculate an arbitrary average. In particular, on can take thus value to be (5.7), so that the RI invariants holds.

The operators and the average sign being defined by (5.6) and (5.7), respectively, the Jones polynomial for knot diagram 5 is calculated as follows:

$$\begin{aligned} \langle S_{ab}^{ij} S_{lc}^{ak} S_{mi}^{bc} S_{kj}^{ml} \rangle &= a^4 \langle (\delta_b^i \delta_a^j) (\delta_c^a \delta_l^k) (\delta_i^b \delta_m^c) (\delta_j^m \delta_k^l) \rangle + b^4 \langle (\epsilon^{ak} \epsilon_{lc}) (\epsilon^{bc} \epsilon_{mi}) (\epsilon^{ml} \epsilon_{kj}) (\epsilon^{ij} \epsilon_{ab}) \rangle + \\ &+ a^3 b \langle (\delta_b^i \delta_a^j) (\delta_c^a \delta_l^k) (\delta_i^b \delta_m^c) (\epsilon^{ml} \epsilon_{kj}) + (\delta_b^i \delta_a^j) (\delta_c^a \delta_l^k) (\epsilon^{bc} \epsilon_{mi}) (\delta_l^m \delta_k^j) + \\ &+ (\delta_b^i \delta_a^j) (\epsilon^{ak} \epsilon_{lc}) (\delta_i^b \delta_m^c) (\delta_l^m \delta_k^j) + (\epsilon^{ij} \epsilon_{ab}) (\delta_c^a \delta_l^k) (\delta_i^b \delta_m^c) (\delta_j^m \delta_k^l) \rangle + \\ &+ a b^3 \langle (\delta_b^i \delta_a^j) (\epsilon^{ak} \epsilon_{lc}) (\epsilon^{bc} \epsilon_{mi}) (\epsilon^{ml} \epsilon_{kj}) + (\epsilon^{ij} \epsilon_{ab}) (\delta_c^a \delta_l^k) (\epsilon^{bc} \epsilon_{mi}) (\epsilon^{ml} \epsilon_{kj}) + \\ &+ (\epsilon^{ij} \epsilon_{ab}) (\epsilon^{ak} \epsilon_{lc}) (\delta_i^b \delta_m^c) (\epsilon^{ml} \epsilon_{kj}) + (\epsilon^{ij} \epsilon_{ab}) (\epsilon^{ak} \epsilon_{lc}) (\epsilon^{bc} \epsilon_{mi}) (\delta_j^m \delta_k^l) \rangle + \\ &+ a^2 b^2 \langle (\delta_b^i \delta_a^j) (\delta_c^a \delta_l^k) (\epsilon^{bc} \epsilon_{mi}) (\epsilon^{ml} \epsilon_{kj}) + (\delta_b^i \delta_a^j) (\epsilon^{ak} \epsilon_{lc}) (\delta_i^b \delta_m^c) (\epsilon^{ml} \epsilon_{kj}) + (\delta_b^i \delta_a^j) (\epsilon^{ak} \epsilon_{lc}) (\epsilon^{bc} \epsilon_{mi}) (\delta_j^m \delta_k^l) + \\ &+ (\epsilon^{ij} \epsilon_{ab}) (\delta_c^a \delta_l^k) (\delta_i^b \delta_m^c) (\epsilon^{ml} \epsilon_{kj}) + (\epsilon^{ij} \epsilon_{ab}) (\delta_c^a \delta_l^k) (\epsilon^{bc} \epsilon_{mi}) (\delta_j^m \delta_k^l) + (\epsilon^{ij} \epsilon_{ab}) (\epsilon^{ak} \epsilon_{lc}) (\delta_i^b \delta_m^c) (\delta_j^m \delta_k^l) \rangle + \\ &= a^4 \text{Tr} \langle \mathbf{1} \rangle^3 + 4a^3 b \text{Tr} \langle \mathbf{1} \rangle^2 + a^2 b^2 \left(2 \text{Tr} \langle \mathbf{1} \rangle^3 + 4 \langle \text{Tr} \mathbf{1} \rangle \right) + 4ab^3 \langle \text{Tr} \mathbf{1} \rangle^2 + b^4 \langle \text{Tr} \mathbf{1} \rangle \\ &= (q + q^{-1}) (q^{-2} + q^{-6} - q^{-8}) = q^{-1} + q^{-3} + q^{-5} - q^{-9}. \end{aligned} \quad (5.8)$$

The answer coincides with (5.3) for $A = q^2$, as it should.

5.4.3 Turn-over operators instead of average

One more way to complete the construction is to get read of averaging procedure at all, thus obtaining a fully explicit presentation of the knot polynomial. This is indeed possible, at least in many particular cases, provided that one inserts certain additional operators in some edges of the knot diagram. The corresponding procedure relies on a notion of *cycle*, which is by definition a closed path on a directed graph that can be passed along the directions on edges. We call a cycle a *simple cycle* if each edge and each vertex is passed no more that once. The rule reads then:

- Each simple cycle on the knot diagram must contain exactly one additional operator.

We recall that a simple cycle on a directed graph is a closed directed path passing through no edge or vertex for twice (or for more times). E.g., for the above considered knot diagram the proper operator contraction takes form

$$\langle S_{ab}^{ij} S_{lc}^{ak} S_{mi}^{bc} S_{kj}^{ml} \rangle \equiv S_{ab}^{ij} S_{lc}^{ak} S_{mi}^{bc} S_{\kappa j}^{ml} \mathcal{M}_\alpha^a \mathcal{M}_\beta^b \mathcal{M}_\kappa^c. \quad (5.9)$$

In the case relevant to the Jones polynomial, the new operator \mathcal{M} takes the explicit form

$$\mathcal{M} = \begin{pmatrix} q & 0 \\ 0 & q^{-1} \end{pmatrix}. \quad (5.10)$$

Each averaged unity in the calculation of the previous section is substituted then with the trace of the operator \mathcal{M} ,

$$\langle \delta_a^a \rangle \longrightarrow \mathcal{M}_a^a, \quad (5.11)$$

the result literally reproducing (5.8).

5.4.4 Explicit definition of average

The next variant of the approach is already very close to the variant of our main interest. It relies on the explicit definition of the averaging procedure. Namely, one should first substitute the crossing operators with their projections S_r on certain subspaces, defined with help of the corresponding projectors \mathcal{P}_r as

$$S_r \equiv \mathcal{P}_r S \mathcal{P}_r, \quad (5.12)$$

and then sum the contractions over these subspaces with certain weights w_r ,

$$\langle S \dots S \rangle \equiv_r \sum w_r \langle S_r \dots S_r \rangle, \quad (5.13)$$

To carry out this procedure explicitly, it is useful first to rewrite the contraction of the crossing operators as the trace of a matrix product. For instance, contraction (5) can be rewritten as,

$$S_{\boxed{ab}}^{sj} \delta_{\boxed{\kappa}}^t \cdot S_{\boxed{lc}}^{\alpha\kappa} \delta_{\boxed{u}}^{\beta} \cdot S_{\underline{mv}}^{\underline{uc}} \delta_{\underline{v}}^{\underline{l}} \cdot S_{\underline{tj}}^{\underline{mv}} \delta_{\underline{s}}^i = S_{ucl}^{(2)\beta\alpha\kappa} S_{imv}^{(1)ucl} S_{s jt}^{(2)imv} S_{ba\kappa}^{(1)sjt} = \text{Tr} \left\{ S^{(2)} S^{(1)} S^{(2)} S^{(1)} \right\} \quad (5.14)$$

where each of the matrices $S_L^{(i)I}$, $i = 1, 2$, has the two multi-indices corresponding two the triples of the sub- and superscripts as

$$S_L^{(1)I} \equiv S_{lmn}^{(1)ijk} \equiv S_{\underline{ml}}^{ij} \delta_n^k, \quad S_L^{(2)I} \equiv S_{lmn}^{(2)ijk} \equiv \delta_l^i S_{\underline{nm}}^{jk}. \quad (5.15)$$

We emphasize that reducing of the tensor contraction to the trace of the matrix product requires for introducing the two operators instead of one. The completed operation can be presented graphically, as redrawing initial knot diagram (fig.5) as of a braid closure. In the case relevant to the Jones polynomial, explicit expressions (5.6) for the operators S yield the corresponding expressions for the operators $S^{(1)}$ and $S^{(2)}$,

$$S_{lmn}^{(1)ijk} = q^{-1} \delta_l^i \delta_m^j \delta_n^k - q^{-2} \epsilon^{ij} \epsilon_{ml} \delta_n^k, \quad S_{lmn}^{(2)ijk} = q^{-1} \delta_l^i \delta_m^j \delta_n^k - q^{-2} \delta_l^i \epsilon^{jk} \epsilon_{nm}, \quad (5.16)$$

the matrices of the operators being, respectively,

$$q^2 S^{(1)} = \begin{array}{c} \begin{array}{cccccccc} 111 & 112 & 121 & 122 & 211 & 212 & 221 & 222 & ijk/lmn \end{array} \\ \left\| \begin{array}{cccccccc} q & & & & & & & & 111 \\ & q & & & & & & & 112 \\ & & q+1 & & -1 & & & & 121 \\ & & & q+1 & & -1 & & & 122 \\ & & & & -1 & q+1 & & & 211 \\ & & & & & & -1 & q+1 & 212 \\ & & & & & & & q & 221 \\ & & & & & & & & q & 222 \end{array} \right\|, \quad (5.17) \end{array}$$

and

$$q^2 S^{(2)} = \begin{array}{c} \begin{array}{cccccccc} 111 & 112 & 121 & 122 & 211 & 212 & 221 & 222 & ijk/lmn \end{array} \\ \left\| \begin{array}{cccccccc} q & & & & & & & & \\ & q+1 & -1 & & & & & & \\ & -1 & q+1 & & & & & & \\ & & & q & & & & & \\ & & & & q & & & & \\ & & & & & q+1 & -1 & & \\ & & & & & -1 & q+1 & & \\ & & & & & & & q & \end{array} \right\| \begin{array}{c} 111 \\ 112 \\ 121 \\ 122 \\ 211 \\ 212 \\ 221 \\ 222 \end{array} \end{array} \quad (5.18)$$

The averaging procedure is defined then with help of an additional operator Q , as a sum over the Q eigenvalues of the matrix products projected on the related to each eigenvalue subspaces, with the eigenvalues as the weights,

$$\langle \text{Tr} \{ S^{(2)} S^{(1)} S^{(2)} S^{(1)} \} \rangle \equiv \sum_{\substack{\lambda=q^3, q, \\ q^{-1}, q^{-3}}} \lambda \text{Tr} \{ S_{\lambda}^{(2)} S_{\lambda}^{(1)} S_{\lambda}^{(2)} S_{\lambda}^{(1)} \}, \quad S^{(i)} \equiv \mathcal{P}_{\lambda} S^{(i)} \mathcal{P}_{\lambda}, \quad i = 1, 2. \quad (5.19)$$

Of course, the thus defined averaging procedure is equivalent to just inserting the operator Q under the trace sign,

$$\langle \text{Tr} \{ S^{(2)} S^{(1)} S^{(2)} S^{(1)} \} \rangle \equiv \text{Tr} \{ Q S^{(2)} S^{(1)} S^{(2)} S^{(1)} \}. \quad (5.20)$$

, However, the basic quantities in some variants of the approach, in particular, in the variant we discuss in details in sec.6, are the Q eigenvalues and the projected matrices \mathcal{S}_{λ} , rather than the operators themselves. Hence, it is expression (5.19), and not (5.20), which is taken as a definition of the average then.

In the selected basis, the operator Q and the corresponding projectors are given by the diagonal matrices

$$\begin{array}{l} Q = \text{diag} \begin{pmatrix} q^3 & q & q & q & q^{-1} & q^{-1} & q^{-1} & q^{-3} \end{pmatrix} \\ \mathcal{P}_1 = \text{diag} \begin{pmatrix} 1 & 0 & 0 & 0 & 0 & 0 & 0 & 0 \end{pmatrix} \\ \mathcal{P}_2 = \text{diag} \begin{pmatrix} 0 & 1 & 1 & 1 & 0 & 0 & 0 & 0 \end{pmatrix} \\ \mathcal{P}_3 = \text{diag} \begin{pmatrix} 0 & 0 & 0 & 0 & 1 & 1 & 1 & 0 \end{pmatrix} \\ \mathcal{P}_4 = \text{diag} \begin{pmatrix} 0 & 0 & 0 & 0 & 0 & 0 & 0 & 1 \end{pmatrix} \end{array} \quad (5.21)$$

One can explicitly verify that the operator Q is related to the operators \mathcal{M} from the previous section as

$$Q_L^I \equiv Q_{lmn}^{ijk} = \mathcal{M}_l^i \mathcal{M}_m^j \mathcal{M}_n^k, \quad (5.22)$$

so that the trace in (5.19) coincides with contraction (5.9).

5.4.5 Character expansion

The subspaces and weights entering the definition of the average can not be selected just arbitrarily, because they should provide the invariance of the resulting quantity under RI (see sec.6 for details). However, there are many equivalent ways to present the subspaces and weights, which correspond to rewriting (5.19) various bases. In particular, the approach variant we are mostly interested in relies

on the choice of the subspaces and of the corresponding weights, which leads to presenting the average as the linear combination

$$\left\langle \text{Tr} \left\{ S^{(2)} S^{(1)} S^{(2)} S^{(1)} \right\} \right\rangle \equiv \sum_{r=s,a} [\text{dim}]_q^r \text{Tr} \left\{ S_r^{(2)} S_r^{(1)} S_r^{(2)} S_r^{(1)} \right\} = \text{Tr} \left\{ \mathcal{Q} S^{(2)} S^{(1)} S^{(2)} S^{(1)} \right\}, \quad (5.23)$$

$$S_r^{(i)} \equiv \mathcal{P}_r S^{(i)} \mathcal{P}_r, \quad r = s, f, \quad i = 1, 2,$$

where the quantities $[\text{dim}]_q^f$ and $[\text{dim}]_q^s$ are *quantum dimensions* [60] of the $SU(2)$ representations obtained by the group acting on vectors and rank three permutation tensors, respectively [52]. We postpone the precise definitions of these quantities for the next section, just presenting here the explicit form of the corresponding decomposition for the above example. Expression (5.23) can be derived from expression (5.20), with help of the fact that both the matrices $S^{(1)}$ and $S^{(2)}$ are block-diagonal in some distinguished basis,

$$S_{8 \times 8}^{(i)} = \begin{pmatrix} S_{4 \times 4}^{(i)s} & & \\ & S_{2 \times 2}^{(i)a} & \\ & & S_{2 \times 2}^{(i)a} \end{pmatrix}, \quad i = 1, 2, \quad (5.24)$$

the matrix \mathcal{Q} being just diagonal in the same basis and having the explicit form

$$\mathcal{Q} = \text{diag} \left(\underbrace{q^3 \ q \ q^{-1} \ q^{-3}}_s \ \underbrace{q \ q}_a \ \underbrace{q^{-1} \ q^{-1}}_a \right). \quad (5.25)$$

Trace (5.20) decomposes then into sum (5.23), with traces of the \mathcal{Q} operator over the corresponding subspaces as the weights,

$$[\text{dim}]_q^s = q^3 + q + q^{-1} + q^{-3}, \quad [\text{dim}]_q^f = q + q^{-1}. \quad (5.26)$$

For $q = 1$ these weights reproduce the dimensions $[\text{dim}]_q^f(q = 1) = 2$ and $[\text{dim}]_q^s(q = 1) = 4$ of the fundamental $SU(2)$ representation and of the space of the rank three permutation tensors on it, respectively.

The explicit form of the constituent blocks is

$$S_s^{(1)} = S_a^{(1)} = q^{-1} \mathbb{1}_{4 \times 4}, \quad S_a^{(1)} = \begin{pmatrix} q^{-1} & \\ & -q^{-3} \end{pmatrix}, \quad S_a^{(2)} = \begin{pmatrix} \frac{-1}{q^3 + q^5} & \frac{\sqrt{1+q^2+q^4}}{q^2+q^4} \\ \frac{\sqrt{1+q^2+q^4}}{q^2+q^4} & \frac{q}{1+q^2} \end{pmatrix}, \quad (5.27)$$

We do not give the precise definition of the corresponding subspaces here (see sec.7.6 for it).

Substituting explicit formulas (5.27) and (5.26) for blocks and quantum dimensions in expression for the average (5.23), and using the identities $\text{Tr} A^2 = \sum A_{ij} A_{ji}$ and

$$\left(\frac{-q^{-1}}{q^3 + q^5} \right)^2 + \left(\frac{-q}{q^3(1+q^2)} \right)^2 - 2q^{-1}(-q^{-3}) \frac{1+q^2+q^4}{(q^2+q^4)^2} = -q^{-8}, \quad (5.28)$$

one finally obtains the value of the average

$$\begin{aligned} \left\langle \text{Tr} \left\{ S^{(2)} S^{(1)} S^{(2)} S^{(1)} \right\} \right\rangle &= q^{-4} [\text{dim}]_q^s - q^{-8} [\text{dim}]_q^f = q^{-4} (q^3 + q + q^{-1} + q^{-3}) - q^{-8} (q + q^{-1}) = \\ &= q^{-1} + q^{-3} + q^{-5} - q^{-9} \end{aligned} \quad (5.29)$$

which reproduces the Jones polynomial for the trefoil knot once again.

Unfortunately, such simple expressions for the crossing operators and averages of the unity (or for the edge operators) are unavailable already in case of HOMFLY polynomials, nothing to say about

the colored knot polynomials. A generalization of the above outlined approach is yet possible, and we describe it in the next section.

The last variant of the approach turns out to be very effective as a tool of calculating HOMFLY polynomials, both plain and colored. For instance, the computational technology developed in [17, 18, 19, 43, 44, 45, 9, 11, 10, 13, 12] relies just on this variant. What is even more important, expression (5.23) gives rise to a new interesting quantity, which is obtained by substituting the quantum dimensions $[\dim]_q^f$ and $[\dim]_q^s$ of the $SU(2)$ representations by *characters* of these representations, $\chi_f = t_1$ and $\chi_s = \frac{1}{2}(t_1^2 + t_2)$, respectively. Substituting the special values $t_1 = q + q^{-1}$ and $t_2 = q^2 + q^{-2}$ for the formal variables, obtains the quantum dimensions again. The new quantity is referred to as *extended HOMFLY polynomial* [17]. Such quantity is no longer a *knot* invariant, being a *braid* invariant instead (see sec.6 for details). The extended HOMFLY polynomial is expected to arise naturally in the context of the matrix models [8] and integrable hierarchies [17], where a character decomposition for an average is widely used technic.

A drawback of the above representation for the average is that it relies on representing a knot as the closure of a braid. However, there is a vast amount of knots with the braid representations being much more involved than other representations of the same knots (the most common example is given by the *twist* knots [1]). Such knots can be effectively treated with by means of different variants of the operator contraction approach [55, 80, 75, 78, 56, 32]. Apart from that, such an interesting knot invariant as a *Khovanov polynomial* [57, 30] is also introduced with help of the same operators related to the crossings on the knot diagram, but the *homologies* of the operators matter in this case. Expressions for averages like (5.19,5.23) turn out to be insufficient then, explicit expressions for the very operators like (5.6) being needed instead.

6 Knot polynomial as an averaged trace of a braid group element

Braid group	Symmetric group	Hecke algebra	Colored Hecke algebra
$b_i b_{i+1} b_i = b_{i+1} b_i b_{i+1}$	$\sigma_i \sigma_{i+1} \sigma_i = \sigma_{i+1} \sigma_i \sigma_{i+1}$	$h_i h_{i+1} h_i = h_{i+1} h_i h_{i+1}$	$H_i H_{i+1} H_i = H_{i+1} H_i H_{i+1}$
$b_i b_j = b_j b_i, i-j \neq 1$	$\sigma_i \sigma_j = \sigma_j \sigma_i, i-j \neq 1$	$h_i h_j = h_j h_i, i-j \neq 1$	$H_i H_j = H_j H_i, i-j \neq 1$
	$\sigma_i^2 = \mathbb{1}$	$h_i^2 = \mathbb{1} + (q - q^{-1})h_i = 0$	$H_m = \sum_{k=0}^{m-1} a_k H_i^k$
	\Downarrow	\Downarrow	\Downarrow
	$(\sigma_i - 1)(\sigma_i + 1) = 0$	$(h_i - q)(h_i + q^{-1}) = 0$	$\prod_{k=1}^m (H_k - \lambda_k) = 0$

(6.1)

In this section, we discuss one more approach to the knot polynomials. Namely, the knot polynomials that are obtained in the framework of the state model approach [53] can be alternatively presented with help of matrix representations of the braid group [52]. This is not a coincidence, but rather a demonstration of a deep relation between the two approaches. This relation becomes clear from the standpoint of the \mathcal{R} -matrix approach, which we address to in sec.7, and which is in fact a version of the both approaches at the same time. Hence, the present section, together with the preceding one, should be considered as two preliminary parts of the subject presented in the following section.

6.1 Properties of braids and braid closures

The below discussed representation for knot polynomials relies on representing a knot as a braid closure. Hence, we start from recalling the basic properties of such representation. Throughout the section, we put attention of a relation between the braid group and the permutation group, this relation implying that the discuss knot invariants may naturally arise as the observable quantities in any physical model, which possess the permutation symmetry.

6.1.1 The braid group an extension of the permutation group

In the present section, we recall the definitions of the braid and permutation groups, and briefly review their properties essential for the following presentation. We also discuss a permutation group extension known as *Hecke algebra*, on which the below procedure of constructing a knot invariant essentially relies on.

Equivalence transformations of braids

$$\begin{array}{ccc}
 \text{I} & \text{II} & \text{III} \\
 \begin{array}{c} \text{Diagram I} \\ b_1 b_2 b_1 \end{array} = \begin{array}{c} \text{Diagram I} \\ b_2 b_1 b_2 \end{array} & \begin{array}{c} \text{Diagram II} \\ b_1 b_3 \end{array} = \begin{array}{c} \text{Diagram II} \\ b_3 b_1 \end{array} & \begin{array}{c} \text{Diagram III} \\ b_1 \tilde{b}_1 \end{array} = 1
 \end{array} \tag{6.2}$$

Generators of the permutation group. By definition, a generator σ_i of the permutation group of $n + 1$ elements corresponds to a transposition of the elements i and $i + 1$ in the sequence. Taking product of two the permutations is merely doing them successively. The group unity $\mathbf{1}$ corresponds to the trivial permutation (all the elements remain on their positions).

Generators of the braid group. A generator b_i of the $n + 1$ -strand braid group corresponds to a intertwining of the strands i and $i + 1$ in a braid section. Taking a product of two braids is, by definition, plating one after the other on the same strands. The unity in the $n + 1$ -strand braid group is the trivial $n + 1$ -strand braid, which consists of $n + 1$ unintertwined strands.

Symmetric group constraints. Two products of the permutation group generators are equivalent if and only if they realize the same permutation, e.g.,

$$\sigma_1 \sigma_1 xy = \sigma_1 yx = \mathbf{1} xy, \quad \sigma_1 \sigma_3 xyz = \sigma_3 \sigma_1 xyz = yxz, \quad \text{and} \quad \sigma_1 \sigma_2 \sigma_1 xyz = \sigma_2 \sigma_1 \sigma_2 xyz = zyx. \tag{6.3}$$

In fact, all relations between the permutation group generators are exhausted by the above examples. Namely, the products of the group generators are in one to one correspondence with the permutations provided that the group generators satisfy [42]:

$$\sigma_i \sigma_{i+1} \sigma_i = \sigma_{i+1} \sigma_i \sigma_{i+1}, \quad i = 1, \dots, n - 1, \tag{6.4}$$

$$\sigma_i \sigma_j = \sigma_j \sigma_i, \quad i, j = 1, \dots, n, \quad |i - j| \neq 1, \tag{6.5}$$

$$\sigma_i^2 = \mathbf{1}, \quad i = 1, \dots, n. \tag{6.6}$$

Braid group constraints. In turn, the braid group generators satisfy their own constraints, accordingly with that two braids, differing when projected on a plane, may be *isotopic*, i.e., being continuously transformed into each other in the three-dimensional space. According to the Artin theorem [94], such a transformation may be presented as a sequence of the elementary transformations shown in fig.6.2. While transformation (6.2-III) just determines the inverse of a braid group generators, transformations (6.2-I,II) give rise the following identities for the braid group generators:

$$b_i b_{i+1} b_i = b_{i+1} b_i b_{i+1}, \quad i = 1, \dots, n - 1, \tag{6.7}$$

$$b_i b_j = b_j b_i, \quad i, j = 1, \dots, n. \quad |i - j| \neq 1, \tag{6.8}$$

Relating a permutation to a braid. Constraints (6.7,6.8) coincide with constraints (6.4,6.5) for the permutation group generators. Hence, one may relate a permutation to a braid, intertwining strands i and $i + 1$ when the elements i and $i + 1$ are permuted, isotopic braids being related to the same permutation due to (6.7,6.8). However, the inverse is generally wrong, since there is no analog of constraint (6.6) for the braid group. In particular, any two-strand braid corresponds either to the permutation xy or to the permutation yx , when containing even or odd number of crossings, respectively, while any two-strand braids with the different numbers of crossings are not isotopic.

A one to one correspondence may be established between $n + 1$ -strand braids and replacements of $n + 1$ indistinguishable points in the plane, a generator b_i of the braid group corresponding to moving the points i and $i + 1$ *continuously* on the positions of each other, in the selected, e.g., clockwise, direction. Although the final arrangement of points coincides with the initial one, such operation may have a non-trivial effect, e.g., when acting on a function with algebraic or logarithmic singularities in the given points [85].

Relating a “quantum permutation” to a braid. The continuous transposition operators described above may still satisfy some relations, apart from braid group relations (6.7,6.8), in each particular case. The simplest non-trivial and important in many respects example is given by *Hecke algebra* [54]. By definition, generators h_i with $i = \overline{1, n}$ of the Hecke algebra satisfy the constraints

$$h_i h_{i+1} h_i = h_{i+1} h_i h_{i+1}, \quad i = 1, \dots, n - 1, \quad (6.9)$$

$$h_i h_j = h_j h_i, \quad i, j = 1, \dots, n. \quad |i - j| \neq 1, \quad (6.10)$$

$$h_i^2 = (q - q^{-1})h_i + 1, \quad q^n \neq 1, \quad n \in \mathbb{Z}, \quad (6.11)$$

where q is a new formal variable, and thorough the present text we suppose q being not a root of unity (since the properties of the Hecke algebra strictly differ in the opposite case [60]).

A Hecke algebra may be considered as a deformation of the permutation group, with the elements being enumerated, a transposition respecting the order numbers, and, apart from the permutations, their formal linear combinations being considered, namely,

$$h_i \left\{ \underbrace{\dots x_k x_l}_{i-1} \underbrace{\dots}_{n-i} \right\} = \{ \dots x_l x_k \dots \}, \quad l > k, \\ h_i \{ \dots x_k x_l \dots \} = (q - q^{-1}) \{ \dots x_k x_l \dots \} + \{ \dots x_l x_k \dots \}, \quad l < k. \quad (6.12)$$

From this stand point, an element of a Hecke algebra is sometimes referred to as a *quantum* or *q-permutation* [54].

Extensions of the permutation group with the polynomial constraints. Hecke algebra constraint (6.11) can be considered as a particular case of a more general constraint, having the form

$$H_m = \sum_{k=0}^{m-1} a_k H_i^k, \quad (6.13)$$

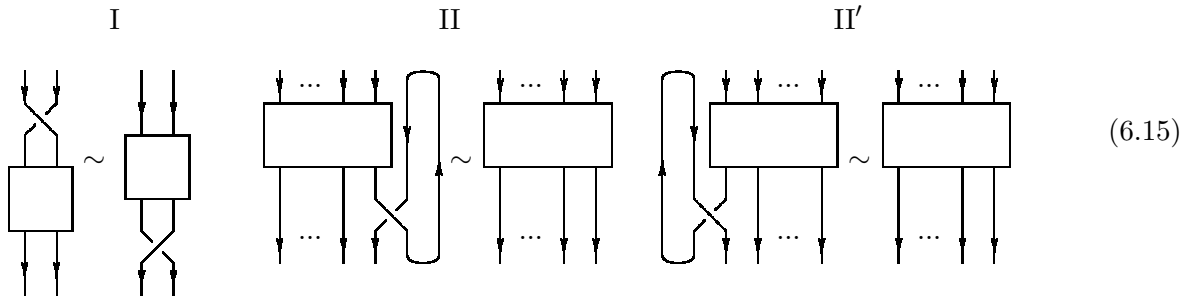
where generators H_i the new algebra are supposed to satisfy (6.9,6.10) as well. Moreover, all three relations (6.6), (6.11), and (6.13) can be considered as the spectral equations for the algebra generators,

$$(\sigma_i - \mathbb{1})(\sigma_i + \mathbb{1}) = 0, \quad (h_i - q\mathbb{1})(h_i + q^{-1}\mathbb{1}) = 0, \quad \text{and} \quad \prod_{k=1}^m (H_k - \lambda_k \mathbb{1}) = 0, \quad (6.14)$$

respectively. The braid group representations with a general form of constraint (6.13) give rise to the *colored HOMFLY* polynomials. Yet, we do not go into further details here, this point is much more natural to discuss in from the standpoint of the \mathcal{R} -matrix approach, we address to in section 7.

6.1.2 Braids closures and knots

Equivalence transformations of braids closures.



So far we have considered the braids and their equivalence transformations. However, a knot is the closure of a braid [94]. Hence, to construct a knot invariant, one should treat braids closures instead. Their equivalence transformations include those of the braids, as well as two more transformations. The first one is pulling a sequence of crossings $b_1 b_2 \dots b_k$ from the beginning of the braid to its end through the closure; the reversed sequence, $b_k \dots b_2 b_1$, appears then at the braids end, (6.15-I). The transformation is called the first Markov transform.

The second transformation consists in contracting a loop in fig.6.15-II or that in fig.6.15-II', and is referred to the second Markov transformation.

According to the Markov theorem [94], any two isotopic (related by a continuous deformation in the three-dimensional space) braid closures are transformed into each other by a sequence elementary transformations, which include group multiplication law (6.2-III), Artin transformations (6.2-I,II), and Markov transformations, (6.15-I,II). In particular, transformation (6.15-II') can be performed this way, and hence should not be included in the list.

There are some other knot representations of a similar kind, as the braid representation of a knot [1]. In particular, a knot can be related to a braid, the strands being directed differently (several ones “upwards”, the remaining ones “downwards”). A “closure” of such a braid includes an auxiliary element, [19]. A conventional notation for Pretzel knots [1],[33],[20] is this type one. All such braid-like representations can be used to represent a knot invariant in a similar way, as we discuss in what follows.

6.1.3 Unlinked knots and multiplication property

One degenerated case was left thus far beyond the scope of our consideration. Namely, if a strand of braid is never intertwined with the other ones (it can be either the first or the last strand in a braid section, see fig.6), then the closure of the strand, which is just a circle, is separated from the closure of the braid. More generally, the first k strands may never cross the $m - k$ last ones, or the braid may be reduced to one of the type by the equivalence transformations; the closure is a disjoint union of two or more knots or links. From the formal stand point, an invariant of a disjoint union a quantity, independent of the invariants of the components. However, many link invariants, among them Alexander, Jones, Kauffman, and HOMFLY polynomials, by definition possess a *multiplication property* [94]. Namely,

- An invariant of a disjoint union of links is equal to the product of the invariants of the components.

In fact, it suffices to require for factorization of the invariant related to braid with last strand unlinked, the general property following from this fact [52].

The multiplication property for the braid in fig.6 completes the list of the constraints fig.6.2,6.15 on a quantity related to a braid, in order the one to be a knot invariant.

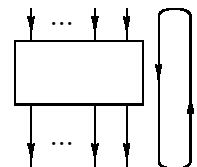


Figure 6: A braid closure with a “free” strand.

6.2 Algorithm of constructing a knot invariant

Completed a general discussion on constructing a knot invariant as a braid group invariant, we proceed with presenting the precise algorithm. First,

Step 6.1 *A knot is represented as the closure of a braid.*

Then, one should construct a representation of a braid group, i.e., to

Step 6.2 *Associate each of braid group generator b_i with a matrix B_i , a product of generators corresponding to the product of the matrices.*

The next step relies on the correspondence discussed above and summarized in tab.6.1. Namely, a representation of the permutation group, as well as a representation of the Hecke algebra is at the same time a representation of the braid group with the same number of generators [51] (we recall that we suppose the parameter q entering the Hecke algebra constraints to be not a root of unity). Moreover, the finite-dimensional irreducible representation of the Hecke algebra and of the permutation group are known then be in a one to one correspondence, the latter ones being obtained from the former ones for $q = 1$. In turn, dimensions of all the permutation group irreducible representations are well known in representation theory [42, 64], what enables explicitly making the following ansatz:

Step 6.3 *Dimension of the matrices is the dimension of an irreducible representation of the permutation group.*

E.g., for the one-strand braid they are 1×1 since the only (irreducible) representation of permutation group one generator is the one-dimensional representation. As we demonstrate in sec.6.3.1, matrices for the two-strand braid are of the same size, since both (irreducible) representations of the permutation group with two elements are one-dimensional. In turn, the permutation group with three elements has one- and two-dimensional irreducible representations, hence the three-strand matrices can be either one-, or two-dimensional (see sec.6.3.2), etc.

Explicit matrix expressions for Hecke algebra generators are in fact also known in representation theory (they are given, e.g., in [52]), However, we find it more illustrative not just present the corresponding expressions, but to derive them from the first principles in the particular cases. Namely, we are going to

Step 6.4 *Write down the matrices B_i of the proper size with undefined matrix elements and impose the braid group constraints (6.7,6.8) on them. (6.8)*

Using a freedom in selected the basis, we suppose the matrix B_1 to be diagonal. We will then

Step 6.5 *Solve the obtained system of equations w.r.t. to the elements of the matrices B_i , $i > 1$, expressing them via the eigenvalues of the matrix B_1 .*

After that, a matrix representing an arbitrary braid can be calculated explicitly by taking the proper product of the matrices B_i representing the braid group generators. This matrix depends on $\dim B_i$ of formal parameters λ_j , which are the B_1 eigenvalues.

The above steps provide a braid group representation, i.e., a braid is related to a matrix invariant under transformations (fig.6.2) of the braid. To pass to a knot invariant, one must construct a quantity that is invariant under braid closure transformations (fig.6.15,6) as well. To guarantee the invariance under transformation (fig.6.15-I) one can just

Step 6.6 *Take the trace of the matrix B related to the braid.*

To achieve the invariance under remaining transformations (fig.6.15-II,III) and (fig.6) is much more difficult. As we discussed in sec.5, “extra” conditions can be taken into account by taking a kind of “average” (see sec.5). If we continue following from the first principles, in the case to take the average implies to

Step 6.7 Write a linear combination of the traces $\text{Tr } B$ of matrices from different braid group representations with undefined coefficients,

then

Step 6.8 impose (fig.6.15-II,III) and (fig.6) on the obtained expressions,

and, finally,

Step 6.9 Solve the resulting equations w.r.t. the coefficients, expressing them via the B_1 eigenvalues.

We interrupt the general description at this point, sending a reader to [52] for the sequel, and proceed with carrying out the formulated steps explicitly in the particular cases.

6.3 Explicit calculating of the knot invariant in particular cases

6.3.1 Two-strand braids

Step 1. A two strand braid has the form b_1^n , where b_1 is the only braid group generator. The closures of various two-strand braids (fig.14) represent the so named series $T^{2,n}$ of torus knots (for n odd) and links (for n even). In particular, $T^{2,0}$ is a pair of unlinked unknots, and $T^{2,1}$ is the once intertwined unknot (fig.9-I), $T^{2,2}$ is the Hopf link, $T^{2,3}$ is a trefoil knot (fig.12), $T^{2,4}$ is the Solomon link, etc. (see figures at [1]).

Step 2. There are $2! = 2$ permutations of two elements, xy and yx . The space of their formal linear combinations is the two-dimensional, a basis can be chosen as

$$X_S = \frac{1}{2}(xy + yx), \quad X_A = \frac{1}{2}(xy - yx). \quad (6.16)$$

One refers to the formal expressions X_S and X_A as to one-dimensional representations of the permutation group S_2 , implying that are conserved, up to factor, subjected to the permutation group generator b_1 that permutes x and y ,

$$b_1 X_S = X_S, \quad b_1 X_A = -X_A. \quad (6.17)$$

Step 3. According to the ansatz of **Step 6.3**, one should take two matrices 1×1 , denote them λ and μ . No constraints are imposed on the single generator of the two-strand braid group, hence **Steps 6.4-6.5** are omitted, and we go to

Step 6. According to the ansatz of **Step 6.2** a two-strand braid is associated with a matrix product

$$B(b_1^n) = (h_1^I)^n, \quad I = S \text{ or } A. \quad (6.18)$$

where n is the number of crossings, positive or negative depending if the crossings are of direct or inverse orientation, respectively (see fig.7).

Finally, the indeed non-trivial step, already in the case concerned, is

Step 7. Following the ansatz of **Step 6.7**, we write the invariant of a braid in the form

$$\lambda^n \chi_S + \mu^n \chi_A, \quad (6.19)$$

where n is the number of crossings, positive or negative depending on their orientation (see 6.2-II), the eigenvalues λ and μ are considered as formal variables, while χ_S and χ_A are (*weight*) coefficients to define.

To obtain a knot (or link), not just a braid invariant, one has to impose some extra conditions on (6.19). E.g., one may observe that the closure of the two parallel strands reproduces a pair of unlinked unknots, while the closure of the two once intersected strands reproduces the single unknot with a contractible loop. The value of invariant of the unknot is not defined at the moment, and we denote it just χ ; due to the multiplication property discussed in sec.6.1.3, the invariant of a pair of unlinked unknots equals χ^2 . The resulting constraints read:

$$\begin{aligned} \mathbb{1}^{(2)} &\sim \mathbb{1}^{(1)} \otimes \mathbb{1}^{(1)} \Rightarrow \chi^2 = \chi_S + \chi_A, \\ h_1^{(2)} &\sim \mathbb{1}^{(1)} \Rightarrow \chi = \lambda\chi_S + \mu\chi_A, \end{aligned} \quad (6.20)$$

System (6.20) enables one to express the coefficients of irreducible representations in terms of the eigenvalues of the corresponding operators and value of the invariant for the unknot:

$$\chi_S = \frac{(\mu\chi - 1)\chi}{\mu - \lambda}, \quad \chi_A = \frac{(\lambda\chi - 1)\chi}{\lambda - \mu}. \quad (6.21)$$

The resulting expression for invariant of the knot represented as the closure of a two-strand braid with n crossings oriented the upper one in 6.2-II, or with $-n$ crossings oriented as the lower one, is

$$H(\mathfrak{B}^{(2)}; \lambda, \mu) = \lambda^n \frac{(\mu\chi - 1)\chi}{\mu - \lambda} + \mu^n \frac{(\lambda\chi - 1)\chi}{\lambda - \mu}, \quad (6.22)$$

where λ and μ can be substituted by arbitrary numbers or just left as formal parameters.

6.3.2 Three-strand braids

Step 1. A three-strand braid has the form $b_1^{a_1} b_2^{b_1} b_1^{a_2} b_2^{b_2} \dots$, where b_1 and b_2 are the braid group generators, while a_1, a_2, \dots and b_1, b_2, \dots are integer numbers, positive or negative. Not all braids with various a and b are inequivalent; many of them are isotopic, and hence must be equivalent as braid group elements. The corresponding formal expressions are brought to each other with help of the braid group relation

$$b_1 b_2 b_1 = b_2 b_1 b_2, \quad (6.23)$$

which is a particular case of (6.7) for $m = 3$. The smallest values of a and b correspond to unknots, there unlinked ones for the trivial braid $\mathbb{1}$ (all a and b equal zero), two unlinked ones (one once intertwined) for the braids $b_1^{\pm 1}$ and $b_2^{\pm 1}$, and one twice intertwined for the braids $b_1^{s_1} b_2^{s_2} \sim b_2^{s_2} b_1^{s_1}$, where s_1 and s_2 equal 1 or -1 independently of each other. The first non-trivial knot is obtained for $a_1 = a_2 = 1$, and $b_1 = b_2 = 1$; this is the trefoil knot with an additional contractible loop on a wire (fig.5). Setting all a and b equal one ($2n$ of them non-zero), one obtains a braid of the form $(b_1 b_2)^n$, whose close is a torus knot (for n not multiplies 3) or link (otherwise) out of the series named $T^{3,n}$, which starts form the twice intertwined unknot ($n = 1$), the trefoil knot with a contractible loop ($n = 2$), and the Borromean rings link ($n = 3$, $L6a4$ or 6_3^3 in [1]). The simplest so called twist knots are represented by three-stand braids, namely, the figure-eight, or two half-twist knot (4_1 in [1]) is the closure of the braid $b_1(b_2)^{-1}b_1(b_2)^{-1}$, and the next, three half-twist knot (5_2 in [1]) is the closure of the braid $b_1^3 b_2 b_1^{-1} b_2$. An infinitely many topologically different non-torus and non-twist knots are among the closures of three-strand braids, see [1].

Step 2. There are $3! = 6$ permutations of six elements, $\{xyz, xzy, yxz, yzx, zxy, zyx\}$. In analogy with the permutation group of two elements, two linear combinations are conserved up to a factor by all permutations,

$$X_S = xyz + yxz + xzy + yzx + zxy + zyx \equiv (xyz), \quad b_1 X = b_2 X = X, \quad (6.24)$$

and

$$X_A \equiv xyz - yxz - xzy + yzx + zxy - zyx \equiv [xyz]. \quad b_1 X = b_2 X = -X, \quad (6.25)$$

Hereafter, we use parentheses for a full symmetrization, i.e., for the sum over all permutations, and we use square brackets for a full antisymmetrization, i.e., for the sum over all even permutations minus the sum over all odd permutations.

The linear space spanned by the permutations of three elements has the dimension $3! = 6$, a generic vector being of the form⁴

$$X = xyz + a_1 yxz + a_2 xzy + a_{12} yzx + a_{21} zxy + a_{121} zyx. \quad (6.26)$$

The cases, (6.24) with $a = a_1$, $a_2 = a_{12}$, $a_{21} = a_{121}$, and (6.25) with $a = a_2$, $a_1 = a_{21}$, $a_{12} = a_{121}$, correspond to the two common eigenvectors of the group generators, and thus to the two one-dimensional eigenspaces of the permutation group. Apart from that, the generators have a common four-dimensional eigenspace (complementary to the subspace spanned by the two common eigenvectors), given by the system of constraints:

$$\begin{cases} a + a_1 + a_2 + a_{12} + a_{21} + a_{121} = 0, \\ a - a_1 - a_2 + a_{12} + a_{21} - a_{121} = 0 \end{cases} \Leftrightarrow \begin{cases} a + a_{12} + a_{21} = 0, \\ a_1 + a_2 + a_{121} = 0 \end{cases}, \quad (6.27)$$

i.e. coefficients of the permutations mutually related by a cyclic shift must sum up to zero. It is straightforward to verify that this property is covariant under the transpositions, both of the first two and of the last two elements. Hence, (6.27) indeed defines a subspace of (6.26) invariant under the action of the permutation group.

The four-dimensional space given by (6.27) is by definition a representation of the permutation group, but not an irreducible one. It turns out to decompose into two two-dimensional irreducible representations. More precisely, it includes the two-dimensional subspace

$$\begin{aligned} X_{AS} = a(xyz)z + b(yzx)x + c(zxy)y &\equiv axyz + ayxz + byzx + bzyx + czxy + cxzy, \\ a + b + c &= 0. \end{aligned} \quad (6.28)$$

each vector of which generates a two-dimensional irreducible representation of the permutation group. Indeed, X_{AS} is, by construction, an eigenvector of the first generator:

$$b_1 X_{AS} = X_{AS}; \quad (6.29)$$

in addition, it satisfies the identity

$$X_{AS} + b_2 X_{AS} + b_1 b_2 X_{AS} = (a + b + c)(xyz) = 0. \quad (6.30)$$

To verify it, let us notice, that (6.30) contains $3 \cdot 6 = 18$ summands and includes each of 6 monomials exactly 3 times, with different coefficients, as they arise from different brackets in (6.28), e.g.,

$$\begin{aligned} (a + b + c)xyz &= (axyz + b_2 cxzy + b_1 b_2 byzx), \\ (a + b + c)yxz &= (ayxz + b_2 byzx + b_1 b_2 cxzy), \end{aligned} \quad (6.31)$$

and similarly for the other monomials. Relations (6.29) and (6.30) guarantee that the representation in question is two-dimensional, since any X_{AS} from subspace (6.28) and the corresponding $b_2 X_{AS}$ are turned by the group generators into linear combinations of each other,

	X	$b_2 X$
b_1	X	$-X - b_2 X$
b_2	$b_2 X$	X

(6.32)

⁴subscripts of the coefficients reflect the sequence of permutations that yields a given element, i.e., a_{121} is the coefficient of $zyx = b_1 b_2 b_1 xyz$.

In fact, it is not necessary to start exactly from (6.28) to construct a two-dimensional irreducible representation of the permutation group. Subspace (6.27) is a direct sum of two two-dimensional subspaces of the first generators eigenvectors, with the eigenvalues 1 and -1 , respectively. On the other hand, same subspace (6.27) is a similar direct sum w.r.t. the second generator. A plane containing simultaneously two first generators eigenvectors and two second generators eigenvectors (the ones with distinct eigenvalues, otherwise there would be more common eigenvectors, while their is non) is a two-dimensional common eigenspace of the generators. One has to parameterize all these planes in one or another way. In the what follows, we checked and used, that each first generators eigenvector with the eigenvalue 1 from subspace (6.27) generates, together with its image under the second generator, a two-dimensional common eigenspace of the generators; hence, these eigenspaces are in one to one correspondence with the first generators eigenvectors. One can use the first generators eigenvectors with the eigenvalue -1 equally well. The latter ones also lie in subspace (6.27) and have the form

$$X_{SA} = a[xy]z + b[yz]x + c[zx]y \equiv axyz - ayxz + byzx - bzyx + czxy - cxy, \quad a + b + c = 0, \quad (6.33)$$

and satisfy the identities, similar to (6.29,6.30):

$$b_1 X_{SA} = -X_{SA}, \quad (6.34)$$

and

$$X_{SA} - b_2 X_{SA} + b_1 b_2 X_{SA} = (a + b + c)(xyz) = 0, \quad (6.35)$$

the last one being verified with help of the equalities

$$\begin{aligned} (a + b + c)xyz &= (axyz - b_2(-cxy) + b_1 b_2 byzx), \\ -(a + b + c)yxz &= (-ayxz - b_2 byzx - b_1 b_2 cxy), \end{aligned} \quad (6.36)$$

etc. One could also start from eigenvectors of the second generator instead. Of course, in all cases one will obtain the same set of two-dimensional planes, just differently parameterized. Each of these planes is a common eigenspace of the two permutation group generators, thus being an invariant subspace (in other words, a space of a representation) of the entire permutation group. The group generators acting on such a subspace can be presented as 2×2 matrices. In particular, if one selects a basis as $\{X_{AS}, b_2 X_{AS}\}$, for any X_{AS} from (6.27), the matrices are read from table (6.32),

$$b_1 = \begin{pmatrix} 1 & -1 \\ 0 & -1 \end{pmatrix}, \quad b_2 = \begin{pmatrix} 0 & 1 \\ 1 & 0 \end{pmatrix}, \quad X \equiv \begin{pmatrix} 1 \\ 0 \end{pmatrix}, \quad b_2 X \equiv \begin{pmatrix} 0 \\ 1 \end{pmatrix} \quad (6.37)$$

For practical purposes, a basis of eigenvectors of b_1 (or b_2) is more convenient:

$$b_1 = \begin{pmatrix} 1 & 0 \\ 0 & -1 \end{pmatrix}, \quad b_2 = \begin{pmatrix} -\frac{1}{2} & \frac{\sqrt{3}}{2} \\ \frac{\sqrt{3}}{2} & \frac{1}{2} \end{pmatrix}, \quad X \equiv \begin{pmatrix} 1 \\ 0 \end{pmatrix}, \quad \frac{1}{\sqrt{3}}(X + 2b_2 X) \equiv \begin{pmatrix} 0 \\ 1 \end{pmatrix}. \quad (6.38)$$

where the normalization factor in front of the second eigenvector is chosen so that the matrix of b_2 is permutation. Independence of these matrices of a , b , and c , entering expression (6.28) for X , means that all the representations with various a , b , and c are isomorphic.

In explicit calculations, it is convenient to take a certain X_{AS} from (6.28), the conventional choice is

$$\begin{aligned} a = -b = 1 \text{ in (6.28)} &\Rightarrow X = (xy)z - (zx)y, \quad X + 2b_2 X = 2[yz]x - [xy]z - [zx]y, \quad (6.39) \\ a = b = 1, \quad c = -2 \text{ in (6.28)} &\Rightarrow X = (xy)z + (zx)y - 2(yz)x, \quad X + 2b_2 X = 3[xy]z - 3[zx]y. \end{aligned}$$

Finally, we have constructed three distinct representations of the permutation group with three elements, two one-dimensional ones, (6.24), (6.25), and a two-dimensional one, generated by any vector of form (6.28). In fact, there is an entire two-dimensional space of such a vectors, given by (6.28). Each of these vectors generates a two-dimensional representation, altogether filling a four-dimensional space, and, together with the two one-dimensional representations, covering the entire six-dimensional space spanned by the $3! = 6$ permutations of six elements.

Step 3. We have obtained three distinct irreducible representations of the permutation group with three elements, one-dimensional ones (6.24) and (6.25), and a two-dimensional one (6.28); a known theorem claims that there no other ones [42]. The ansatz of **Step 6.3** dictates then to take three pairs of matrices, h_i^{SS} and h_i^{AA} of the size 1×1 , and h_i^{AS} of the size 2×2 , with $i = 1, 2$. The next step is to determine the explicit form of the matrices from the braid group relations.

Step 4. Matrices h_1 and h_2 must satisfy group relations (6.23). For the one-dimensional representations, it gives merely

$$h_1^{SS} = h_2^{SS} = \alpha, \quad h_1^{AA} = h_2^{AA} = \delta, \quad (6.40)$$

while for the two dimensional representation a non-trivial equations is obtained,

$$h_1^{SA} h_2^{SA} h_1^{SA} = h_2^{SA} h_1^{SA} h_2^{SA},$$

$$\begin{pmatrix} \beta & 0 \\ 0 & \gamma \end{pmatrix} \begin{pmatrix} a & b \\ c & d \end{pmatrix} \begin{pmatrix} \beta & 0 \\ 0 & \gamma \end{pmatrix} = \begin{pmatrix} a & b \\ c & d \end{pmatrix} \begin{pmatrix} \beta & 0 \\ 0 & \gamma \end{pmatrix} \begin{pmatrix} a & b \\ c & d \end{pmatrix}, \quad (6.41)$$

Step 5. Equality (6.41) is satisfied if $h_2 = h_1$. Apart from that, there is the non-trivial solution for h_2 :

$$a = \frac{\gamma^2}{\gamma - \beta}, \quad bc = \frac{\beta\gamma(\beta\gamma - \beta^2 - \gamma^2)}{(\beta - \gamma)^2}, \quad d = \frac{\beta^2}{\beta - \gamma}. \quad (6.42)$$

Since (6.42) gives the value only of the product bc , there remains an arbitrariness, which, however, will not affect on the invariants, where only the traces of matrix products enter. Indeed, the matrices h_1^{SA} and h_2^{SA} satisfy group relation (6.23) and the eigenvalue equation

$$(h_1^{SA} - \beta)(h_1^{SA} - \gamma) = 0, \quad (h_2^{SA} - \beta)(h_2^{SA} - \gamma) = 0. \quad (6.43)$$

As already said, the matrices lie in a representation of the Hecke algebra, whose dimension is the same to that of the corresponding permutation group [52], i.e., equals $(2 + 1)! = 6$ for the case. Hence, a product of the matrices, each one equals h_1^{SA} or h_2^{SA} or is inverse to one of them, reduces, with help of eigenvalue equation (6.43) and relation (6.23), to a linear combination of 6 basis elements, which can be chosen, e.g., as

$$\text{Id}, \quad h_1, \quad h_2, \quad h_1 h_2, \quad h_2 h_1, \quad h_2 h_1 h_2. \quad (6.44)$$

This is easy to verify in each particular case, e.g. (the omitted superscript SA is assumed),

$$\begin{aligned} \underbrace{h_2 h_1 h_2}_{=h_1 h_2 h_1} h_1^{-1} \underbrace{h_2 h_1 h_2}_{=h_1 h_2 h_1} &= h_1 \underbrace{h_2 h_1 h_2}_{h_1 h_2 h_1} h_1 = h_1^2 h_2 h_1^2 = ((\beta + \gamma)h_1 - \beta\gamma)h_2((\beta + \gamma)h_1 - \beta\gamma) = \\ &= \beta^2 \gamma^2 h_2 - (\beta + \gamma)\beta\gamma(h_1 h_2 + h_2 h_1) + (\beta + \gamma)^2 h_1 h_2 h_1. \end{aligned}$$

A trace of a braid group element, which enters the knot invariant definitions, therefore, expands over the basis traces as well; the latter ones are independent of b ,

$$\text{Tr } \mathbb{1} = 2, \quad \text{Tr } h_1 = \text{Tr } h_2 = \beta + \gamma, \quad \text{Tr } h_1 h_2 = \text{Tr } h_2 h_1 = a\beta + d\gamma, \quad \text{Tr } h_1 h_2 h_1 = a\beta^2 + d\gamma^2,$$

and, hence, so does the knot invariant. When discussing the matrices themselves, we will fix this arbitrariness so that the matrices turn permutation; the result then is

$$\begin{aligned} h_1^{SA} &= \begin{pmatrix} \beta & 0 \\ 0 & \gamma \end{pmatrix}, \quad (h_1^{SA})^{-1} = \begin{pmatrix} \beta^{-1} & 0 \\ 0 & \gamma^{-1} \end{pmatrix} \\ h_2^{SA} &= \begin{pmatrix} \frac{\gamma^2}{\gamma-\beta} & \frac{\sqrt{\beta\gamma(\beta\gamma-\beta^2-\gamma^2)}}{\beta-\gamma} \\ \frac{\sqrt{\beta\gamma(\beta\gamma-\beta^2-\gamma^2)}}{\beta-\gamma} & \frac{\beta^2}{\gamma-\beta} \end{pmatrix}, \\ (h_2^{SA})^{-1} &= \begin{pmatrix} \frac{\beta}{\gamma(\gamma-\beta)} & \frac{1}{\beta-\gamma} \sqrt{\frac{(\beta\gamma-\beta^2-\gamma^2)}{\beta\gamma}} \\ \frac{1}{\beta-\gamma} \sqrt{\frac{(\beta\gamma-\beta^2-\gamma^2)}{\beta\gamma}} & \frac{\gamma}{\beta(\gamma-\beta)} \end{pmatrix}. \end{aligned} \quad (6.45)$$

Step 6. Following the ansatz of **Step 6.2**, we write the invariant of a three-strand braid in the form

$$h^I \left(b_1^{a_1} b_2^{b_1} \dots b_1^{a_k} b_2^{b_k} \right) = \prod_{i=1}^k (h_1^I)^{a_i} (h_2^I)^{b_i}, \quad I = SS, AS, AA. \quad (6.46)$$

Step 7. At this step, we have obtained an invariant of a braid group conjugation class. The ansatz of **Step 6.7** dictates then to search for invariant of a knot presented as the closure of a three-strand braid $b_1^{a_1} b_2^{b_1} \dots b_1^{a_k} b_2^{b_k}$ in the form

$$\sum_{I=S,A,SA} \chi_I \text{Tr} \prod_k (h_1^I)^{a_k} (h_2^I)^{b_k} = \chi_{SS} \alpha^n + \chi_{SA} \text{Tr} \left\{ (h_1^{SA})^{a_1} (h_2^{SA})^{b_1} \dots \right\} + \chi_{AA} \delta^n, \quad (6.47)$$

and we proceed with determining the there standing weight coefficients from matching the invariant values for braids with different numbers of strands representing same knots. For three-strand braids, this step is even less trivial compared to that for two-stand braid, so we split it into two substeps.

Step 7-a: co-product for operators and weight coefficients. This step is based on the multiplication property (see sec.6.1.3), which implies that

$$\left(b_1^{(3)} \right)^n \sim \left(b_1^{(2)} \right)^n \otimes \mathbb{1}^{(1)} \Rightarrow \lambda^n \chi_{S\chi} + \mu^n \chi_{A\chi} = \alpha^n \chi_{SS} + (\beta^n + \gamma^n) \chi_{SA} + \delta^n \chi_{AA} \quad (6.48)$$

for an arbitrary n . Relation (6.48) can be considered as a system of infinitely many homogeneous linear equations. The only solution is

$$\chi_{S\chi} = \chi_{A\chi} = \chi_{SS} = \chi_{SA} = \chi_{AA} = 0, \quad (6.49)$$

unless the equations are linearly dependent. A principle minor occupying in the lines with $n = 0, \dots, 5$ is a Vandermonde determinant,

$$\det \begin{vmatrix} 1 & 1 & 1 & 1 & 1 & 1 \\ \lambda & \mu & \alpha & \beta & \gamma & \delta \\ \lambda^2 & \mu^2 & \alpha^2 & \beta^2 & \gamma^2 & \delta^2 \\ \lambda^3 & \mu^3 & \alpha^3 & \beta^3 & \gamma^3 & \delta^3 \\ \lambda^4 & \mu^4 & \alpha^4 & \beta^4 & \gamma^4 & \delta^4 \\ \lambda^5 & \mu^5 & \alpha^5 & \beta^5 & \gamma^5 & \delta^5 \end{vmatrix} = (\alpha - \beta)(\alpha - \gamma)(\alpha - \delta)(\beta - \gamma)(\beta - \delta)(\gamma - \delta) \cdot (\lambda - \alpha)(\lambda - \beta)(\lambda - \gamma)(\lambda - \delta) \cdot (\mu - \alpha)(\mu - \beta)(\mu - \gamma)(\mu - \delta); \quad (6.50)$$

any other one differs just by a factor of type $\lambda^{m_1} \mu^{m_2} \alpha^{m_3} \beta^{m_4} \gamma^{m_5} \delta^{m_6}$. Analysis of smaller sized minors shows, that rank of the matrix in the l.h.s. of (6.50), which is the number of linearly independent solutions of (6.48), is equal to the number of distinct eigenvalues among $\lambda, \mu, \alpha, \beta, \gamma, \delta$, the coefficient before each one becoming one of the relations generating the space of solutions of (6.48).

There is a distinguished solution, which has a profound group theory sense:

$$\begin{aligned} \lambda &= \alpha = \beta, \quad \mu = \gamma = \delta \\ \chi\chi_S &= \chi_{SS} + \chi_{SA}, \quad \chi\chi_A = \chi_{SA} + \chi_{AA}. \end{aligned} \quad (6.51)$$

Relations (6.51) are produced by a coproduct structure on the braid group [79].

Note, that (6.48) is satisfied as long as (6.51) does; in particular, the coefficients are thus far completely independent of eigenvalues. The last step consists in relating them two.

Step 7-b. It remaining step relies on transformation (6.15-II). As already mentioned, it is the corresponding constraint on the coefficients and eigenvalues that turn a braid invariant to a knot invariant. There is an infinite set on constraints of the form

$$\left(b_1^{(3)}\right)^{n-1} b_2^{(3)} \sim \left(b_1^{(2)}\right)^{n-1} \Rightarrow \lambda^{n-1} \chi_S + \mu^{n-1} \chi_A = \lambda^n \chi_{SS} + \frac{\lambda^{n+1} - \mu^{n+1}}{\lambda - \mu} \chi_{SA} + \mu^n \chi_{AA}, \quad (6.52)$$

for all integer n . Any three of these equations are linearly dependent since

$$\lambda \begin{vmatrix} \lambda^n \\ \lambda^m \\ \lambda^k \end{vmatrix} - \mu \begin{vmatrix} \mu^n \\ \mu^m \\ \mu^k \end{vmatrix} = \begin{vmatrix} \lambda^{n+1} - \mu^{n+1} \\ \lambda^{m+1} - \mu^{m+1} \\ \lambda^{k+1} - \mu^{k+1} \end{vmatrix}. \quad (6.53)$$

Hence, one can determine all three three-strand coefficients, selecting any two of constrains (6.52), e.g. with $n = 1, 2$ and completing them by any one of (6.51), e.g. with $n = 0$:

$$\begin{aligned} \mathbf{1}^{(3)} &\sim \mathbf{1}^{(2)} \otimes \mathbf{1}^{(1)} \Rightarrow \chi\chi_S + \chi\chi_A = \chi_{SS} + 2\chi_{SA} + \chi_{AA}, \\ b_2^{(3)} &\sim \mathbf{1}^{(2)} \Rightarrow \chi_S + \chi_A = \lambda\chi_{SS} + (\lambda + \mu)\chi_{SA} + \mu\chi_{AA}, \\ b_1^{(3)} b_2^{(3)} &\sim h_1^{(2)} \Rightarrow \lambda\chi_S + \mu\chi_A = \lambda^2\chi_{SS} + \lambda\mu\chi_{SA} + \mu^2\chi_{AA}, \end{aligned} \quad (6.54)$$

wherefrom, taking into account (6.21), one gets

$$\chi_{SS} = \frac{\chi(\mu\chi - 1)(\lambda^2\chi + \mu - \lambda)}{(\mu - \lambda)\lambda\mu}, \quad \chi_{AA} = \frac{\chi(\lambda\chi - 1)(\mu^2\chi + \lambda - \mu)}{(\lambda - \mu)\lambda\mu}, \quad (6.55)$$

and

$$\chi_{SA} = \frac{\chi(\mu\chi - 1)(\lambda\chi - 1)}{\lambda\mu}.$$

It can be checked that selecting any other three linearly independent constrains from of (6.52) and (6.51) provides the same answer.

The result. Finally, the invariant of the knot presented as the closure of a three-strand braid is expressed via the two-strand eigenvalues as

$$\begin{aligned} H \left(b_1^{a_1} b_2^{b_1} \dots b_1^{a_k} b_2^{b_k} \right) &= \lambda^n \frac{\chi(\mu\chi - 1)(\lambda^2\chi + \mu - \lambda)}{(\mu - \lambda)\lambda\mu} + \mu^n \frac{\chi(\lambda\chi - 1)(\mu^2\chi + \lambda - \mu)}{(\lambda - \mu)\lambda\mu} + \\ &+ \text{Tr} \prod_k (h_1^{SA})^{a_k} (h_2^{SA})^{b_k} \frac{\chi(\mu\chi - 1)(\lambda\chi - 1)}{\lambda\mu}, \end{aligned} \quad (6.56)$$

where h_1^{SA} and h_2^{SA} , as well as the inverse matrices, are given by (6.45) with $\beta = \lambda$ and $\gamma = \mu$. Let us emphasize, that λ and μ enter (6.56) just as formal variables; substituting for them *arbitrary* numbers, or, equivalently, taking the coefficient of their *any* powers provides a numeric knot invariant.

6.3.3 Four-strand braids

Step 1. A four-strand braid has the form

$$\mathfrak{h}^{(4)} = b_1^{a_1} \sigma_2^{b_1} \sigma_3^{c_1} b_1^{a_1} \sigma_2^{b_1} \sigma_3^{c_1} \dots b_k^{a_1} \sigma_k^{b_1} \sigma_k^{c_1}. \quad (6.57)$$

The particular case of $h^{(4)} = (b_1 b_2 b_3)^k$ corresponds to the torus knots (even k) and links (odd k) of the so named series $T^{4,k}$. The four and five half-twist knots (6_1 and 7_2 in [1], respectively), as well as all knots with no more than 7 crossings can be presented as the closures of four-strand braids [1].

Step 2. As usual, we begin from listing the irreducible representations of the permutation group, this time acting on four elements. Similarly to the previous cases, there are two one-dimensional representations, fully permutation one,

$$X_{SSS} = (xyzt), \quad b_1 X_{SSS} = b_2 X_{SSS} = b_3 X_{SSS} = X_{SSS}, \quad (6.58)$$

where all the permutations of $xyzt$ enter with the same coefficient, and fully antisymmetric one,

$$X_{AAA} = [xyzt], \quad b_1 X_{AAA} = b_2 X_{AAA} = b_3 X_{AAA} = -X_{AAA}, \quad (6.59)$$

where coefficients of all the permutations are equal up to a sign, being plus for even permutations, and minus for odd permutations (we recall that in all formulas parentheses and the square brackets stand for stand, correspondingly, for the fully symmetric and antisymmetric combinations constructed from the embarked elements). Apart from the one-dimensional representations, the permutation group with four elements has several more complicated ones. These representations are constructed even less trivial than a two dimensional representation of the permutation group with three elements. For this reason, we sketch briefly the common representation theory approach to the problem, before listing the representations in question explicitly.

An important here theorem states that the irreducible representations of a permutation group with k elements are in one-to one correspondence with the partitions of k

$$k = k_1 + k_2 + \dots + k_m, \quad k_1 \geq k_2 \geq \dots \geq k_m, \quad k_1, k_2, \dots, k_m \in \mathbb{N} \quad (6.60)$$

Moreover, an irreducible representation corresponding to a given partition of k is constructed within the approach explicitly, as a formal linear combination of permutations. We start from revising the cases of two and three elements on this language. A partition of k defined as (6.60) we denote by $[k_1 k_2 \dots k_m]$.

There two partitions of 2, 2 and 1 + 1 (we write [2] and [11] for them). They correspond to two irreducible representations (6.16) of the permutation group with two elements, where the elements are distributed over the round brackets as 2, $X_S \equiv X_2 = (xy)$, and as 1 + 1, $X_A \equiv X_{11} = a(x)(y) + b(y)(x) = axy + byx$ with $a + b = 0$. Similarly, three elements are distributed over the three round brackets in there irreducible representations (6.24,6.28,6.25) of the permutation group according to one of three partitions of 3, $X_S \equiv X_3$, $X_{SA} \equiv X_{21}$, $X_A \equiv X_{111}$.

In turn, all the irreducible representations of the permutation group with four elements the are enumerated by partitions of 4 [42, 64]. The representation corresponding to a partition $[k_1 \geq k_2 \geq k_3 \geq k_4]$ ($k_1 + k_2 + k_3 + k_4 = 4$) is constructed in the two following steps. First, one writes $xyzt$, putting the parentheses around the first k_1 , next k_2 , next k_3 , and last k_4 elements; the parentheses (symmetrization sign) are separated by a group product, e.g.,

$$(xy)(zt) \equiv (xy + yx)(zt + tz) = xyzt + yxzt + xytz + yxtz. \quad (6.61)$$

Then, one lists all permutations of $xyzt$ that remained inequivalent provided the parentheses standing as described. These permutations are assembled then to a linear combination, with the coefficient satisfying a certain system of linear equations. We do not describe here neither a general form of

this system, nor rules for constructing it, restricting ourselves by listing it explicitly in the particular cases. Roughly speaking, a linear combination associated with a given partition is to be, first, an eigenspace of the entire permutation group, second, linearly independent of the linear combinations for the previous partitions (in the inverse lexicographic order). Such a system is in the most cases excessively defined, and we also verify, for the cases considered, that each solution of this system gives rise to an irreducible representation of the permutation group. However, it can be shown, that all the representations corresponding to a given partition are isomorphic [42]. One can equivalently start from putting the square brackets (antisymmetrization sign) in accordance with each partition, and then impose some other (constructed in a similar manner as for expressions with the parentheses) systems of linear equations on the coefficients of the corresponding linear combinations. The representation with parentheses for a certain partition will be then isomorphic to the representation with the square brackets for the dual partition (in the case [4] is dual to [1111], [31] is dual to [211], and [22] is dual to itself). We use the easiest way of these two in each case, in one case demonstrating their equivalence.

The simplest representations correspond to the partitions [4] and [1111]; they are already listed fully symmetric and antisymmetric representations correspondingly, $X_4 \equiv X_{SSS}$ and $X_{[1111]} \equiv X_{AAA}$. Next comes the partition [31]. The corresponding irreducible representation of the permutation group with four elements is a straightforward analog of [21]-type representation of the permutation group with three elements:

$$X_{31} = a(xyz)t + b(yzt)x + c(ztx)y + d(txy)z, \quad a + b + c + d = 0 \quad (6.62)$$

The general form of the linear combination is dictated by the ansatz for a [31]-type representation, while the constraint on the coefficients arises as a condition of linear independence of X_{31} and X_4 (which is obtained for $a = b = c = d$), being formulated in a permutation (i.e., invariant under entire permutation group) form. The constructed linear combination is fully permutation under the permutations of the first three elements, i.e.,

$$b_1 X_{31} = b_2 X_{31} = X_{31}, \quad (6.63)$$

and also satisfies the identity

$$(\mathbb{1} + b_3 + b_2 b_3 + b_1 b_2 b_3) X_{31} = (a + b + c + d)(xyz)t = 0. \quad (6.64)$$

Identity (6.64) is similar to identity (6.30) for 21-type representation of a permutation group. Each permutation of xyz appears in the resulting expression for the four times, picked up from one of the four summands in (6.62) by one of the four group elements entering (6.64), e.g.,

$$axyzt + db_3 xyzt + cb_2 b_3 xzty + bb_1 b_2 b_3 ztyx = (a + b + c + d)xyz, \quad (6.65)$$

and similarly for other monomials. The constructed representation turns out to be three-dimensional, with a basis can be chosen as $\{X, b_3 X, b_2 b_3 X\}$. To verify that, it suffices to check that the action of the permutation group generators on the basis elements expands, in account for (6.63,6.64), over the same basis; the corresponding expressions are summarized in the table:

		X	$b_3 X$	$b_2 b_3 X$	
b_1	X	$b_3 X$	$-X - b_3 X - b_2 b_3 X$		
b_2	X	$b_2 b_3 X$	$b_3 X$		
b_3	$b_3 X$	X	$b_2 b_3 b_2 X = b_2 b_3 X$		

(6.66)

Note that *any* linear combination of type (6.62), there is a three-dimensional space of them, gives rise to a three-dimensional representation of the permutation group; all these representations are isomorphic, since the action of the group generators on the basis vectors is given in all cases by the same table (6.66). According the above mentioned rule, the representation for the transposed partition,

which is for the case is [211], is obtained by substituting all parentheses with the square brackets, and demanding (in a permutation manner) that all the obtained expression is linearly independent of X_{1111} (which corresponds to $a = -b = c = -d = 1$).

$$X_{211} = a[xyz]t + b[yzt]x + c[ztx]y + d[txy]z, \quad a - b + c - d = 0 \quad (6.67)$$

Similarly to X_{31} , their are the identities valid for this representation

$$\begin{aligned} b_1 X_{211} &= b_2 X_{211} = -X_{211}, \\ (\mathbb{1} - b_3 + b_2 b_3 - b_1 b_2 b_3) X_{211} &= (a + b + c + d)(xyzt) = 0, \end{aligned} \quad (6.68)$$

the latter one being verified for each permutation, e.g., for $xyzt$, as

$$(a + b + c + d)xyzt = axyzt - b_3(-dxytz) + b_2 b_3 cxzty - b_1 b_2 b_3(-byztx). \quad (6.69)$$

As a result, a [211]-type representation of the permutation group is of the same dimension three, as a [31]-type one. Basisses can be chosen similarly in both cases; in case of [211], the group generators act on the basis vectors as:

	X	$b_3 X$	$b_2 b_3 X$	
b_1	$-X$	$b_3 X$	$-X + b_3 X - b_2 b_3 X$	
b_2	$-X$	$b_2 b_3 X$	$b_3 X$	
b_3	$b_3 X$	X	$b_2 b_3 b_2 X = -b_2 b_3 X$	

(6.70)

The above table confirm that the presented X_{211} indeed gives rise to a three-dimensional representation of the permutation group. Again, (6.67) sets an entire three-dimensional set of isomorphic [211]-type representations, each one can be alternatively defined via action (6.70) of the group generators on the basic elements.

One more partition remains, namely [22]. The corresponding irreducible representation of the permutation group has a slightly more involved structure, than the above listed ones. A general linear combination fitting the [22]-type ansatz includes six summands:

$$X_{22} = a_1(xy)(zt) + a_2(zt)(xy) + a_3(xzr)(yt) + a_4(yt)(xz) + a_5(yz)(xt) + a_6(xt)(yz). \quad (6.71)$$

The very ansatz implies that

$$X_{22} = b_1 X_{22} = b_3 X_{22}. \quad (6.72)$$

A linear space spanned by all permutations of 4 elements has the dimension $4! = 24$. We have already established, that there are two one-dimensional representations ([4]- and [1111]-type ones), and two tree-dimensional spaces of three-dimensional representations ([31]- and [211]-type ones). According the mentioned theorem [42], each vector of the remained subspace belongs to in a [22]-type representation. Hence, the dimension of this subspace, which is $4! - 2 \cdot 1 \cdot 1 - 2 \cdot 3 \cdot 3 = 4$, equals the dimension [22]-type representation multiplied by its multiplicity, i.e., by the number of linearly independent (6.71)-type expressions allowed by the corresponding constraints. Actually, the representation in question has the dimension two and the multiplicity two, as we demonstrate in the below. Four constraints on six coefficients are imposed in accordance with that. These constraints can be presented in one of two equivalent forms:

$$\left\{ \begin{array}{l} a_1 + a_2 + a_6 = 0, \\ a_1 + a_3 + a_5 = 0, \\ a_2 + a_3 + a_4 = 0, \\ a_4 + a_5 + a_6 = 0 \end{array} \right. \Leftrightarrow \left\{ \begin{array}{l} a_3 + a_4 + a_5 = 0, \\ a_2 + a_4 + a_6 = 0, \\ a_1 + a_5 + a_6 = 0, \\ a_1 + a_2 + a_3 = 0 \end{array} \right. \quad (6.73)$$

The second equations are obtained from the first ones by a termwise subtraction from the equality

$$a_1 + a_2 + a_3 + a_4 + a_5 + a_6 = 0, \quad (6.74)$$

which, in turn, arises as a termwise sum (being canceled by 2) of all the equations, either the first ones, or the second ones. Each of the first equations collects the coefficients of terms in (6.71) that have in the second parentheses x , y , z , or t in the second parenthesis. The second equations are organized in a similar manner w.r.t. to the first parenthesis. Such combinations of the coefficients arise in the expressions of the form

$$\begin{aligned} a_1xyzt + a_2b_2xzyt + a_6b_1b_2yzxt &= (a_1 + a_2 + a_6)xyzt, \\ a_1xyzt + a_2b_2xzyt + a_3b_3b_2xtyz &= (a_1 + a_2 + a_3)xyzt, \end{aligned} \quad (6.75)$$

and in the similar ones for other permutations. Hence, a combination of form (6.71) constrained by (6.73) satisfies, in addition to (6.72), the identities

$$\begin{aligned} (\mathbb{1} + b_2 + b_1b_2)X_{22} &= \\ (a_1 + a_2 + a_6)(xyz)t + (a_1 + a_3 + a_5)(txy)z + (a_2 + a_3 + a_4)(ztx)y + (a_4 + a_5 + a_6)(yzt)x &= 0, \\ (\mathbb{1} + b_2 + b_3b_2)X_{22} &= \\ (a_3 + a_4 + a_5)t(xyz) + (a_2 + a_4 + a_6)z(txy) + (a_1 + a_5 + a_6)y(ztx) + (a_1 + a_2 + a_3)x(yzt) &= 0. \end{aligned} \quad (6.76)$$

Dimension of the examined representation equals two, what is checked by acting by the group generators on the basic elements, which can be chosen as $\{X, b_2X\}$:

	X	b_2X	
b_1	X	$-X - b_2X$	
b_2	b_2X	X	
b_3	X	$-X - b_2X$	

(6.77)

To summarize, we have constructed formal linear combinations of permutations of four elements, corresponding to two one-dimensional representations ([4]- and [1111]-type ones), two three-dimensional spaces of vectors, each one giving rise to a three-dimensional representation of the permutation group (a [31]- and [211]-type one, correspondingly), and a two dimensional space of vectors, each one giving rise to a two-dimensional representation of the permutation group (a [22]-type one). The described spaces do not intersect by construction and form altogether a linear space of the dimension $2 \cdot 1 \cdot 1 + 2 \cdot 3 \cdot 3 + 1 \cdot 2 \cdot 2 = 24 = 4!$. Hence, any linear combination of the $4!$ permutations of four elements is expanded over vectors from the spaces of the listed irreducible representations.

Step 3. We have constructed five distinct irreducible representations of the permutation group with four elements, one-dimensional ones (6.58) and (6.59), two-dimensional one (6.71), and three-dimensional ones (6.62) and (6.67). It is known that there are no other, inequivalent ones [42]. **Step 6.3** then tells one to take five triples matrices of the corresponding sizes. After the general scheme of constructing the irreducible representation was discussed, it is natural to label these matrices with the partitions. There are 1×1 matrices h_i^4 and h_i^{1111} , three-dimensional ones h_i^{31} and h_i^{211} , and two-dimensional ones h_i^{22} , with $i = 1, 2, 3$. We omit the superscripts unless the size of matrices is essential.

Step 4. The next step is to impose on the matrices the group relations, which for the case take the form

$$b_1b_2b_1 = b_2b_1b_2, \quad b_3b_2b_3 = b_2b_3b_2, \quad b_1b_3 = b_3b_1. \quad (6.78)$$

Step 5. One must then solve the constraints w.r.t. to the matrix elements, expressing them all via a necessary number of free parameters. Similarly to the three-strand case, ones of the matrices eigenvalues can be taken as such parameters. We approach to the problem at several steps.

Step 5-a: coinciding of eigenvalues from the II Artin constraint. One conclusion can be done for an arbitrary braid. Namely, the matrices h_i^Y , a partition Y given, a position i in a braid section vary, have the same eigenvalues. This follows from the II Artin constraint, which can be brought to the form

$$(h_i - \lambda)h_{i+1}h_i = h_{i+1}h_i(h_{i+1} - \lambda), \quad (6.79)$$

Taking the determinants from both sides, one obtains that the characteristic polynomials of the matrices coincide,

$$\det(h_i - \lambda) = \det(h_{i+1} - \lambda), \quad (6.80)$$

what is equivalent to the coincidence of all the eigenvalues up to a permutation; it is natural then to enumerate the basis vectors $e^{(k)}$ so that $\lambda_i^{(k)} = \lambda_{i+1}^{(k)}$.

Step 5-b: commuting of non-adjacent operators. Other steps in solving (6.78) are not so straightforward. The next in simplicity one concerns the third the constraints, which reflects the commutation of the non-adjacent crossings. For one-dimensional matrices the property is held trivially. The corresponding two-dimensional matrices must be both diagonal, their eigenvalues coincide, as already established,

$$h_1^{22} = \begin{pmatrix} \lambda_{22,1} & \\ & \lambda_{22,2} \end{pmatrix} \Rightarrow h_3^{22} = \begin{pmatrix} \lambda_{22,1} & \\ & \lambda_{22,2} \end{pmatrix}, \text{ or } h_3^{22} = \begin{pmatrix} \lambda_{22,1} & \\ & \lambda_{22,2} \end{pmatrix}. \quad (6.81)$$

The same might be true for the three-dimensional matrices. A case is more involved if two of three eigenvalues coincide; the corresponding matrices then commute provided that they have a block structure:

$$h_1^{31} = \begin{pmatrix} \lambda_{31,1} & & \\ & \lambda_{31,1} & \\ & & \lambda_{31,2} \end{pmatrix} \Rightarrow h_3^{31} = \begin{pmatrix} a & b & \\ b & c & \\ & & \lambda_{31,2} \end{pmatrix}, \quad (6.82)$$

and similarly for the other three-dimensional representations

$$h_1^{211} = \begin{pmatrix} \lambda_{211,1} & & \\ & \lambda_{211,1} & \\ & & \lambda_{211,2} \end{pmatrix} \Rightarrow h_3^{211} = \begin{pmatrix} \tilde{a} & \tilde{b} & \\ \tilde{b} & \tilde{c} & \\ & & \lambda_{211,2} \end{pmatrix}. \quad (6.83)$$

We examine this possibility in the next paragraph, postponing the question of whether this is the case until **Step 6.7**.

Step 5-b: form of blocks from the II Artin constraint. We return now to the first two of constraints (6.78), this time using them to express the non-diagonal matrix elements via the eigenvalues; for three-dimensional matrices we take ansätze (6.82, 6.83).

The first of equations (6.78) reduces to (6.41), both for the two-dimensional matrices, and for the two-by blocks in the three-dimensional matrices. The only difference is that β and γ are substituted by the corresponding eigenvalues. Since (6.41) has the only (modulo the above mentioned subtleties) solution, one just writes

$$h_2^{22} = h_2^{SA}(\beta = \lambda_{22,1}, \gamma = \lambda_{22,2}),$$

$$h_2^{31} = \begin{pmatrix} \lambda_{31,1} & & \\ & h_1^{SA}(\lambda_{31,1}, \lambda_{31,2}) & \\ & & \end{pmatrix}, \quad h_2^{211} = \begin{pmatrix} \lambda_{211,1} & & \\ & h_2^{SA}(\lambda_{211,1}, \lambda_{211,2}) & \\ & & \end{pmatrix}. \quad (6.84)$$

The second of equations (6.78) makes one to select the first possibility for h_3^{22} in (6.81). For each of the three-dimensional matrices, a separate non-trivial matrix equation is obtained. There are no non-trivial solutions for arbitrary 2×2 blocks entering h_2^{31} and h_2^{211} . For the two by two blocks as in (6.84), one obtains that the matrix elements in (6.82) and (6.83) are

$$a = \frac{\lambda_2^3}{\lambda_1^2 - \lambda_1\lambda_2 + \lambda_2^2}, \quad c = \frac{\lambda_1^3}{\lambda_1^2 - \lambda_1\lambda_2 + \lambda_2^2}, \quad b^2 = \frac{(\lambda_1 - \lambda_2)\sqrt{-\lambda_1\lambda_2(\lambda_1^2 + \lambda_2^2)}}{\lambda_1^2 - \lambda_1\lambda_2 + \lambda_2^2}, \quad (6.85)$$

where λ_1 and λ_2 should be substituted by the eigenvalues of the corresponding matrices.

Step 6. As **Step 6.2** prescribes, an invariant of a four-strand braid has the form

$$h^I \left(b_1^{a_1} \sigma_2^{b_1} \sigma_3^{c_1} \dots b_1^{a_k} \sigma_2^{b_k} \sigma_3^{c_k} \right) = \prod_{i=1}^k (h_1^I)^{a_i} (h_2^I)^{b_i} (h_3^I)^{c_i}. \quad (6.86)$$

Step 7. It remains to specify the coefficients in the linear combination

$$H \left(\mathfrak{B}^{(4)} \right) = \sum_{\substack{I=4,311,22 \\ 211,1111}} \chi_I \text{Tr} h^I \left(\mathfrak{B}^{(4)} \right) \quad (6.87)$$

that yields a knot invariant. Again, we split this step into two ones.

Step 7-a: co-product for operators and weight coefficients. If the last two strands of a four-strand braid enter no crossings, then the closure of the braid consists of pairwise unlinked two unknots and the knot or link that is the closure of the braid placed in the first two strands. Due to the multiplication property (see sec.6.1.3), the invariant of the former one must decompose into the product of the three latter ones. In the sense specified in sec.6.1.3, we write

$$\left(\sigma_1^{(4)} \right)^n \sim \left(\sigma_1^{(2)} \right)^n \otimes \mathbb{1}^{(1)} \otimes \mathbb{1}^{(1)}, \quad (6.88)$$

with the corresponding constraints on knot invariants being

$$\begin{aligned} & \lambda_4^n \chi_4 + (\lambda_{31,1}^n + \lambda_{31,2}^n + \lambda_{31,3}^n) \chi_{31} + (\lambda_{22,1}^n + \lambda_{22,2}^n) \chi_{22} + \\ & + (\lambda_{211,1}^n + \lambda_{211,2}^n + \lambda_{211,3}^n) \chi_{211} + \lambda_{1111}^n \chi_{1111} = \lambda^n \chi_2 \chi_1^2 + \mu^n \chi_{11} \chi_1^2. \end{aligned} \quad (6.89)$$

Similarly to that in the three-strand case, a homogenous linear system of constraints on $\chi_2 \chi_1^2$, $\chi_{11} \chi_1^2$, and $\chi_{Y,i} \equiv \chi_Y$ (with Y running over the partitions of 4, and i running from 1 to the number of corresponding eigenvalues) was obtained. It is straightforward to verify that a principle minor of this system is proportional to the Wandermund determinant composed of the eigenvalues. Hence, non-trivial solution for characters are their for some of the eigenvalues coincide. In particular, the system is satisfied if

$$\begin{aligned} \chi_2 \chi_1^2 &= (\chi_3 + \chi_{21}) \chi_1 = \chi_4 + 2\chi_{31} + \chi_{22} + \chi_{211}, \\ \chi_{11} \chi_1^2 &= (\chi_{21} + \chi_{111}) \chi_1 = \chi_{31} + \chi_{22} + 2\chi_{211} + \chi_{1111}. \end{aligned} \quad (6.90)$$

and

$$\begin{aligned} \lambda_4 &= \lambda, \quad \lambda_{31,1} = \lambda_{31,2} = \lambda, \lambda_{31,3} = \mu, \quad \lambda_{22,1} = \lambda, \quad \lambda_{22,2} = \mu, \\ & \lambda_{211,1} = \lambda, \quad \lambda_{211,2} = \lambda_{211,3} = \mu, \lambda_{1111} = \mu. \end{aligned} \quad (6.91)$$

This is the solution, which enters in the definition of the knot invariant of the interest. The case is that rules (6.90) and (6.91) reflect a co-algebra structure on the braid group, similarly to (6.51) in case of three-strand braids. Although any other solution might give rise to a knot invariant, only the named one is systematically studied. The reason is, probably, in that the additional structure enables to re-define the knot invariant in an explicit and concise manner [90, 79, 71], not just as a solution of infinitely many equations. We will partially approve the made choice in sec.7.6, by arriving at the same answer by at the first glance completely different method.

Step 7-b: weight coefficients via eigenvalues. It remains to express the weight coefficients via eigenvalues. Just as in the previous cases, some of the necessary relations follow from the second of the equivalence transformations, specific for braid closures, (6.15-I,II). To determine the five characters, one needs overall five independent equations, e.g.,

$$\begin{aligned} \mathbb{1}^{(4)} \sim \mathbb{1}^{(3)} \otimes \mathbb{1} &\Rightarrow \chi_4 + \chi_{31} + \chi_{22} + \chi_{211} + \chi_{1111} = \\ &= \chi_1 \chi_3 + \chi_1 \chi_{21} + \chi_1 \chi_{111}, \end{aligned} \quad (6.92)$$

$$\begin{aligned} h_3^{(4)} \sim \mathbb{1}^{(3)} &\Rightarrow \lambda \chi_4 + (2\lambda + \mu) \chi_{31} + (\lambda + \mu) \chi_{22} + (\lambda + 2\mu) \chi_{211} + \mu \chi_{1111} = \\ &= \lambda \chi_3 + (\lambda + \mu) \chi_{21} + \mu \chi_{111}, \end{aligned} \quad (6.93)$$

$$\begin{aligned} h_2^{(4)} h_3^{(4)} \sim h_2^{(3)} &\Rightarrow \lambda^2 \chi_4 + (\lambda^2 + \lambda \mu) \chi_{31} + \lambda \mu \chi_{22} + (\lambda \mu + \mu^2) \chi_{211} + \mu^2 \chi_{1111} = \\ &= \lambda^2 \chi_3 + \lambda \mu \chi_{21} + \mu^2 \chi_{111}, \end{aligned} \quad (6.94)$$

$$\begin{aligned} h_1^{(4)} h_2^{(4)} h_3^{(4)} \sim h_1^{(3)} h_2^{(3)} &\Rightarrow \lambda^3 \chi_4 + \mu \lambda^2 \chi_{31} + \mu^2 \lambda \chi_{211} + \mu^3 \chi_{1111} = \\ &= \lambda^2 \chi_3 + \lambda \mu \chi_{21} + \mu^2 \chi_{111}, \end{aligned} \quad (6.95)$$

$$\begin{aligned} h_1^{(4)} h_2^{(4)} h_1^{(4)} h_2^{(4)} h_1^{(4)} h_2^{(4)} h_3^{(4)} \sim h_1^{(3)} h_2^{(3)} h_2^{(3)} h_1^{(3)} h_2^{(3)} &\Rightarrow \\ \lambda^7 \chi_4 - \lambda^4 \mu^3 \chi_{31} - \lambda^3 \mu^3 (\lambda + \mu) \chi_{22} - \lambda^3 \mu^4 \chi_{211} + \mu^7 \chi_{1111} &= \\ = \lambda^6 \chi_3 - 2\lambda^3 \mu^3 \chi_{21} + \mu^6 \chi_{111}. & \end{aligned} \quad (6.96)$$

Note, that to produce five linearly independent equations, one has to take at least one braid with a strand entering no crossings, and at least one three-strand braid not reducible to a two-strand one. The solution reads,

$$\chi_4 = \frac{\chi_1 (\mu \chi_1 - 1) (\mu^2 \chi_1 + \lambda - \mu) (\mu^3 \chi_1 + \lambda^2 - \lambda \mu + \mu^2)}{(\lambda - \mu)^2 (\lambda^2 + \mu^2) (\lambda^2 + \mu^2 - \lambda \mu)}, \quad (6.97)$$

$$\chi_{31} = -\frac{\chi_1 (\lambda \chi_1 - 1) (\mu \chi_1 - 1) (\mu^2 \chi_1 + \lambda - \mu)}{(\lambda - \mu)^2 (\lambda^2 + \mu^2)},$$

$$\chi_{22} = \frac{\lambda \mu \chi_1^2 (\mu \chi_1 - 1) (\lambda \chi_1 - 1)}{(\lambda - \mu)^2 (\lambda^2 + \mu^2 - \lambda \mu)},$$

$$\chi_{211} = -\frac{\chi_1 (\lambda \chi_1 - 1) (\mu \chi_1 - 1) (\lambda^2 \chi_1 + \mu - \lambda)}{(\lambda - \mu)^2 (\lambda^2 + \mu^2)},$$

$$\chi_{1111} = \frac{\chi_1 (\lambda \chi_1 - 1) (\lambda^2 \chi_1 + \mu - \lambda) (\lambda^3 \chi_1 + \lambda^2 - \lambda \mu + \mu^2)}{(\lambda - \mu)^2 (\lambda^2 + \mu^2) (\lambda^2 + \mu^2 - \lambda \mu)}. \quad (6.98)$$

The result. Putting everything together, we obtain that the invariant of the knot presented as the closure of a four-strand braid is computed as

$$H \left(b_1^{a_1} \sigma_2^{b_1} \sigma_3^{c_1} \dots b_1^{a_k} \sigma_2^{b_k} \sigma_3^{c_k} \right) = \sum_{Y \vdash 4} \chi_Y \text{Tr} \prod_{i=1}^k (h_1^I)^{a_i} (h_2^Y)^{b_i} (h_3^Y)^{c_i}, \quad (6.99)$$

where $Y \vdash 4$ means that Y runs over partitions of 4 ($Y = [4], [31], [22], [211], [1111]$), the matrices h^Y are

$$\begin{aligned}
h_1^4 &= h_2^4 = \lambda, & h_1^{1111} &= h_2^{1111} = \mu, \\
h_2^{22} &= h_2^{SA}(\lambda, \mu) = \begin{pmatrix} \frac{\mu^2}{\mu-\lambda} & \frac{\sqrt{\lambda\mu(\lambda\mu-\lambda^2-\mu^2)}}{\lambda-\mu} \\ \frac{\sqrt{\lambda\mu(\lambda\mu-\lambda^2-\mu^2)}}{\lambda-\mu} & \frac{\lambda^2}{\mu-\lambda} \end{pmatrix}, \\
h_2^{31} &= \begin{pmatrix} \lambda & \\ & h_1^{SA}(\lambda, \mu) \end{pmatrix}, & h_2^{211} &= \begin{pmatrix} \mu & \\ & h_2^{SA}(\lambda, \mu) \end{pmatrix}.
\end{aligned} \tag{6.100}$$

and the weight coefficients χ_I are given by (6.98).

6.4 Weight coefficients as $SU(N)$ characters

The obtained expressions for the weight coefficients have a remarkable property, which reveals a deeper underlining structure. Namely, the crossing matrices arise as a deformation of the permutation group generators. If one substitutes now the two-strand eigenvalues in (6.21,6.55,6.98) by the eigenvalues of the rang two permutation groups generator on the symmetric and antisymmetric representations (6.16), respectively, i.e., $\lambda = 1$ and $\mu = -1$, the weight coefficients turn into the quotients of the gamma function resembling expressions,⁵

$$\chi_2 = \frac{\chi(\chi+1)}{2}, \quad \chi_{11} = \frac{\chi(\chi-1)}{2} \tag{6.101}$$

$$\chi_3 = \frac{\chi(\chi+1)(\chi+2)}{6}, \quad \chi_{21} = \frac{\chi(\chi+1)(\chi-1)}{3}, \quad \chi_{111} = \frac{\chi(\chi-1)(\chi-2)}{6} \tag{6.102}$$

$$\begin{aligned}
\chi_4 &= \frac{\chi(\chi+1)(\chi+2)(\chi+3)}{24}, \quad \chi_{31} = \frac{\chi(\chi+1)(\chi+2)(\chi-1)}{8}, \quad \chi_{22} = \frac{\chi_1^2(\chi+1)(\chi-1)}{3}, \\
\chi_{211} &= \frac{\chi(\chi+1)(\chi-1)(\chi+2)}{8}, \quad \chi_{1111} = \frac{\chi(\chi+1)(\chi+2)(\chi+3)}{24}.
\end{aligned} \tag{6.103}$$

In particular, for χ being equal to any integer N , a coefficient χ_Y for a Young diagram Y equals the dimension of $su(N)$ representation corresponding to the Young diagram Y ; as well as permutation group irreducible representations, $su(N)$ irreducible representations are in one-to-one correspondence with the Young diagrams [42, 64].

The observed property admits a generalization. As already mentioned in sec.6.1.1, the permutation group admires a deformation called Hecke algebra, or q -permutation group. As we will see in sec.7.6, the generator of the q -permutation group acts on its two irreducible representation with the eigenvalues $\lambda = q$ and $\mu = -q^{-1}$, with q begin a formal parameter entering group relations. Substituting the so deformed eigenvalues in (6.21,6.55,6.98), one obtains that (6.101-6.103) is substituted by

$$\chi_2 = \frac{[N][N+1]}{[2]}, \quad \chi_{11} = \frac{[N][N-1]}{[2]} \tag{6.104}$$

$$\chi_3 = \frac{[N][N+1][N+2]}{[2][3]}, \quad \chi_{21} = \frac{[N][N+1][N-1]}{[3]}, \quad \chi_{111} = \frac{[N][N-1][N-2]}{[2][3]}, \tag{6.105}$$

⁵We label all the coefficients by partitions this times; in particular, $\chi_2 \equiv \chi_S$, $\chi_{11} \equiv \chi_A$, $\chi_{SS} \equiv \chi_3$, $\chi_{SA} \equiv \chi_{21}$, and $\chi_{AA} \equiv \chi_{111}$.

$$\chi_4 = \frac{[N][N+1][N+2][N+3]}{[2][3][4]}, \quad \chi_{31} = \frac{[N][N+1][N+2][N-1]}{[2][4]}, \quad \chi_{22} = \frac{[N]^2[N+1][N-1]}{[3]},$$

$$\chi_{211} = \frac{[N][N+1][N-1][N-2]}{[2][4]}, \quad \chi_{1111} = \frac{[N][N+1][N+2][N+3]}{[2][3][4]}.$$

with the standard notation $[N] \equiv \frac{q^N - q^{-N}}{q - q^{-1}} = q^{N-1} + q^{N-3} + \dots + q^{-N-1}$ used. For $q = 1$, $[N] = N$, and (6.104-6.106) reduce to (6.101-6.103) with $\chi_1 = N$. Quantities (6.104 – 6.106) are referred to as *quantum dimensions* of *quantum group* $U_q(SU(N))$ irreducible representations [79]. They can be considered traces of the exponentiated quadratic Casimir operator over the corresponding $SU(N)$ representations [71].

7 Constructing a knot polynomial from \mathcal{R} -matrices

In this section, we finally address to the approach we are especially interested in. As we already mentioned, this approach can be developed either on the ground of the state model approach (see sec.5), or on the ground of the braid group approach (see sec.6). Below we outline the construction, which we discuss in details throughout the section.

In complete analogy with state model approach the with braid group approach, we first pass from the knot diagram to a *cut* knot diagram, and relate it to an operator product, which is invariant under Reidemeister moves II (fig.7.1) and III (fig.7.10) and depending on some additional parameters. Afterwards, we define an “average” over these parameters, which will be invariant under the Reidemeister move I (fig.7.15) as well. This procedure has different versions, already outlined in sec.5. We mostly concentrate here on the turn-over operators approach introduced in sec.5.4.3, since it being very poorly presented in literature. We also give a notion of the more common approach, or rather the approaches, which are based on selecting a certain direction on the projection plane [58, 71, 55, 80, 75, 78, 98, 86, 56, 46, 68, 69, 32, 41, 49, 48, 35, 34].

7.1 The notion of \mathcal{R} -matrix

In sec.6 we considered the Hecke algebra elements, discussing there how a symmetry generalizing the permutation symmetry can be realized with help of these elements. In fact, Hecke algebra elements are particular cases of the *quantum \mathcal{R} -matrices* [94, 91, 24, 60]. Namely, an operator satisfying permutation group constraints (6.4,6.5), generally *not* satisfying (6.6) is by definition \mathcal{R} -matrix. An eigenvalue equation of a general form (6.13) holds for an \mathcal{R} -matrix instead of (6.6).

As we discussed above, symmetric group constraints (6.4),6.5) can be associated with the transformations of a knot diagram in lines 1 and 2 of tab.5.2, respectively. These transformations, it turn, give rise to the operator equations the right column of the table. A four script operator satisfying these constraints is thus another representation of an \mathcal{R} -matrix. Equation (6.6,5.2 — line 2), represented in any of the two equivalent forms, is referred to as *the Yang-Baxter equation* [94].

The \mathcal{R} -matrices the most naturally arise in the context of *quantum groups* [60]. However, this subject is beyond the scope of our presentation. Here we just outline the several properties of a quantum \mathcal{R} -matrix, which are essential for using it as a tool for constructing the knot polynomials. Namely,

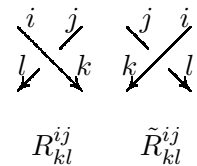


Figure 7:
Direct and
inverse crossings.

A quantum \mathcal{R} -matrix

- Is explicitly constructed for each representation of each Lie group
- Depends on a formal variable q (which is referred to as a *quantum* parameter)

- Satisfies the Yang-Baxter equation, which is associated with the III Reidemeister transformation of the knot planar diagram.

We also present the explicit form of the simplest \mathcal{R} -matrix and verify that it indeed satisfies the Yang-Baxter equation in sec.7.3.

7.2 A contraction of \mathcal{R} -matrices as a cut knot diagram invariant

7.2.1 The general part of the state model approach adopted to the \mathcal{R} -matrix approach

We start from recalling the first steps of the constructing a knot polynomial in the state model approach (see sec.5), this time formulating them in a way especially convenient for the following presentation.

First,



Step 7.1 *A knot is related to a knot diagram.*

The definition of a knot diagram is given in sec.5. Now we pass from a knot diagram to a *cut* knot diagram. Namely, we

Figure 8: Cutting of the edge on a knot diagram.

Step 7.2 *Cut some edges on the knot diagram so that the cut diagram is related to a collection of self-crossing free curves.*

To cut an internal edge directed from vertex A to vertex B means substitute the edge with the pair of edge incoming the vertex A and the edge outgoing the vertex B . (see fig.8).

The proper cutting of a knot diagram can be carried out as follows. The first cut is made on an arbitrary edge. Then, one follows in the direction selected on the edges, at each crossing selecting the edge corresponding to the proceeding of an already passed edge on the original curve (i.e., edge k proceeds edge i , and edge l proceeds edge j in fig.7). Following the edges in a knot diagram this way, one stops before encountering with the already passed edge for the first time. The next cut is done on the edge where one stopped. The procedure is then repeated, the made cut as a new starting point. In case of a knot, one terminates at the first cut by the end. In case of a link, the procedure is carried out for each connection component separately. An example of the resulting cut diagram is presented in fig.12. After the procedure is completed,

Step 7.3 *Each incoming edge on the cut diagram acquires its own number.*

The same number can be related to the corresponding segment of the original curve after being cut. One obtains then a collection of enumerated directed curve segments, corresponding to unclosed polygons composed of edges of the cut knot diagram, the crossing on the diagram corresponding now to intersections of these segments. Hence, a crossing is related now to a pair of numbers associated with the corresponding curve segments. The following two steps then are to

Step 7.4 *Associate the polygon on the cut diagram attached with incoming edge α to a vector space \mathcal{L}_α ,*

and to

Step 7.5 *Associate a direct crossing (see fig.7) of polygons α and β with a linear operator $S^{(\alpha,\beta)}$ acting in the space $\mathcal{L}_\alpha \otimes \mathcal{L}_\beta$.*

Written down in components, this operator has four tensor indices, $S_{kl}^{(\alpha,\beta)ij}$, the superscripts running in the space of origin, $i \in \mathcal{L}_\alpha, j \in \mathcal{L}_\beta$ and being related to the incoming strands, the subscripts running in the space of image, $k \in \mathcal{L}_\alpha, l \in \mathcal{L}_\beta$ and being related to the outgoing strands; the first script in each pair being related to the edge corresponding to the upper curve segment in the planar projection, fig.7.

We reflect this fact by labeling each edge by an index running in the corresponding \mathcal{L} . Alternatively, one may write the operator with one superscript and one subscript, $S_J^{(\alpha,\beta)I}$, both running in the space $\mathcal{L}_\alpha \otimes \mathcal{L}_\beta$.

The general part of the construction is completed by assuming that

Step 7.6 Associate an inverse crossings (see fig.7) of polygons α and β with the operator $\tilde{S}^{(\alpha,\beta)}$ inverse to operator $S^{(\alpha,\beta)}$ on the space $\mathcal{L}_\alpha \otimes \mathcal{L}_\beta$.

Other words, the operators $S^{(\alpha,\beta)}$ and $\tilde{S}^{(\alpha,\beta)}$ by definition satisfy the identities in line 3 of tab.5.2.

Once each edge of the cut knot diagram is labeled by a script,

Step 7.7 The cut knot diagram is related to a certain contraction of (yet undefined) operators $S^{(\alpha,\beta)}$ and $\tilde{S}^{(\alpha,\beta)}$, the contractions coinciding identically for a pair of diagrams related a sequence of the second Reidemeister moves (line 3 in tab.5.1).

7.2.2 The \mathcal{R} -matrices as crossing operators.

The last step completes the general part of the construction, we now turning to the specific R -matrix part of it. Namely, one takes the following ansatz,

Step 7.8 A space \mathcal{L}_α is the space representation Q_α of a Lie group G ,

and

Step 7.9 The operator $S^{(\alpha,\beta)}$ is the corresponding quantum $\mathcal{R}_{Q_\alpha, Q_\beta, G}(q)$ -matrix.

The general definition of the quantum \mathcal{R} -matrix is given above in sec.7.1 (rigorously speaking, G is not a Lie group but the corresponding *quantum group*, but we ignore the difference here modulo the remark in sec.7.1). Here we emphasize once again that the *explicit*, although very complicated expressions for arbitrary quantum \mathcal{R} -matrices are available in representation theory [60]. Substituting one of the corresponding expressions for the crossing operators in the previously obtained operator contraction, one obtains that

Step 7.10 A cut knot diagram with n incoming and n outgoing edges corresponds to an (n, n) type tensor depending on the Lie group G , its representation Q , and on the formal parameter q .

Moreover, by definition of the \mathcal{R} -matrix,

Step 7.11 The same tensors correspond to any pair of cut knot diagrams related by a sequence of the second (line 3 of tab.5.2) and third (line 2 of tab.5.2) Reidemeister moves.

In the following, we concentrate on the particular case of the representations Q being the **fundamental** representation of the $SU(N)$ group, keeping N as a free parameter. The obtained knot invariants are (uncolored) HOMFLY polynomials (see sec.2 and 5) in the case, after the substitution $A = q^N$ and analytic continuation to arbitrary complex A being done. Although the same knot polynomial can be obtained equally in many other approaches (e.g., in the once discussed in 5.4.1 and 6), we chose this simplest case as an illustration to the \mathcal{R} -matrix approach, which, as already mentioned, enables constructing the colored HOMFLY polynomials for knots [43, 44, 45, 11, 13, 83, 46] and multi-colored HOMFLY polynomials for links (taking higher representations of $SU(N)$ as the representation Q) [98, 97, 86, 13, 68, 69, 32], as well as Kauffman polynomials [53], plain [71, 82] and colored [66] (considering the $SO(N)$ group instead of $SU(N)$), and even more general knot invariants [6] (considering the exceptional groups; very few explicit answers is yet available for these cases).

7.3 Explicit verifying the topological invariance constraints for the simplest \mathcal{R} -matrix

In the present section, we complete presentation of the \mathcal{R} -matrix approach to the knot invariants by writing out explicitly the form of these operators in the simplest case (the obtained knot invariant is an (uncolored) HOMFLY polynomial in this case), and by verifying for them the constraints providing a topological invariance of the contraction. According to the Reidemeister theorem [94], three constraints are enough to impose; they are illustrated in (7.10),(7.1), and (7.15) and referred to as Reidemeister moves. Each of these constraints is associated with a singular transformation of a planar diagram corresponding to non-singular transformation of the knot. The theorem states that any two diagrams of the (topologically) same knots can be transformed into each other by a combination of three Reidemeister moves. Hence, any quantity that satisfy the three corresponding constraints would be a knot invariant.

7.3.1 Yang-Baxter equation

The next constraint corresponds to the third Reidemeister move (in the next coming evaluation, these are delta-symbols, not the R -matrices, stand in all crossings; the crossings where R -matrices still stand are labeled by dots):

$$R_{ba}^{ji} R_{cm}^{bk} R_{nl}^{ac} = R_{ac}^{ik} R_{bn}^{jc} R_{ml}^{ba} \quad (7.1)$$

This constraint is called a Yang-Baxter equation, and its solutions are studied in the integrable models theory under the name of R -matrices [24]. In particular, a one-parametric family of solutions is constructed explicitly for a finite-dimensional representation of a regular Lie group [47]. Here we restrict ourselves by verifying the Yang-Baxter equation for the simplest of the solution, which corresponds to the fundamental representation of the group $su(N)$. Non-zero elements of the examined solution are:

$$R_{ii}^{ii} = q; \quad R_{ij}^{ij} = 1, \quad i \neq j; \quad R_{ji}^{ji} = q - q^{-1}, \quad 1 \leq i < j \leq N, \quad (7.2)$$

where N is an integer number, and q is a formal parameter of the family. This solution gives rise to (uncolored) HOMFLY polynomials (see examples below).

Let us verify that (7.2) satisfies the Yang-Baxter equation explicitly. Since we write the solution in a certain basis, the notations are *not* covariant any longer; in particular, *no sum* after repeated indices is assumed default. Solution (7.2) can be presented as

$$R_{kl}^{ij} = a_{ij} \delta_i^j \delta_k^l + b_{ij} \delta_i^j \delta_k^l, \quad a_{ij} = 1 + (q - 1) \delta_{ij}, \quad b_{ij} = (q - q^{-1}) \theta_{ij} \quad (7.3)$$

with $\theta_{ij} \equiv 1$ for $i < j$, and $\theta_{ij} \equiv 0$ otherwise. Verifying of the YB equation can be then carried out graphically. Four out of eight pairs of diagrams merely coincide:

equalities termwise, one gets correct in the case in case identity,

$$\begin{array}{c}
 \begin{array}{c} i \\ \diagdown \\ \text{---} \\ \diagup \\ n \end{array} \begin{array}{c} | \\ i \\ \text{---} \\ l \end{array} \begin{array}{c} \curvearrowright \\ m \\ \curvearrowleft \end{array} \\
 \\
 a_{ii}^2 b_{ik}
 \end{array}
 \quad
 \boxed{i = j < k}
 \quad
 =
 \quad
 \begin{array}{c}
 \begin{array}{c} i \\ \text{---} \\ n \end{array} \begin{array}{c} \curvearrowright \\ m \\ \curvearrowleft \end{array} \begin{array}{c} | \\ i \\ \text{---} \\ l \end{array} \begin{array}{c} \curvearrowright \\ k \\ \text{---} \\ m \end{array} \\
 \\
 a_{ik} a_{ki} b_{ik}
 \end{array}
 \quad
 +
 \quad
 \begin{array}{c}
 \begin{array}{c} i \\ \text{---} \\ n \end{array} \begin{array}{c} \curvearrowright \\ m \\ \curvearrowleft \end{array} \begin{array}{c} | \\ i \\ \text{---} \\ l \end{array} \begin{array}{c} \curvearrowright \\ k \\ \text{---} \\ m \end{array} \\
 \\
 a_{ii} b_{ik}^2
 \end{array}
 \quad
 (7.8)$$

due to the identity $q^2 = 1 + q(q - q^{-1})$. Similarly, for $i = j < k$, equality takes place for the sums of

diagrams (7.7) and (7.8) contributing to the component $\begin{pmatrix} ij & i \\ lnm \end{pmatrix}$,

$$\begin{array}{c}
 \begin{array}{c} j \\ \diagdown \\ \text{---} \\ \diagup \\ n \end{array} \begin{array}{c} | \\ i \\ \text{---} \\ l \end{array} \begin{array}{c} \curvearrowright \\ m \\ \curvearrowleft \end{array} \\
 \\
 a_{ji} a_{ij} b_{ji}
 \end{array}
 \quad
 \boxed{j < i = k}
 \quad
 +
 \quad
 \begin{array}{c}
 \begin{array}{c} j \\ \text{---} \\ n \end{array} \begin{array}{c} \curvearrowright \\ m \\ \curvearrowleft \end{array} \begin{array}{c} | \\ i \\ \text{---} \\ l \end{array} \begin{array}{c} \curvearrowright \\ k \\ \text{---} \\ m \end{array} \\
 \\
 a_{ii} b_{ji}^2
 \end{array}
 \quad
 =
 \quad
 \begin{array}{c}
 \begin{array}{c} j \\ \text{---} \\ n \end{array} \begin{array}{c} \curvearrowright \\ m \\ \curvearrowleft \end{array} \begin{array}{c} | \\ i \\ \text{---} \\ l \end{array} \begin{array}{c} \curvearrowright \\ i \\ \text{---} \\ m \end{array} \\
 \\
 b_{ji} a_{ii}
 \end{array}
 \quad
 (7.9)$$

7.3.2 Inverse crossings

The next (in fact, the most simple out of the three ones) constraint reflects the invariance under the second Reidemeister move, (7.10).

$$\begin{array}{c}
 \begin{array}{c} i \swarrow \quad \searrow j \\ \text{---} \\ b \quad | \quad a \\ \text{---} \\ k \swarrow \quad \searrow l \end{array} \\
 \\
 \sum_{a,b} R_{ab}^{ij} \tilde{R}_{kl}^{ab}
 \end{array}
 \quad
 =
 \quad
 \begin{array}{c}
 \begin{array}{c} i \swarrow \quad \searrow j \\ \text{---} \\ \text{---} \\ \text{---} \\ k \swarrow \quad \searrow l \end{array} \\
 \\
 \delta_k^i \delta_l^j
 \end{array}
 \quad ,
 \quad
 (7.10)$$

The condition gives rise to the constraints, which relates the operators corresponding to the crossings of the mutually inverse orientations. Because (7.10) is a system of N^2 linear equations on N^2 variables (which can be verified to non-degenerate), matrix elements of the inverse crossing operators are determined therefrom explicitly and unambiguously. The most simple is to write for them the ansatz, similar to expression (7.3),

$$\tilde{R}_{kl}^{ij} = \tilde{a}_{ij} \delta_k^i \delta_l^j + \tilde{b}_{ij} \delta_l^i \delta_k^j. \quad (7.11)$$

Equations (7.10) then take the form

$$\sum_{p,q} \tilde{R}_{pq}^{ij} R_{kl}^{pq} = (\tilde{a}_{ij} a_{ij} + \tilde{b}_{ij} b_{ji}) \delta_k^i \delta_l^j + (\tilde{a}_{ij} b_{ij} + \tilde{b}_{ij} a_{ji}) \delta_l^i \delta_k^j = \delta_k^i \delta_l^j. \quad (7.12)$$

With a_{ij} and b_{ij} from (7.3), there are three distinct non-trivial cases, which give (note that $\tilde{b}_{ii} = 0$ by definition)

$$\begin{aligned}
i = k \leq j = l &\Rightarrow \tilde{a}_{ij}a_{ij} = 1 &\Rightarrow \tilde{a}_{ii} = q^{-1}, \tilde{a}_{ij} = 1, i > j \\
i = k > j = l &\Rightarrow \tilde{a}_{ij}a_{ij} + \tilde{b}_{ij}b_{ji} = 1 &\Rightarrow \tilde{b}_{ij} = 0, i > j, \\
i = l < j = k &\Rightarrow \tilde{a}_{ij}b_{ij} + \tilde{b}_{ij}a_{ji} = 0 &\Rightarrow \tilde{b}_{ij} = q^{-1} - q.
\end{aligned} \tag{7.13}$$

Yang-Baxter equation (7.1) holds for the obtained solution automatically, since the matrix elements for the inverse crossing operators appeared to be related with that for the direct ones by a plain change of parameter, $\tilde{a}_{ij}(q) = a_{ij}(q^{-1})$ and $\tilde{b}_{ij}(q) = b_{ij}(q^{-1})$, while (7.3) satisfies (7.1) for an *arbitrary* value of q .

Thereby, if one puts operators (7.3) in the direct crossings, one should must put the operators (recall that $\theta_{ij} = 1$ for $i < j$, and $\theta_{ij} = 0$ for $i \geq j$)

$$R_{kl}^{ij} = \tilde{a}_{ij}\delta_i^j\delta_k^l + \tilde{b}_{ij}\delta_i^j\delta_k^l, \quad \tilde{a}_{ij} = 1 + (q^{-1} - 1)\delta_{ij}, \quad \tilde{b}_{ij} = (q^{-1} - q)\theta_{ij} \tag{7.14}$$

in the inverse crossings.

7.4 First Reidemeister move and turn-over operators

7.4.1 RI invariance as a condition on the R -matrix contraction

One more transformation of the knot, which is smooth though looking singular at a planar projection, is contracting of a loop:



$$\sum_{a,b} \mathcal{M}_a^b R_{bk}^{ia} = \delta_k^i \tag{7.15}$$

The above rules relate the left and right figures with the partial contraction of the R -matrix $\sum_{a,b} R_{bk}^{ia}$ and with the unity operator δ_k^i , respectively. It is straightforward to verify that these expressions are not equal; the R -matrix do not possess the desired property.

7.4.2 Turn-over operators

To make a contraction of the R -matrices invariant under transformation (7.15) as well, one introduces one more element in the construction [79],[58],[71]. Namely, the scripts of R -matrix are contracted now with help of a new operator \mathcal{M} , which we call a *turn-over operator*. Equality (7.15) is a definition of the operator \mathcal{M} , and it enables one to determine elements of the turn-over operator explicitly.

Explicit expression for the turn-over operators We will use the explicit expression (7.3) for elements of the R -matrix in a selected basis, and we suppose that the operator \mathcal{M} is diagonal in the same basis,

$$\mathcal{M}_j^i = m_i \delta_j^i; \tag{7.16}$$

as we will verify, such a solution exists, and it is unique, as follows from the dimension counting. Let us start from the particular values of N in (7.3). For $N = 2$, constraints (7.15) take the explicit form

$$\begin{cases} m_1 R_{11}^{11} + m_2 R_{21}^{12} \\ m_2 R_{22}^{22} \end{cases} = \begin{cases} 1 \\ 1 \end{cases} \Rightarrow \begin{cases} qm_1 + (q - q^{-1})m_2 \\ qm_2 \end{cases} = \begin{cases} 1 \\ 1 \end{cases}, \tag{7.17}$$

and have the solution

$$m_1 = q^{-3}, \quad m_2 = q^{-1} \quad (7.18)$$

For $N = 3$, one has the system

$$\begin{cases} m_1 R_{11}^{11} + m_2 R_{21}^{12} + m_3 R_{31}^{13} = 1, \\ m_2 R_{22}^{22} + m_3 R_{32}^{23} = 1, \\ m_3 R_{33}^{33} = 1 \end{cases} \Rightarrow \begin{cases} qm_1 + (q - q^{-1})(m_2 + m_3) = 1, \\ qm_2 + (q - q^{-1})m_3 = 1, \\ qm_3 = 1, \end{cases} \quad (7.19)$$

the solution being

$$m_1 = q^{-5}, \quad m_2 = q^{-3}, \quad m_3 = q^{-1}. \quad (7.20)$$

Now it is easy to write down both the constraints and their solution for generic N . Equations (7.15) can be rewritten as

$$m_i R_{ii}^{ii} + \sum_{j=i+1}^N m_j R_{ji}^{ij} = 1 \Rightarrow qm_i + (q - q^{-1}) \sum_{j=i+1}^N m_j = 1, \quad (7.21)$$

wherefrom one expresses explicitly the non-zero elements of the turn-over operator,

$$\boxed{m_i = q^{2i-2N-1}, \quad i = 1, \dots, N.} \quad (7.22)$$

A contraction of the R -matrix in the other two scripts, in turn, corresponds contracting loop (7.24-II), and should be carried out with help of another operator, \mathcal{M}' , which is determined by the system of constraints

$$\sum_{a,b} \mathcal{M}'_a{}^{ab} R_{ab}^{aj} = \delta_l^j. \quad (7.23)$$

$\mathcal{M}R$
I

$\mathcal{M}'R$
II

$\tilde{\mathcal{M}}\tilde{R}$
III

$\tilde{\mathcal{M}}'\tilde{R}$
IV

(7.24)

E.g., the system for $N = 2$ takes the explicit form

$$\begin{cases} m'_1 R_{11}^{11} = 1, \\ m'_1 R_{21}^{12} + m'_2 R_{22}^{22} = 1, \end{cases} \Rightarrow \begin{cases} qm'_1 = 1, \\ (q - q^{-1})m'_1 + qm'_2 = 1, \end{cases} \quad (7.25)$$

and it has the solution

$$m'_1 = q^{-1}, \quad m'_2 = q^{-3}. \quad (7.26)$$

For $N = 3$, one has

$$\begin{cases} m'_1 R_{11}^{11} = 1, \\ m'_1 R_{21}^{12} + m'_2 R_{22}^{22} = 1, \\ m'_1 R_{31}^{13} + m'_2 R_{32}^{23} + m'_3 R_{33}^{33} = 1, \end{cases} \Rightarrow \begin{cases} qm'_1 = 1, \\ (q - q^{-1})m'_1 + qm'_2 = 1, \\ (q - q^{-1})(m'_1 + m'_2) + qm'_3 = 1, \end{cases} \quad (7.27)$$

what gives

$$m'_1 = q^{-1}, \quad m'_2 = q^{-3}, \quad m'_3 = q^{-5}. \quad (7.28)$$

Finally, the constraints on the non-zero matrix elements and their solutions for generic N are, respectively,

$$\sum_{j=1}^{i-1} m'_j R_{ij}^{ji} + m'_i R_{ii}^{ii} = 1 \Rightarrow (q - q^{-1}) \sum_{j=1}^{i-1} m'_j + qm'_i = 1, \quad (7.29)$$

and

$$\boxed{m'_j = q^{-2j+1}, \quad j = 1, \dots, N.} \quad (7.30)$$

Loops attached to the inverse vertices. To complete the construction under discussion, One also should introduce the operators $\tilde{\mathcal{M}}$ and $\tilde{\mathcal{M}}'$ to be inserted in contractions of the *inverse* R -matrix in one and in the other pairs of scripts, and associated with contractions of the loops in fig.7.24-III and -IV, respectively. The matrix elements of the operators must satisfy the system of constraints, which, according to (7.14), are obtained from (7.21) and (7.29), correspondingly, by changing q for q^{-1} . Therefore, the same change of parameters relates the unique solutions of the systems,

$$\boxed{\tilde{m}_i = q^{2N-2i+1}, \quad i = 1, \dots, N,} \quad (7.31)$$

and

$$\boxed{\tilde{m}'_i = q^{2i-1}, \quad i = 1, \dots, N.} \quad (7.32)$$

Hence, there are in fact only two independent operators,

$$\mathcal{M} = \tilde{\mathcal{M}}^{-1} \quad \text{and} \quad \mathcal{M}' = \tilde{\mathcal{M}}'^{-1}. \quad (7.33)$$

7.4.3 Topological normalization of the turn-over operators and framing of a knot

A priori, there are four distinct turn-over operators associated with contractions of the four distinct loops in fig.7.24, two including the direct crossing, the other two the inverse one. However, we will see that in a more general case a turn-over operator can be inserted in an arbitrary edge that belongs to a cycle on a knot diagram. Hence, there should be just two distinct operators, inserted in the counter-clock and clock-wise cycles, respectively. Yet, we obtained four explicit distinct expressions (7.22,7.30,7.31,7.32) for the operators associated with the corresponding loops. This problem is resolved if one rescales the turn-over operators in some proper way, bringing them in a so called *topological* normalization. The four turn-over operators equal pairwise in this normalization.

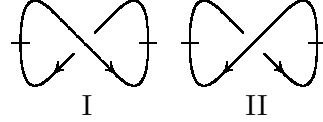


Figure 9: Diagrams of the twisted circles, both are equivalent to the unknot.

Rigorously speaking, equation (7.15), which follows from RI invariance, determines the turn-over operators uniquely, not up to a factor. Rescaling of the operators, hence, is possible only together with deformation of the equation itself. The operators R - and \mathcal{M} - satisfying the resulting deformed equations give rise to so called *framed* knot invariants, which generalize the notion of plain knot invariants. The latter ones still can be obtained as contractions of the rescaled R - and \mathcal{M} - operators, if one properly rescales the entire contraction at the last step of the computation.

Twisted circles as full contractions of R -matrices As the first demonstration of a problem with inserting the correct turn-over operator, consider an invariant of the twisted circle (fig.9-I). Following the algorithm of sec.7.2, one makes two cuts as in the diagram. There is only one crossing, and the corresponding invariant equals the contraction of the R -matrix with two \mathcal{M} -matrices inserted in the two pairs of indices,

$$\sum_{i,j,a,b} R_{ab}^{ij} \mathcal{M}_b^i \mathcal{M}_a^{j'} = \sum_{i,j} R_{ji}^{ij} m_i m'_j = \sum_{i=1}^N m_i = \sum_{j=1}^N m'_j = \sum_{i=1}^N q^{-2i+1} = q^{-N} \frac{q^N - q^{-N}}{q - q^{-1}} \equiv q^{-N} [N]. \quad (7.34)$$

In turn, a similar diagram with the crossing substituted with the inverse one (fig.9-II) gives the value of the invariant

$$\sum_{i,j,a,b} \tilde{R}_{ab}^{ij} \mathcal{M}_b^i \mathcal{M}_a^{j'} = \sum_{i,j} \tilde{R}_{ji}^{ij} \tilde{m}_i \tilde{m}'_j = \sum_{i=1}^N \tilde{m}_i = \sum_{j=1}^N \tilde{m}'_j = \sum_{i=1}^N q^{2i-1} = q^N [N]. \quad (7.35)$$

On the other hand, (7.34) must coincide with (7.35) for a properly defined knot invariant, since both diagrams in fig.9 are projections of the curves that can be continuously transformed into a plain circle, i.e. to the unknot. One can cure this problem by putting one more element into the R -matrix construction.

Topological normalization The problem is considered even clearly as one considers a plain circle. Following the program of sec.7.2, one should treat its planar projection as a diagram with no vertices and with one cut (fig.10). Rigorously speaking, the above rules do not determine the corresponding value of the invariant at all. In analogy with (7.15), one may associate with this diagram the trace of a turn-over operator. One of the four turn-over operators \mathcal{M} , \mathcal{M}' , $\tilde{\mathcal{M}}$, $\tilde{\mathcal{M}}'$ can be taken equally well in the case. Unfortunately, their traces differ, as we already verified above,

$$\sum_{i=1}^N \mathcal{M}_i^i = \sum_{i=1}^N \mathcal{M}'_i^i = q^{-N}[N], \quad \sum_{i=1}^N \tilde{\mathcal{M}}_i^i = \sum_{i=1}^N \tilde{\mathcal{M}}'_i^i = q^N[N]. \quad (7.36)$$

Invariants of framed knots in R -matrix construction A clue to the resolution is given by the following observation. The expressions (7.34) and (7.35) are obtained from the knot diagrams with the different values of a *relative* invariant, a *writhe number*, which by definition equals the number of direct crossings minus the number of inverse crossings (see fig.7). A writhe number remains unchanged under the second and third Reidemeister moves, (7.10) and (7.1), respectively, but increases or decreases by one by the first Reidemeister move, (7.15). Answers (7.34) and (7.35) coincide provided that one multiplies them by factors q^{wN} with the corresponding writhe numbers $w = 1$ and $w = -1$ for figs.9-I and II, respectively. This observation, however, does not solve the problem with plain circle, for which $w = 0$. This problem can be avoided by rescaling of the crossing operators as

$$\mathcal{M} \rightarrow \mathfrak{M} \equiv q^{-N} \mathcal{M}, \quad \text{and} \quad \mathcal{M}' \rightarrow \mathfrak{M}' \equiv q^{-N} \mathcal{M}', \quad (7.37)$$

The non-vanishing matrix elements then become

$$\mathfrak{m}_i = q^{2i-N-1}, \quad \mathfrak{m}'_i = q^{N-2i+1}, \quad \tilde{\mathfrak{m}}_j = q^{N-2i+1}, \quad \tilde{\mathfrak{m}}'_i = q^{2i-N-1}, \quad i = 1, \dots, N. \quad (7.38)$$

All the four traces in (7.36) equal then $[N]$; (7.34) then matches (7.35) and the answer for the plain circle after each expression is multiplied on the factor of q^{-wN} with its own w (the factor is inverse to the previously suggested ones). Motivated by these considerations, one may introduce then two more rules,

Step 7.12 *Rescale the turn-over operators so that traces of all the four operators equal,*

and

Step 7.13 *Multiply the result of Steps 7.1-7.2.2 by q^{-wN} , with w being the writhe number of knot diagram involved in the evaluation.*

If one follows the above rules, both diagrams in fig.9, as well that in fig.10, yield one and the same value $[N]$ of the invariant for the unknot. However, one has to check whether the suggested rescaling does not break already imposed constraints (7.1,7.10,7.15). Equalities (7.1) and (7.10) which do not involve turn-over operators, indeed, remain unaffected. Unlike them, condition (7.15) gains an extra factor of q^N for loops in fig.7.24-I,II, and q^{-N} for loops in fig.7.24-III,IV. Deformed this way, relation (7.15) is called a *q -Reidemeister-I move*. Since a loop in (7.15) can be contracted in the three-dimensional space, a supposed deformation of the constraint is inept, unless one endows a knot with an additional structure. The needed structure can be represented graphically, by substituting a knot by a knotted *ribbon*. The first Reidemeister move is not an equivalence transformation of such knots, since it causes a twist of the ribbon. Formally speaking, a knot, or each component of a link should be associated now with an integer number, which equals a number of the ribbon intertwinings and is changed by one under the first Reidemeister move. The obtained object is called a *framed* knot or link [94]. We have demonstrated in the elementary example that a knot invariant of the studied type is, in fact, an

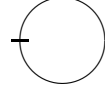


Figure 10: A plain circle (the unknot) requires for inserting a turn-over operator.

invariant not just of a knot, but of a *framed* knot⁶ [79]. Somewhat surprisingly, attempt of interpreting the same invariant as a QFT observable lead one to the same conclusion [37] (see sec.4.5 for details).

Although required in the definition of the knot invariant of the studied type, choice of framing does not affect the answer, provided that one follows **Step 7.13** (the corresponding factor is called a *framing factor*). The independence of the answer on the writhe number used in the calculation knot diagram becomes even more explicit if the multiplying of the entire answer on a framing factor is substituted by the rescaling of each crossing operator as $R \rightarrow q^{-N}R$, and each inverse crossing operator as $\tilde{R} \rightarrow q^N\tilde{R}$. Both constraints (7.1), (7.10) are preserved by such a change, and (7.15) holds again without any extra factors. However, the framing independence property breaks both for knots in topologically non-trivial (other than R_3 or S_3) spaces [94] and for some other (yet conjectured) generalizations of the studied quantities [29].

7.4.4 Turn-over operators and loop version of the RII move.

$$\mathcal{R}_{bl}^{ia} \tilde{\mathcal{R}}_{ka}^{cj} \mathcal{M}_c^a = \delta_k^i \mathcal{M}_l^j. \quad (7.39)$$

Attempt of constructing a topologically invariant contraction of the R -matrices comes across with another problem as well. Namely, the Reidemeister theorem [94] is related to *undirected* knot diagrams. The elementary equivalence transformation of *directed* graphs, in turn, include several versions of (7.1) and (7.1) with variously directed edges (compare, e.g., fig.7.10 and 7.39).

The Reidemeister [94] claims that two knot diagrams are equivalent if and only if they are related by a combination of Reidemeister moves (7.1), (7.10) and (7.15). However, R -matrix contractions are invariant only under versions of the transformations with certain directions of edges, as in (7.10) and (7.1). In particular, they are *not* invariant under transformation (7.39), as one can verify straightforwardly.

This problem is closely related to the problem of RI invariance, since the both transformations delete a *cycle*, i.e., a closed directed curve on a knot diagram. Similarly to the former case, transformation (7.39) can be associated with the corresponding equality, which also includes a turn-over operator.

A difference between the directed graphs in the l.h.s. of (7.10) and (7.39) is that the latter one contains a *cycle* (one can pass a closed path following the direction of arrows on the diagram), while the former one does not. One can then extract from here the empiric rule to

Step 7.14 *Insert exactly one turn-over operator in one cycle, using the operators \mathcal{M} and \mathcal{M}' for the counter-clock and clock-wise oriented cycles, respectively.*

For instances, possible placements of the cuts for the two different diagrams of the trefoil knot are shown in fig.12-I and fig.5. However, the above rule sets a new problem.

7.4.5 Commutation of the turn-over operators with the R -matrices

Rule (**Step 7.14**) does not specify where exactly one should insert the turn-over operators. Moreover, the construction would be self-consistent only if *all* ways to insert the turn-over operators in accordance

⁶In fact, framing of a knot consists in substituting a curve with a ribbon, or, equivalently, in introducing a normal vector bundle on it. The power of the framing factor equals then the number on ribbon intertwinings [94].

with the rule gave the same result. It is not straightforward to understand whether such independence takes place generally. On the one hand, the turn-over operator does *not* commute with the R -matrix, what follows just from the explicit expressions for the operators in the considered particular case,

$$\sum_a \mathcal{M}_k^a R_{al}^{il} \neq \sum_a \mathcal{M}_a^i R_{kl}^{aj} \Leftrightarrow m_k R_{kl}^{ij} \neq m_i R_{kl}^{ij}. \quad (7.40)$$

On the other hand, one generally can *not* just move a turn-over operator from one edge to another since this would violate rule **Step** 7.14.

The considered particular (su_n fundamental) case. One may observe here that the R -matrix commutes with a *pair* of the turn-over operators instead,

$$\sum_{a,b} \mathcal{M}_a^i \mathcal{M}_b^j R_{kl}^{ab} = \sum_{a,b} \mathcal{M}_k^a \mathcal{M}_l^b R_{kl}^{ij}. \quad (7.41)$$

The above equality is straightforward to verify for the here considered (su_n fundamental) R -matrices and the corresponding \mathcal{M} -matrices, which satisfy

$$m_i m_j R_{kl}^{ij} = m_k m_l R_{kl}^{ij}, \quad (7.42)$$

wherefrom comes (7.41) in this particular case.

General case. Commutation relation (7.41) holds for generic R - and \mathcal{M} -operators as well, as a corollary of certain group theory facts [71]. To sketch the prove, let us rewrite (7.41) in the script-free form,

$$\mathcal{M} \otimes \mathcal{M} \cdot R = R \cdot \mathcal{M} \otimes \mathcal{M}, \quad (7.43)$$

where both the operators $\mathcal{M} \otimes \mathcal{M}$ and R are maps of the space $V \otimes V$ (recall that a vector space V of a Lie algebra representation is attached to each edge on the cut diagram, see sec.7.2). Equality (7.43) then follows of the well-known R -matrix property [24]. Namely, the R -matrix commutes with each algebra operator when acting on the tensor product of the representations. The operator \mathcal{M} , in turn, can be presented a formal series in the algebra operators, only pairwise commuting operators entering the series [71]. For an ordinary Lie algebra, these generators act on the tensor product of the representations merely as $V \otimes V \rightarrow TV \otimes V + V \otimes TV$. However, in the construction that we consider T are in fact generators of a *quantum* Lie algebra; they satisfy somehow deformed commutation relations and act on a tensor product of the representations yielding a more generic linear combination of tensor monomials, $\Delta(T)(V \otimes V) \equiv \sum T_{a_1} \dots T_{a_i} V \otimes T_{b_1} \dots T_{b_j} V$, which, for instance, is not necessary permutation w.r.t. a permutation of the tensor factors (the rule specifying this combination for each algebra operators is called a *co-product* rule). The commutative subalgebra is yet the same for the corresponding ‘‘classical’’ and quantum Lie algebras, operators H of the subalgebra still acting on the tensor product just as $HV \otimes V + V \otimes HV$. Hence, the turn-over operator, being the exponential of such an operator, acts on the same space as $MV \otimes MV$, i.e., just with the operator entering (7.43). This proves the equality.

$$\begin{array}{c} \times \quad \times \\ \diagdown \quad \diagup \\ \times \quad \times \end{array} \longrightarrow \begin{array}{c} \diagdown \quad \diagup \\ \times \quad \times \end{array} \quad (7.44)$$

Move of the turn-over operators (fig.7.44) corresponding to commutation relation (7.44) might imply that one operator is removed from a loop, being substituted by another one. Were any two allowed by **Step** 7.14 placements of the turn-over operators related by a sequence of (7.24)-type moves, (7.41) would ensure equality of the operator contractions for all such placements. However, a more careful treatment is needed before one can make a general statement.

7.4.6 Conventional non-covariant approach: the extremum point operators

A conventional approach to the problem of the turn-over operators [58],[71] is to refuse from the “covariance” of the construction. Namely, **Steps** 7.12- 7.14 are substituted by the following

Step 7.15 *A direction on the projection plane is selected, and an operator (which we call an extremum point operator) is inserted in each extremum point, where a tangent to the knot diagram vector is orthogonal to the direction.*

Hence, there are four operators, Q_+ , Q_- , \tilde{Q}_+ , \tilde{Q}_- for the four distinct extremum points, two minimum and two maximum, each pair differing by the direction selected on the curve. The pairwise products of the extremum point operators must be equal to either to the unity operator,

$$Q_+Q'_- = Q'_-Q_+ = \mathbb{1}, \quad Q'_+Q_- = Q_-Q'_+ = \mathbb{1}. \quad (7.45)$$

or to a turn over operators, there being two distinct ones the topological normalization,

$$Q_-Q_+ = Q_+Q_- = \mathfrak{M}, \quad Q'_+Q'_- = Q'_-Q'_+ = \tilde{\mathfrak{M}}. \quad (7.46)$$

The corresponding theorem [58] claims that the conditions (7.46) together with defining constraints (7.1), (7.10) and (7.15) on the R - and M - matrices ensure invariance of the operators contraction constructed with help of **Steps** 7.1-7.2.2 and 7.15 under all elementary equivalence transformations of directed graphs. Moreover, we already mentioned above that the vector space where run the scripts of the operators is a representation space of a Lie group, or, more precisely, of its certain deformation referred to as *quantum group*; the obtained contraction is be invariant of this groups transformations as well [58].

Condition (7.46) in fact does not specify the extremum point operators uniquely. In particular, one may additionally require that the minimum or maximum point operator equals the unity operator, the other one being then equal to the corresponding turn-over operator.

Following another version of the non-covariant approach [55, 80, 75, 78, 98, 86, 56, 46, 68, 69, 32], one, instead of introducing the extremum point operators, takes a “*matrix element*”, i.e., a certain component of the tensor related to a cut knot diagram, or, more precisely, a linear combinations of these components, the coefficients provide the RI invariance. This approach can be shown to be equivalent to the extremum point operators approach [58], but we are not to go in details the present text.

7.4.7 Examples of using the covariant approach

One can still operate in covariant terms of the turn-over operators at least in certain particular cases.

To complete our discussion on the turn-over operators, let is illustrate that the covariant “one operator for one loop” approach works at least in particular cases. We consider explicitly three examples of the knot, corresponding to the closure of a two-strand braid, a multiply intertwined circle, and to a pair of counter-oriented strands that can be separated in the three-dimensional space. Each case has its own points to discuss. It seems especially interesting to us that the topological invariance constrains can be formulated, at least for the particular case of the (su_N fundamental) R - and M -matrices that we consider, intermediately for the operator products, not only for the full contractions that yield the knot invariants.

Examples. I. Two-strand braids. We start with evaluating the invariant of a torus knot or link $T^{2,n}$, presented as the closure of a two-strand braid with n crossings. A main subtlety arises here is that one should insert the *different* turn-over operators for the counter-clock wise and clock-wise

closures. The obtained values of the invariant yet must be the same.⁷ Below we demonstrate this being indeed true for turn-over operators (7.22,7.30), although looking out as a non-trivial fact.

A two-strand braid with n crossings corresponds to an operator (all scripts run from 1 to N),

$$h_{kl}^{ij} \equiv \mathcal{R}_{j_2 i_2}^{i_1 j_1} \mathcal{R}_{j_3 i_3}^{i_2 j_2} \dots \mathcal{R}_{l_k}^{i_n j_n}. \quad (7.47)$$

The matrix forms of the operators are (R differs from \mathcal{R} by the permutation of the subscripts, $\mathcal{R}_{kl}^{ij} \equiv R_{lk}^{ij}$, and matrix indices are a multi-index $I = (ij)$ with i, j running from 1 to N and $i < j$)

$$R = \begin{array}{c|c|c} \dots & ii & \dots & \dots & ij & ij & \dots & \vdots \\ \vdots & & & & & & & ii \\ & q & & & & & & \vdots \\ & & \ddots & & & & & \vdots \\ \hline & & & \ddots & & & & \vdots \\ & & & & q - q^{-1} & 1 & & ij \\ & & & & 1 & & & ji \\ & & & & & & \ddots & \vdots \end{array}, \quad (7.48)$$

and

$$B = R^n = \begin{array}{c|c|c} \dots & ii & \dots & \dots & ij & ij & \dots & \vdots \\ \vdots & & & & & & & ii \\ & q & & & & & & \vdots \\ & & \ddots & & & & & \vdots \\ \hline & & & \ddots & & & & \vdots \\ & & & & P_{n+1} & P_n & & ij \\ & & & & P_n & P_{n-1} & & ji \\ & & & & & & \ddots & \vdots \end{array}, \quad (7.49)$$

where $P_n = P_n(q)$ are determined from the recurrent relations

$$P_0 = 0, \quad P_1 = 1, \quad P_{n+1} = (q - q^{-1}) P_n + P_{n-1} \quad \Rightarrow \quad P_n = \sum_{k=0}^{n-1} (-1)^k q^{n-2k-1} = \frac{q^n + (-1)^{n+1} q^{-n}}{[2]}. \quad (7.50)$$

All the non-zero matrix elements of B have the form either h_{ij}^{ij} or h_{ji}^{ij} , i.e., the subscripts are a permutation of the superscripts. Hence, the partial contraction corresponding to closing of the second strand is diagonal in the selected basis,

$$b_l^i \equiv h_{kl}^{ij} \mathcal{M}_j^l = \sum_{l=1}^N h_{lk}^{ik} m_k = \delta_l^i \sum_{k=1}^N h_{ik}^{ik} m_k \equiv b_i \delta_l^i. \quad (7.51)$$

Moreover, all diagonal elements turn out to be equal to each other,

$$\begin{aligned} b_i &= h_{ii}^{ii} m_i + \sum_{j=1}^{i-1} h_{ij}^{ij} m_j + \sum_{j=i+1}^N h_{ij}^{ij} m_j = q^n m_i + P_{n+1} \sum_{j=1}^{i-1} m_j + P_{n-1} \sum_{j=i+1}^N m_j = \\ &= q^n \sum_{i=1}^N m_i - P_n \left(q \sum_{j=1}^{i-1} m_j + q^{-1} \sum_{j=i+1}^N m_j \right) = q^n [N] - P_n [N-1]. \end{aligned} \quad (7.52)$$

⁷The two described planar figures, although representing the same braid closure, can *not* be continuously transformed one into the other in the projection plane. The mirror reflection of an arc, which relates two such figures, should be considered as one more equivalence transformation of a knot diagram, the transformation being referred to as *zero Reidemeister move*. We did not consider this transformation yet, because the tensor contractions associated with the two diagrams in the state model approach, as well as the related to them the braid group elements in another approach, coincide *identically*, and the same is true for averages of these quantities. However, the situation turns different as soon one introduces the turn-over operators.

where we substituted $m_i = q^{N-2i+1}$ and used the relations

$$P_{n+1} = q^n - q^{-1}P_n \quad \text{and} \quad P_{n-1} = q^n - qP_n, \quad (7.53)$$

following from (7.50). Substituting the explicit expression for P_N from (7.50) into (7.51), one obtains that partial contraction (7.51) takes form

$$h_{kl}^{ij} \mathcal{M}_j^l = \delta_l^k \left(\frac{q^n [N+1] + (-1)^n q^{-n} [N-1]}{[2]} \right) \equiv \delta_l^k \mathcal{H}_r^{2,n}, \quad (7.54)$$

where a factor of delta-symbol is the *reduced* HOMFLY polynomial for the $T^{2,n}$ knot or link, which is the closure of the considered braid. Hence, both possible full contractions give the *unreduced* HOMFLY polynomial of the same link,

$$h_{kl}^{ij} \mathcal{M}_j^l \mathcal{M}_i^k = h_{kl}^{ij} \mathcal{M}_j^l \mathcal{M}_i^k = \mathcal{M}_i^i \mathcal{H}_r^{2,n} = \mathcal{M}_i^i \mathcal{H}_r^{2,n} = [N] \mathcal{H}_r^{2,n} \equiv \mathcal{H}^{2,n}. \quad (7.55)$$

II. Multiply intertwined circle. The next example that we consider is a two-strand antiparallel braid. According to the general rule, one should insert the turn-over operators not only in the “closure”, but in *each* section, since a section of an antiparallel braid is related to a cycle (fig.11). We restrict ourselves by considering the simplest case, when the strands of the braids are matched as in fig.11, so that the braid can be unplaited in the three-dimensional space. We demonstrate explicitly that the proper partial contraction of the R - and M - matrices is proportional to the unity operator, as it should be.

An antiparallel two-strand braid one can associate with the contraction of the crossing and turn-over operators

$$\mathcal{R}_{kl}^{ia} \mathcal{M}_a^j \mathcal{R}_{jm}^{nb} \mathcal{M}_b^k \dots \equiv (RM)^n, \quad (7.56)$$

where for R one should substitute the sl_n solution

$$R_{ii}^{ii} = q, \quad R_{ij}^{ij} = 1 \text{ for } i \neq j, \quad R_{ji}^{ji} = q - q^{-1} \text{ for } i < j, \quad (7.57)$$

and M is determined form the RI invariance condition (are factor of q^{-N} is present since we use the so called topological framing, which is a separate story),

$$R_{bj}^{ia} M_a^b = q^{-N} \delta_j^i \quad \Rightarrow \quad M_a^b = m_a \delta_a^b, \quad m_a = q^{N-2a+1}. \quad (7.58)$$

The matrix forms of the operators are

$$R = \begin{pmatrix} S_{N \times N} & \\ & \text{Id}_{N(N-1)} \end{pmatrix}, \quad S = \begin{pmatrix} q & & & \\ q - q^{-1} & q & & \\ q - q^{-1} & q - q^{-1} & q & \\ \dots & \dots & \dots & \dots \end{pmatrix}, \quad (7.59)$$

and $M = \text{diag}(m_1, m_2, \dots, m_N, 0, \dots, 0)$. The “fake” closure on the one end gives an n times intertwined line; the corresponding partial contraction might be

$$\mathcal{M}_l^k \mathcal{R}_{kl}^{ia} \mathcal{M}_a^j \mathcal{R}_{jm}^{nb} \mathcal{M}_b^k \dots \equiv \mu (RM)^n = q^{-Nn} (1, 1, \dots, 1, 0, \dots, 0) = q^{-Nn} \delta_q^p, \quad (7.60)$$

with $\mu = (m_1, m_2, \dots, m_N, 0, \dots, 0)$. Hence, the RI invariance holds as an operator identity in this particular case, if one inserts one turn-over operator for one cycle.

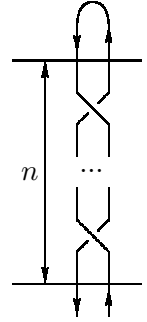


Figure 11: The “fake closure” of the antiparallel braid.

III. Loop version of RII. As the last example, let us demonstrate that relation (7.39) holds as an operator identity provided that one inserts the turn-over operator in the loop,

$$\mathcal{R}_{bl}^{ia} \tilde{\mathcal{R}}_{ka}^{cj} \mathcal{M}_c^a = \delta_k^i \mathcal{M}_l^j. \quad (7.61)$$

Indeed, using explicit expressions (7.3) and (7.22) for elements of the \mathcal{R} - and \mathcal{M} -matrices, one obtains for the components of (7.61) that do not vanish identically,

$$\begin{aligned} i = k = j = l, \quad \sum_{a=1}^N \mathcal{R}_{aj}^{ja} \tilde{\mathcal{R}}_{ja}^{aj} m_a &= \mathcal{R}_{jj}^{jj} \tilde{\mathcal{R}}_{jj}^{jj} m_j = qq^{-1} m_j = m_j, \\ i = k \neq l = j, \quad \sum_{a=1}^N \mathcal{R}_{ai}^{ia} \tilde{\mathcal{R}}_{ja}^{aj} m_b &= \mathcal{R}_{ij}^{ij} \tilde{\mathcal{R}}_{ij}^{ij} m_i = 1 \cdot 1 \cdot m_i = m_i, \\ i = l \neq k = j, \quad \sum_{a=1}^N \mathcal{R}_{bj}^{ia} \tilde{\mathcal{R}}_{ia}^{bj} m_b &= \mathcal{R}_{ii}^{ii} \tilde{\mathcal{R}}_{ji}^{ij} m_i + \sum_{a=i+1}^{j-1} \mathcal{R}_{ai}^{ia} \tilde{\mathcal{R}}_{ja}^{aj} m_a + \mathcal{R}_{ji}^{ij} \tilde{\mathcal{R}}_{jj}^{jj} m_j, \end{aligned} \quad (7.62)$$

i.e., in all cases one reproduces the r.h.s. of (7.61), which equals $\delta_k^i \delta_l^j m_j$.

7.5 Explicit evaluation of the invariant for the trefoil knot

After all discussions, we are finally ready to complete an explicit evaluation of the studied invariant for the simplest knot, which is the trefoil knot. The \mathcal{R} matrix construction dictates, with all conclusions and assumptions of sec.7.2-7.3 taken into account, to related with the knot diagram in 12 the expression

$$q^{-wN} \sum_{\substack{i,j,k,l, \\ a,b,c,d}} R_{ai}^{kc} R_{bl}^{ia} R_{dj}^{lb} \mathfrak{M}_c^d \mathfrak{M}_k^j = q^{-3N} \sum_{\substack{i,k,l, \\ a,b,c}} R_{ai}^{kc} R_{bl}^{ia} R_{ck}^{lb} \mathfrak{m}_c \mathfrak{m}_k. \quad (7.63)$$

Form of solution (7.3) for \mathcal{R} -matrix implies that scripts of the non-zero summands in (7.63) are related according to one of the lines in the tabular

	$k \ c$	$i \ a$	$l \ b$	k	c
	$a \ i$	$b \ l$	$c \ k$	c	k
$k = a = l = c = i = b$	$i \ i$	$i \ i$	$i \ i$	i	i
	$i \ i$	$i \ i$	$i \ i$	i	i
$k = a = l < c = i = b$	$k \ i$	$i \ k$	$k \ i$	k	i
	$k \ i$	$i \ k$	$i \ k$	i	k
$k = a = b < c = i = l$	$k \ i$	$i \ k$	$i \ k$	k	i
	$k \ i$	$k \ i$	$i \ k$	i	k
$k = i = b < c = a = l$	$k \ l$	$k \ l$	$l \ k$	k	l
	$l \ k$	$k \ l$	$l \ k$	l	k
$k = a = b = c = i = l < k$	—				
$k = i = b = c = a = l < k$	—				
$k = i = l = c = a = b < k$	—				
$k = i = l < c = a = b$	$k \ a$	$k \ a$	$k \ a$	k	a
	$a \ k$	$a \ k$	$a \ k$	a	k

(7.64)

Assembling all listed in (7.64) contributions and substituting the values of the R -matrix elements from (7.3), we get

$$\begin{aligned} H_N^{31} &= q^{-3N} \left\{ \sum_{i=1}^N R_{ii}^{ii} R_{ii}^{ii} R_{ii}^{ii} \mathfrak{m}_i \mathfrak{m}_i + \sum_{\substack{i,k=1, \\ i < k}}^N \left(3R_{ik}^{ik} R_{ik}^{ik} R_{ki}^{ik} + R_{ik}^{ki} R_{ik}^{ki} R_{ik}^{ki} \right) \mathfrak{m}_i \mathfrak{m}_k \right\} \equiv \\ &\equiv q^{-3N} \left\{ q^3 \alpha_N + (3(q - q^{-1}) + (q - q^{-1})^3) \beta_N \right\} = q^{-3N} \left\{ q^3 (\alpha_N + \beta_N) - q^{-3} \beta_N \right\}, \end{aligned} \quad (7.65)$$

where we introduced the notations

$$\alpha_N \equiv \sum_{i=1}^N (\mathfrak{m}_i)^2, \quad \beta_N \equiv \sum_{\substack{i,k=1, \\ i < k}}^N \mathfrak{m}_i \mathfrak{m}_k \quad \Rightarrow \quad \alpha_N + \beta_N = \sum_{\substack{i,k=1, \\ i \leq k}}^N \mathfrak{m}_i \mathfrak{m}_k. \quad (7.66)$$

Calculating the sums explicitly for \mathbf{m} from (7.22), we obtain them to be related with the already familiar from sec.6.4 quantities,

$$\begin{aligned}\beta_N &= \sum_{1 \leq i < j \leq N} q^{2i+2j-2N-2} = \frac{[N][N-1]}{[2]} = \chi_{11}, \\ \alpha_N + \beta_N &= \sum_{1 \leq i \leq j \leq N} q^{2i+2j-2N-2} = \frac{[N][N+1]}{[2]} = \chi_2.\end{aligned}\tag{7.67}$$

Finally, we get the answer

$$H_N^{3_1}(N, q) = q^{-3N} \left\{ q^3 \frac{[N][N+1]}{[2]} - q^{-3} \frac{[N][N-1]}{[2]} \right\}.\tag{7.68}$$

The formula enables an analytic continuation to arbitrary values of N , merely by substituting q^N for a new independent variable A . Divided by the value of the invariant for the unknot $[N] \equiv \frac{A-A^{-1}}{q-q^{-1}}$, the resulting expression yields the HOMFLY polynomial for the trefoil knot [1] (with $a = A^{-1}$ and $z = q - q^{-1}$),

$$\mathcal{H}_N^{3_1}(A, q) = \frac{A^{-3}}{[2]} \left\{ q^3 \frac{Aq - A^{-1}q^{-1}}{q - q^{-1}} - q^{-3} \frac{Aq^{-1} - A^{-1}q}{q - q^{-1}} \right\} = A^{-2}(q^2 + q^{-2}) - A^{-4}.\tag{7.69}$$

7.5.1 Mirror symmetry

If one changes all crossings in fig.12-I for the inverse ones, one obtains the knot diagram in fig.12-II. Evaluation of the associated knot invariant repeats the above calculation almost literally, with only difference that the operators R and \mathfrak{M} are substituted by the corresponding inverse operators \tilde{R} and $\tilde{\mathfrak{M}}$. The matrix elements of the latter ones are given by (7.11,7.13), and (7.31), respectively, and they are obtained from the corresponding elements of R and \mathfrak{M} by substituting $q \rightarrow q^{-1}$. In addition, the writhe number in the framing factor changes for the opposite one. Hence, the answer for the reflected diagram is

$$H_N^{\tilde{3}_1}(N, q) = H_N^{3_1}(N, q^{-1}) = q^{3N} \left\{ q^{-3} \frac{[N][N+1]}{[2]} - q^3 \frac{[N][N-1]}{[2]} \right\}.\tag{7.70}$$

Expressions (7.68) and (7.70) are *different*, they are not even proportional to each other. This agrees with the inequivalence of knots represented by diagrams in figs.12-I and II, which are named as *left-* and *right-*hand trefoils, respectively. The above reasoning applies to an arbitrary knot diagram, and one obtains that the HOMFLY polynomials of the knot \mathcal{K} and its mirror image $\tilde{\mathcal{K}}$ are related as $H^{\tilde{\mathcal{K}}}(q) = H^{\mathcal{K}}(q^{-1})$.

In contrast to the considered transformation, reversing the orientation of a knot diagram (i.e., reflecting the directions of arrows) does *not* affect the answer at all, since all the direct crossings remain direct ones, and the inverse crossings remain the inverse ones (fig.12-III). The result is a diagram of the same knot, just projected on the “ceiling” instead of the “floor”.

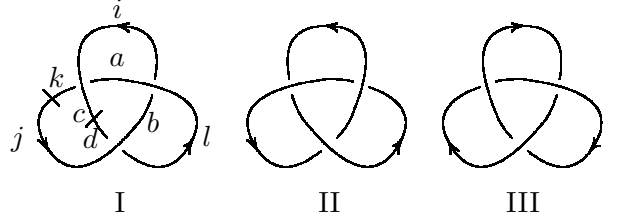


Figure 12: I. Cut diagram of the trefoil knot. II. Diagram of the reflected knot I, *inequivalent* to the original one. III. Another projection of knot I.

7.6 From \mathcal{R} -matrices approach to the braid group approach

In this section, we discuss how the \mathcal{R} -matrix approach is related to the braid group approach (see sec.6). A naive guess might be that the braid crossing operators B are just particular cases of the \mathcal{R} -matrix, written down in a certain basis. The real case is very close to that, but is still somewhat different. In the current section, we discuss the relation between the \mathcal{R} -matrices and the matrices representing the braid group elements, which we considered in sec.6, comparing them explicitly in the simplest examples.

As we already mentioned, the history went just the opposite way. The R -matrices approach was originally formulated applied to braids only [90, 79]. The method was then developed into a fine working computational tool in the same terms, and was extended to wider class of knot representations only recently [43, 44, 45, 11, 13, 98, 97, 13, 68, 69, 32, 86, 83, 46]. Constructing a consistent R -matrix formalism valid for *arbitrary* knot diagrams is a separate problem [71], and it is still far from being solved exhaustively.

7.6.1 Reduction of four-indices operators to matrices. Twisted R -matrices

A serial connection of crossings, as in fig.13, is associated with a contraction of the R -matrices in a *pair* of indices, as we already have considered when we considered the second Reidemeister move. Such a combination can be considered as a matrix product. Namely, one can introduce a *twisted* R -matrix, which differs by a permutation of the subscripts

$$\mathcal{R}_{kl}^{ij} \equiv R_{lk}^{ij}. \quad (7.71)$$

In both matrices the superscripts are placed at the incoming and the lowers ones at the outgoing strands; however, while the two left scripts of R are related to the upper line w.r.t. to the projection plane, while the two left scripts of \mathcal{R} are related to the left strand in the braid. Contraction in fig.13 is rewritten by this trick as a matrix product

$$\sum_{a,b} R_{ba}^{ij} R_{lk}^{ab} = \sum_{a,b} \mathcal{R}_{ab}^{ij} \mathcal{R}_{kl}^{ab} \equiv \sum_J \mathcal{R}_J^I \mathcal{R}_K^J, \quad (7.72)$$

with the multi-indices I, J , and K standing for the pairs of indices (i, j) , (a, b) , and (k, l) correspondingly. The constraint due to the second Reidemeister move is rewritten then as

$$\sum_J \mathcal{R}_J^I \tilde{\mathcal{R}}_K^J = \delta_K^I \Rightarrow \tilde{\mathcal{R}}_J^I = (\mathcal{R}^{-1})_J^I, \quad (7.73)$$

i.e. successive crossings of mutually inverse orientations correspond to the mutually inverse matrices. Finally, the full contraction, associated with the braid closure, would corresponds to taking the trace, were not there the turn-over operators. Before proceeding with writing out the explicit expression, we discuss one more difference between regular and twisted R -matrices.

7.6.2 Eigenvectors of regular and twisted crossing operators in a two-strand braid

Generally, R (and hence \mathcal{R}) maps a tensor product of vector spaces, associated with the incoming strands to that of the ones associated with the outgoing strands. Since all the four spaces are of the same dimension, either R or \mathcal{R} (but not they both at the same time) can be looked at as an automorphism. In particular, one can find the eigenvalues and eigenvectors of these operators. As we will see in the next section, this will notably simplify the computation in case of several operators R contacted as in fig.14. From the practical point of view, these are eigenvalues of \mathcal{R} (not of R), which are needed, due to the multiplication rule (7.72). Yet, we explore the eigenvalue problem for both matrices to better demonstrate a difference in their properties.

The very form of (7.3) supposes that the entire N^2 -dimensional space spanned by $\xi_i \eta_j$ ($i, j = 1, \dots, n$) decomposes into a sum of N one-dimensional eigenspaces spanned by $\xi_i \eta_i$ ($i = 1, \dots, n$)



$$R_{ba}^{ij} R_{lk}^{ab}$$

Figure 13:
A pair of successive crossings.

and $\frac{N(N-1)}{2}$ two-dimensional spaces spanned by $\xi_i\eta_j$ and $\eta_j\xi_i$ ($i, j = 1, \dots, n$ and $i < j$). The same statement is valid for \mathcal{R} . Hence, one already has N coinciding eigenvalues $R_{ii}^{ii} = \mathcal{R}_{ii}^{ii} = q$ with the corresponding eigenvectors, both of R and \mathcal{R} :

$$\lambda_i = q, \quad X_i = \xi_i\eta_i, \quad i = 1, \dots, N. \quad (7.74)$$

It remains to examine one of $\frac{N(N-1)}{2}$ identical two-dimensional spaces. Making use of expression (7.3) for $i < j$, one gets the eigenvalue problem for R

$$\sum_{i,j} R_{kl}^{ij} (\alpha\xi_i\eta_j + \beta\xi_j\eta_i) = \alpha\xi_k\eta_l + ((q - q^{-1})\alpha + \beta)\xi_l\eta_k = \lambda(\alpha\xi_k\eta_l + \beta\xi_l\eta_k), \quad (7.75)$$

whence $\lambda = 1$, $\alpha = 0$, and the only (for a given pair k, l) eigenvector is $\xi_k\eta_l$; there is also the adjoint vector $\xi_k\eta_l - \xi_l\eta_k$, i.e., R is a Jordan cell w.r.t. to the stated eigenvalue problem. Unlike that, \mathcal{R} , whose eigenvalue problem differs from (7.75) by a permutation of indices k and l in the last term of the equality, has two distinct eigenvalues; they are the two roots of the characteristic equation

$$\lambda^2 - (q - q^{-1})\lambda - 1 = 0, \quad (7.76)$$

which, in turn is obtained as consistency condition of the system

$$\lambda\beta = \alpha, \quad (7.77)$$

$$\lambda\alpha = (q - q^{-1})\alpha + \beta, \quad (7.78)$$

on the eigenvectors components. Hence, the eigenvalues and the corresponding eigenvectors are

$$\lambda_+ = q, \quad x_{ij}^+ = q\xi_i\eta_j + \xi_j\eta_i, \quad (7.79)$$

$$\lambda_- = -1/q, \quad x_{ij}^- = \xi_i\eta_j - q\xi_j\eta_i. \quad (7.80)$$

The observed difference between R and \mathcal{R} is considered especially well from the matrix form of their corresponding cells; say, one has for i, j running the values 1, 2

$$\begin{aligned} R_{(12)}^{(12)} &\equiv \begin{pmatrix} R_{12}^{12} & R_{21}^{12} \\ R_{12}^{21} & R_{21}^{21} \end{pmatrix} = \begin{pmatrix} 1 & q - q^{-1} \\ 0 & 1 \end{pmatrix}, \\ \mathcal{R}_{(12)}^{(12)} &\equiv \begin{pmatrix} R_{21}^{12} & R_{12}^{12} \\ R_{21}^{21} & R_{12}^{21} \end{pmatrix} = \begin{pmatrix} q - q^{-1} & 1 \\ 1 & 0 \end{pmatrix}. \end{aligned} \quad (7.81)$$

Following the general rule, one obtains the eigenvalues and the eigenvectors of the inverse R - and \mathcal{R} -matrices by the substituting $q \rightarrow q^{-1}$. It is straightforward to check that the eigenvectors of the straight and inverse operators coincide.

7.6.3 Turn-over operators in a two-strand braid and character decomposition

As discussed above, an operator contraction yielding a knot invariant contains not only the crossing operators, but also the turn-over operators, their explicit form determined in sec.7.4.2, for crossing operators of form (7.3). Two turn-over operators are needed in the case, since a two strand braid is obtained from its closure by making two cuts. Modulo discussion of sec.7.4.2-7.6, one should write

$$H_N^n(q) \equiv \sum_{\substack{a,b,\dots,c,d \\ i,j,p,q}} \mathcal{R}_{ab}^{ij} \dots \mathcal{R}_{pq}^{cd} \mathfrak{M}_i^p \mathfrak{M}_j^q = \sum_{\substack{A,\dots,C \\ I,P}} \mathcal{R}_A^I \dots \mathcal{R}_P^C (\mathfrak{M} \otimes \mathfrak{M})_I^P = \text{Tr} \{ \mathcal{R}^n \mathfrak{M} \otimes \mathfrak{M} \} \quad (7.82)$$

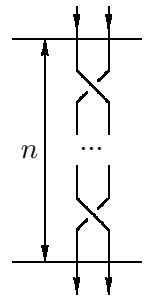


Figure 14: A two-strand braid with n crossings.

with n being the number of crossings in the braid, a positive or negative integer number depending on their orientation (see fig.7).

The tail of the obtained contraction, $\mathfrak{M}_i^p \mathfrak{M}_j^q$, is permutation under a permutation of i and j . Hence, both tensor monomials in expression (7.75), $\xi_i \eta_j$ and $\xi_j \eta_i$, are multiplied at the end of (7.82) on the same factor, thus remaining the eigenvectors of the entire operator $\mathcal{R}^n \mathfrak{M} \otimes \mathfrak{M}$. Moreover, since eigenvectors (7.75) form a basis, the trace can be evaluated as a sum of eigenvalues of the standing under the trace sign product corresponding to all eigenvectors (7.74,7.79,7.80). Similarly to the examples of sec.7.4.3-7.5, each eigenvalue is multiplied on a matrix element of the squared turn-over operator,

$$H_N^n(q) = q^n \underbrace{\sum_{i=1}^N m_i m_i}_{X_i = \xi_i \eta_i} + q^n \underbrace{\sum_{\substack{i,j=1 \\ i < j}}^N m_i m_j}_{x_{ij}^+ = q \xi_i \eta_j + \xi_j \eta_i} + (-q)^{-n} \underbrace{\sum_{\substack{i,j=1 \\ i < j}}^N m_i m_j}_{x_{ij}^- = \xi_i \eta_j - q \xi_j \eta_i} = q^n \alpha_N + (q^n + (-q)^{-n}) \beta_N, \quad (7.83)$$

so that the multiples of similar factors assemble into the quantities α_N and β_N , which we introduced and evaluated in sec.7.5. Substituting the corresponding expressions, one gets

$$H_N^n(q) = q^n \frac{[N][N+1]}{[2]} + (-q)^{-n} \frac{[N][N-1]}{[2]} \quad (7.84)$$

coincides with (6.22) obtained in (6) by the braid group method. The one by one blocks, associated in sec.6 with the symmetric and antisymmetric representations of the permutation group, arose here as eigenvalues of the R -matrix. This is not a coincidence; as was already mentioned in sec.6.1.1, the blocks can be obtained as the eigenvalues of the Hecke algebra, which is an extension of the permutation group [54]. A major difference of the \mathcal{R} -matrices from the braid crossing operators is that the first one has degenerate eigenvalues, q (the ‘‘permutation’’ one) with the multiplicity $\frac{N(N+1)}{2}$, $-q^{-1}$ (the ‘‘antisymmetric’’ one) with the multiplicity $\frac{N(N-1)}{2}$, for the \mathcal{R} -matrix of form (7.3). When one evaluates trace (7.82), each degenerate eigenvalue is multiplied on the trace of the squared turn-over operator over the corresponding ‘‘symmetric’’ and ‘‘antisymmetric’’ subspaces. As a result, one obtains just the weight coefficients, which were determined in (6.22) as solutions of the topological invariance constraints (although (7.84) reproduces just a particular case of (6.22) with $\lambda = q$, $\mu = -q^{-1}$, $\chi = [N]$). Although we solved the topological invariance constraints to determine the matrix elements of the turn-over operators, an explicit expression for the very operators is available in group theory, at least in the particular case of braid representations [79], [71]. It is clear from the form of this expression, that the coefficients of the R -matrix eigenvalues q and q^{-1} are nothing but the *quantum dimensions* of the first symmetric and antisymmetric $SU(N)$ representations, respectively. We came to the same result twice, in 6.22 and in 7.84, with help of straightforward computations.

7.6.4 Common eigenspaces of twisted crossing operators in a three-stand braid

One can derive a generalization of (7.82) for an arbitrary braid [79, 71, 18]. An additional difficulty one encounters with is a presence of several kinds of crossings, each one bringing a contribution to (7.82) of its own form. E.g., there will be two distinct operators for two kinds of crossings in a three-strand braid (fig.15). The operators do not commute, and, hence, can not have a basis of common eigenvectors. Nevertheless, they do have a number of common eigenvectors, while the complimentary subspace decomposes into a sum of two-dimensional common eigenspaces. We demonstrate this explicitly in what follows.

An braid version of the R -matrix approach provides an illustration the fact that twisted R -matrices form the group, which extends the permutation group [91]. Namely, solution to (7.3) for the operator R_{kl}^{ij} can be considered as so referred to q -permutation operator,

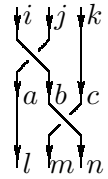


Figure 15: A fragment of a three-strand braid.

whose action is defined on a tensor product of vector spaces $V \otimes V$ as

$$R(q)\xi_i\eta_j = \begin{cases} \xi_j\eta_i, & i > j \\ q\xi_i\eta_i, & i = j, \\ (q + q^{-1})\xi_i\eta_j + \xi_j\eta_i, & i < j. \end{cases} \quad (7.85)$$

where ξ and η are vectors of V , the subscripts run from 1 to $\dim V$. In particular, common eigenspaces of braid R -matrices are constructed similarly to irreducible representations of the permutation group (see sec.6.2). To make this analogy explicit, we briefly review the corresponding formulas from sec.6, this time presenting them in a form generalizable for R -matrices case.

First, let us notice that two irreducible representations (6.16) of rank two permutation group can be rewritten by introducing two linear operators, which are called, correspondingly, symmetriser and antisymmetrizer:

$$(xy) = \frac{1}{2}(\mathbb{1} + b_1) \equiv Sxy, \quad [xy] - \frac{1}{2}(\mathbb{1} - b_1) \equiv Axy, \quad (7.86)$$

and satisfy

$$S^2 = S, \quad A^2 = A, \quad SA = AS = 0, \quad S + A = 1, \quad (7.87)$$

thus being the orthogonal projectors. Relations (7.87) follow straight from definitions (7.86) and from the property $b_1^2 = \mathbb{1}$ of the permutation group generator. The irreducible representations of the permutation group can be determined just in terms of the introduced operators. Since

$$b_1S = S, \quad b_1A = -A, \quad (7.88)$$

any vectors of type SX and AX are eigenvectors of b_1 with the eigenvalues 1 and -1 correspondingly. Similarly, one can introduce three pairwise orthogonal projectors on the common eigenspaces of the permutation group with three elements,

$$\begin{aligned} X_S = (xyz) &= \frac{1}{6}(\mathbb{1} + b_1 + b_2 + b_1b_2 + b_2b_1 + b_1b_2b_1) \equiv SSxyz, \\ X_{SA} &= \frac{1}{2}(1 + b_1)(a + bb_1b_2 + cb_2b_1)xyz \equiv SAxyz, \\ X_A = [xzy] &= -\frac{1}{6}(\mathbb{1} - b_1 - b_2 + b_1b_2 + b_2b_1 - b_1b_2b_1) \equiv AAxyz, \end{aligned} \quad (7.89)$$

so that

$$\begin{aligned} AA \cdot SS = SS \cdot AA = SA \cdot SS = SS \cdot SA = SA \cdot AA = AA \cdot SA = 0, \\ SS^2 = SS, \quad SA^2 = SA, \quad AA^2 = AA. \end{aligned} \quad (7.90)$$

One can verify then, that operators SS_q , AA_q , and S_qSA_q give the projectors on three distinct irreducible representations of the permutation group. In case of the one-dimensional representations, one has to check that $b_1SS = b_2SS = SS$ and $b_1AA = b_2AA = -AA$; this is done by substituting for SS and AA their explicit expressions (7.89) and using that $b_1^2 = b_2^2 = 1$. For the two-dimensional representation, one gets $b_1S \cdot AS = S \cdot AS$, and the check reduces then to ensuring that the expressions S_qSA_q , $b_2S_qSA_q$, and $b_1b_2S_qSA_q$ are linearly dependent, treated as formal polynomials in group generators. This indeed follows from (7.89) given that the squared group generators are the unities:

$$\begin{aligned} \underbrace{\begin{array}{rcl} S \cdot SA & = & 2 \quad +2b_1 \quad -b_2 \quad -b_1b_2 \quad -b_2b_1 \quad -b_1b_2b_1, \\ b_2S \cdot SA & = & -1 \quad -b_1 \quad +2b_2 \quad -b_1b_2 \quad +2b_2b_1 \quad -b_1b_2b_1, \\ b_1b_2b_2SAS & = & -1 \quad -b_1 \quad -b_2 \quad +2b_1b_2 \quad -b_2b_1 \quad +2b_1b_2b_1 \end{array}} \\ \Downarrow \\ (\mathbb{1} + b_2 + b_1b_2)SA = 0. \end{aligned} \quad (7.91)$$

Identity (7.91) implies that any expression of the form $S \cdot SAX$, where X is a formal polynomial in permutations, generates a two-dimensional representation of the permutation group with three elements. Moreover, matrix expressions for group generators in this representations, e.g., (6.38), can be derived from the operator identities

$$\begin{aligned} b_1 \cdot \mathbb{1} &= b_1, & b_1 \cdot \frac{1+2b_2}{\sqrt{3}} &= -\frac{1+2b_2}{\sqrt{3}}, \\ b_2 \cdot \mathbb{1} &= -\frac{1}{2}\mathbb{1} + \frac{\sqrt{3}}{2} \cdot \frac{1+2b_2}{\sqrt{3}}, & b_2 \cdot \frac{1+2b_2}{\sqrt{3}} &= \frac{\sqrt{3}}{2} \cdot \mathbb{1} + \frac{1}{2} \cdot \frac{1+2b_2}{\sqrt{3}}. \end{aligned} \quad (7.92)$$

Similar formulas can be derived for permutation groups with more elements. Then, there is a one-to-one correspondence of the permutation group irreducible representations and common eigenspaces of the braid R -matrices [79, 18]. Moreover, the partition-based approach discussed a little in sec.6.3.3 can be extended to determine the common eigenspaces of the braid R -matrices explicitly [18, 9], in principle, for arbitrary braids. The only reservation should be done here. Practically, the common eigenspaces are found not as irreducible representations of q -permutation group, but as that of the quantum group $U_q(SU(N))$, the two ones are related by the analog of Schur-Weyl duality [64],[42],[31]. An output is an explicit expression for knot polynomials in terms of eigenvalues of quantum R -matrices and quantum Racah coefficients [79],[18]. The first ones are known in full generality, hence the entire problem is concentrated in evaluating the second ones. While the case of $SU(2)$ group is a rather textbook subject [60], a breakthrough beyond was made just recently [45, 87, 46]. In the particular case of R -matrices we discuss here, which are related to the fundamental representation of the quantum group $SU(N)$ and give rise to the HOMFLY polynomials, all needed ingredients are determined explicitly, and a concise and computationally effective procedure is available [10]. The same tools enables to calculate colored HOMFLY polynomials as well, by means of the cabling procedure [13]. Finally, an attempt of applying the approach to studies of superpolynomials was recently performed [12], in the framework of elaborating a modified Khovanov formalism [92].

As usual, we illustrate the approach discussed on the simplest relevant example, that of braid R -matrices for a three-strand braid. We start from recalling the even simpler case of the two-strands. The generalizations of (7.86) by definition satisfy

$$S_q^2 = S_q, \quad A_q^2 = A_q, \quad S_q A_q = A_q S_q = 0, \quad (7.93)$$

and

$$R_1 S_q = q S_q, \quad R_1 A_q = -q^{-1} A_q. \quad (7.94)$$

The operators S_q and A_q are referred to as, correspondingly, q -symmetrizer and q -antisymmetrizer; explicit expressions for them are

$$S_q \equiv \frac{1}{q[2]_q} (\mathbb{1} + q R_1), \quad (7.95)$$

$$A_q \equiv -\frac{q}{[2]_q} (\mathbb{1} - q^{-1} R_1), \quad (7.96)$$

and properties (7.93, 7.94) are verified with help of generalization of the identity $\sigma_1^2 = 1$ for the permutation group generator:

$$R_1^2 - (q - q^{-1}) R_1 - \mathbb{1} = 0 \quad (7.97)$$

Relation (7.75) is a characteristic equation for the braid R -matrix, whose eigenvalues were determined in sec.7.6.2.

In case of three-strand braid, the relevant extension of formulas for the permutation group are less straightforward. Yet, they remain rather simple for projectors on fully permutation and anti-permutation representations. These projectors must satisfy

$$SS_q^2 = SS_q, \quad AA_q^2 = AA_q, \quad SS_q AA_q = AA_q SS_q = 0, \quad (7.98)$$

and

$$R_1SS_q = R_2SS_q = qSS_q, \quad R_1AA_q = R_2AA_q = -q^{-1}AA_q. \quad (7.99)$$

Explicit expressions for SS_q and AA_q are straightforward analogues of formulas (7.89) for SS and AA ; permutation group generators are substituted by the corresponding R -matrices, a factor of q^k is put before a product of k R -matrices, and the normalization factors are changed so that the first and second of equalities (7.98) are satisfied:

$$SS_q \equiv \frac{1}{q^3[2]_q[3]_q} (\mathbb{1} + qR_1 + qR_2 + q^2R_1R_2 + q^2R_2R_1 + q^3R_1R_2R_1), \quad (7.100)$$

$$AA_q \equiv -\frac{q^3}{[2]_q[3]_q} (\mathbb{1} - q^{-1}R_1 - q^{-1}R_2 + q^{-2}R_1R_2 + q^{-2}R_2R_1 - q^{-3}R_1R_2R_1). \quad (7.101)$$

Satisfying of (7.98) and (7.99) is checked with help of (7.75), a similar identity for R_2 , and the Yang-Baxter equation, which in the case takes the form $R_1R_2R_1 = R_2R_1R_2$. An expression for the remaining projector (denote it AS_q) is more involved; the easiest way to obtain it is:

$$AS_q = \mathbb{1} - SS_q - AA_q = \frac{1}{[3]_q} (R_1 - R_2)^2; \quad (7.102)$$

the equalities

$$AS_q^2 = AS_q, \quad AS_qSS_q = SS_qAS_q = AS_qAA_q = AA_qAS_q = 0, \quad (7.103)$$

follow then just from (7.98).

Relations (7.99) already imply that SS_q and AA_q are projectors on the common eigenvectors of R_1 and R_2 , i.e., that for X being any formal polynomial in R -matrices, SS_qX and AA_qX are the eigenvectors, with the values q and $-q^{-1}$, correspondingly. It remains to verify that, in analogy with the permutation group case, the expression S_qAS_q yields a projector on a two-dimensional common eigenspace. One immediately gets that

$$R_1S_qAS_q = S_qAS_q. \quad (7.104)$$

An analog of (7.91) is also derived straightforwardly, though a bit lengthy. Using the eigenvalue equations for R_1 and R_2 , and the Yang-Baxter equation, one obtains that the operators S_qAS_q , $R_2S_qAS_q$, and $R_1R_2S_qAS_q$ are expanded over the six basis products of R -matrices as

	1	R_1	R_2	R_1R_2	R_2R_1	$R_1R_2R_1$
S_qAS_q	$q^2 + 1$	$q^3 + q$	q^{-1}	-1	-1	$-q$
$R_2S_qAS_q$	$-q^{-1}$	-1	$q^2 + q^{-2}$	$-q$	$q^3 + q^{-1}$	$-q^2$
$R_1R_2S_qAS_q$	-1	$-q$	$-q$	$1 + q^{-2}$	$-q^2$	$q + q^{-1}$

(7.105)

wherefrom one derives the identity:

$$(1 + qR_2 + q^2R_1R_2) S_qAS_q = 0. \quad (7.106)$$

Relations (7.104, 7.106) imply that a basis in a two-dimensional common eigenspace of the R -matrices is obtained from an arbitrary formal polynomial in R -matrices X as

$$S_qAS_qX \equiv \begin{pmatrix} 1 \\ 0 \end{pmatrix}, \quad R_2S_qAS_qX \equiv \begin{pmatrix} 0 \\ 1 \end{pmatrix}. \quad (7.107)$$

Alternatively, one can construct a basis of R_1 eigenvectors in the same space. Writing down the corresponding condition

$$R_1(\alpha + \beta R_2) S_qAS_q = \lambda(\alpha + \beta R_2) S_qAS_q \quad (7.108)$$

and solving the system

$$\begin{cases} q\alpha - \beta q^{-2} = \lambda\alpha, \\ \beta q^{-1} = \lambda\beta, \end{cases} \Leftrightarrow \begin{cases} \lambda = q, & \beta = 0, \\ \lambda = -q^{-1}, & \alpha = q^2[2]_q\beta, \end{cases} \quad (7.109)$$

one obtains the corresponding expressions for the basis vectors,

$$SS_qAS_qX \equiv \begin{pmatrix} 1 \\ 0 \end{pmatrix}, \quad \frac{1}{\sqrt{[3]_q}}(\mathbb{1} + q^2[2]_qR_2X)SS_qAS_qX \equiv \begin{pmatrix} 0 \\ 1 \end{pmatrix}, \quad (7.110)$$

and for acting on them R -matrices,

$$R_1 = \begin{pmatrix} 1 & 0 \\ 0 & -1 \end{pmatrix}, \quad R_2 = \begin{pmatrix} -\frac{1}{q^2[2]_q} & \frac{\sqrt{[3]_q}}{[2]_q} \\ \frac{\sqrt{[3]_q}}{[2]_q} & \frac{1}{[2]_q} \end{pmatrix}. \quad (7.111)$$

The result coincides with the formulas for the braid-crossing matrices, derived in the framework of the permutation group approach in sec.6.3.2.

The summary Content of the present section may be reviewed as follows. The contraction of the \mathcal{R} -matrix associated with a closure of a three-strand braid can be presented as a composition of linear operators of two types, $R_1 \equiv R \otimes I$ and $R_2 \equiv I \otimes R$. Both operators acts on the space $V \otimes V \otimes V$, where one can chose a basis of tensor monomials $\xi_i \otimes \xi_j \otimes \xi_k \in V$ composed of basis vectors ξ of the space V , the subscripts running from 1 to N . Operators R_1 and R_2 can be considered then as rank six tensors $(R_a)_{imn}^{ijk}$ for $a = 1, 2$. If we substitute (7.2) for R , all the non-zero elements have the form $(R_a)_{\sigma(ijk)}^{ijk}$, with the subscripts being a permutation of the superscripts. In other words, a linear space \mathcal{V}_{ijk} spanned by all the monomials $(\xi \otimes \xi \otimes \xi)_{\sigma(ijk)}$, where σ runs over all distinct permutations of ijk , is a common eigenspace of R_1 and R_2 . The dimension of this space equals one for $i = j = k$, two for $i = j \neq k$, and six for $i \neq j \neq k$. As we verified above, the subspace \mathcal{V}_{ijk} further decomposes into irreducible common eigenspaces of R_1 and R_2 , which are hence the common eigenspaces of all the three-strand operators. The irreducible common eigenspaces are either one- or two-dimensional, so that the operators R_1 and R_2 acting on these spaces are represented either by 1×1 or by 2×2 matrices. In a certain basis, the matrices reproduce the braid crossing matrices of sec.6.3.2.

The smallest common eigenspaces described above turn out to be nothing but the spaces of the permutation group irreducible representations, as the R -matrices eigenvalues q and $-q^{-1}$ tend to 1 and -1 , respectively. The same spaces for a generic q are the spaces of Hecke algebra (or q -permutation group) irreducible representations.

8 Conclusion

As a closing remark, let us note that this text does not apply in no sense for the full presentation of the questions we referred to. Although the text is a historical review, we have encountered with many subtleties of the discussed notions and constructions, some of them leading to open essential problem. As a conclusion, we formulate two such problem, which seem especially interesting to us.

The first problem is the already mentioned in the introduction problem of relating of the \mathcal{R} -matrix formalism to the perturbation theory for the Chern-Simons theory in the temporal gauge [70, 71]. We add now that a major difficulty on this way is that the \mathcal{R} -matrix is related (if does) to a Wilson line, the classical Chern-Simons fields at different points of the one not commuting with each other. Hence, examining the simple explicit examples of such fields, like the example presented in sec.4.2.2, might spread some light to the problem.

The second problem is to develop the covariant version of the \mathcal{R} -matrix approach, which would involve the turn-over operators instead of the extremum point operators. The problem has at least

two applications. First, a QFT interpretation of the \mathcal{R} -matrix formalism (if any) might be more natural for this version of the covariant version of the formalism. The second application concerns the attempts of involving elements of the \mathcal{R} -matrix approach in evaluating the superpolynomials of the knots [12]. Namely, the morphism act on the Seifert cycles on the resolved knot diagrams in the modified Khovanov contraction [92] might be expressed in terms of the turn-over operators.

Although the above problems thus far attracted undeservedly few attention, we hope for they being studied properly in the nearest future.

9 Acknowledgements

The author would like to thank G.Aminov, D.Vasiliev, D.Galakhov, A.Sleptsov, Sh.Shakirov, and all participants of the ITEP math.phys.group seminar for numerous fruitful discussions. Author is especially grateful to I.Daninlenko, P.Dunin-Barkowski, And.Morozov, A.Popolitov, for reading the preprint and making important remarks. Author also thanks G.Galakhov, S.Mironov and A.Sleptsov for useful comments to the second version. Author is indebted to E.Vyrodov for discussing the physical analogues, and to A.Mironov and A.Morozov for supervising the authors work on \mathcal{R} -matrices approach to knot invariants. The work was partially supported by RFBR grants 14-01-31492_mol_a, 14-01-92691_Ind_a, 15-31-20832_mol_a_ved, 15-51-50034_Yaf, NSH-1500.2014.2.

References

- [1] www.katlas.org.
- [2] www.indiana.edu/~knotinfo.
- [3] www.indiana.edu/~linkinfo.
- [4] <http://www.math.utk.edu/~morwen/knotscape.html>.
- [5]
- [6] M. D. G. A. J. Bracken and R. B. Zhang *Comm. Math. Phys.* **137:1** (1991) 13–21.
- [7] A.A.Belavin, A.M.Polyakov, A.S.Schwartz, and Yu.S.Tyupkin *Phys. Lett.* **B59** (1975) 85–87.
- [8] A.Alexandrov, A.Mironov, A.Morozov, and An.Morozov *JETP Lett.* **100** (2014) 271–278, [arXiv:1407.3754](https://arxiv.org/abs/1407.3754) [hep-th].
- [9] A.Anokhina, A.Mironov, A.Morozov, and An.Morozov *Nucl.Phys.* **B868** (2013) 271–313, [arXiv:1207.0279](https://arxiv.org/abs/1207.0279) [hep-th].
- [10] A.Anokhina, A.Mironov, A.Morozov, and An.Morozov *Adv. in High Energy Phys.* **2013** (2013) 931830, [arXiv:1304.1486](https://arxiv.org/abs/1304.1486) [hep-th].
- [11] A.Anokhina, A.Mironov, A.Morozov, and An.Morozov *Nucl.Phys.* **B882** (2014) 171–194, [arXiv:1211.6375](https://arxiv.org/abs/1211.6375) [hep-th].
- [12] A.Anokhina and A.Morozov *JHEP* **063:07** (2014) , [arXiv:1403.8087](https://arxiv.org/abs/1403.8087) [hep-th].
- [13] A.Anokhina and An.Morozov *Theor.Math.Phys.* **178** (2014) 1–58, [arXiv:1307.2216](https://arxiv.org/abs/1307.2216) [hep-th].
- [14] C. C. Adams, *The Knot Book: an Elementary Introduction to the Mathematical Theory of Knots*. New York: W.H.Freeman, 1994.
- [15] J. W. Alexander *Trans. Amer. Math. Soc.* **30:2** (1928) 275–306.

- [16] A.Mironov and A.Morozov *AIP Conf.Proc.* **1483** (2012) 189–211, [arXiv:1208.2282](#) [hep-th].
- [17] A.Mironov, A.Morozov, and And.Morozov *Strings, Gauge Fields, and the Geometry Behind: The Legacy of Maximilian Kreuzer*, edited by A.Rebhan, L.Katzarkov, J.Knapp, R.Rashkov, E.Scheidegger (World Scientific Publishins) 101–118, [arXiv:1112.5754](#) [hep-th].
- [18] A.Mironov, A.Morozov, and And.Morozov *JHEP* **34:3** (2012) , [arXiv:1112.2654](#) [hep-th].
- [19] A.Mironov, A.Morozov, and An.Morozov *AIP Conf. Proc.* **1562** (2013) , [arXiv:1306.3197](#) [hep-th].
- [20] A.Mironov, A.Morozov, and A.Sleptsov [arXiv:1412.8432](#) [hep-th].
- [21] A. A.Mironov [arXiv:1506.00339](#) [hep-th].
- [22] V. I. Arnold and A. Weinstein, *Mathematical Methods of Classical Mechanics*. Springer, 1997.
- [23] M. F. Atiyah *Proc. Symp. Pure Math.* **48** (1988) 285–299.
- [24] R. J. Baxter, *Exactly Solved Models in Planar Meachnics*. Academic Press Limited, San-Diego, 1989.
- [25] N. Bogolubov, A. A. Logunov, A. Oksak, and I. Todorov, *General Principles of the Quantum Field theory*. Springer Science & Business Media, 2012.
- [26] S.-S. Chern and J. Simons *Ann.Math.* **99** (1974) 48–69.
- [27] S. Chumkov, S. Duzhin, and J.Mostovoy [arXiv:1103.5628v3](#) [math.GT].
- [28] C. H. Clemens, *A Scrapbook of Complex Curve Theory*. American Mathematical Soc., 2002.
- [29] I. Danilenko [arXiv:1405.0884](#) [hep-th].
- [30] D.Bar-Natan *Algebr. Geom. Topol.* **2** (2002) 337–370, [arXiv:0201043](#) [math.QA].
- [31] C. D. Dennis Bonatsos *Prog.Part.Nucl.Phys.* **43** (1999) 537–618, [arXiv:9909003](#) [nucl-th].
- [32] D.Galakhov, D.Melnikov, A.Mironov, and A.Morozov (2015) , [arXiv:1502.02621](#) [hep-th].
- [33] D.Galakhov, D.Melnikov, A.Mironov, A.Morozov, and A.Sleptsov *Phys. Lett.* **B743** (2015) 71–74, [arXiv:1412.2616](#) [hep-th].
- [34] P. Dunin-Barkowski, A. Sleptsov, and A. Smirnov *J. Phys.* **A245** (2012) 385204, [arXiv:1201.0025](#) [hep-th].
- [35] P. Dunin-Barkowski, A. Sleptsov, and A. Smirnov *Int. J. Mod. Phys.* **A28** (2013) 1330025, [arXiv:1112.5406](#) [hep-th].
- [36] G. V. Dunne *Les Houches - Ecole d'Ete de Physique Theorique* **69** (1999) 177–263, [arXiv:9902115](#) [hep-th].
- [37] E.Guadagnini, M.Martellini, and M.Mintchev *Phys. Lett.* **B227** (1989) 111–117.
- [38] E.Guadagnini, M.Martellini, and M.Mintchev *Nucl. Phys.* **B330** (1990) 575–607.
- [39] P. D. Francesco, P. Mathieu, and D.Sènèchal, *Conformal field theory*. Springer-Verlag, New-York, 1997.
- [40] P. Freyd, D. Yetter, J. Hoste, W. B. R. Lickorish, K. Millett, and A. Ocneanu *Bull. Amer. Math. Soc.* **12(2)** (1985) 239–246.

- [41] J. Fröhlich and C. King *Commun. Math. Phys.* **126** (1989) 167–199.
- [42] W. Fulton, *Young Tableaux, with Applications to Representation Theory and Geometry*. Cambridge University Press, 1997.
- [43] H.Itoyama, A.Mironov, A.Morozov, and And.Morozov *Int. J. of Mod. Phys. A***27** (2012) 1250099, [arXiv:1204.4785 \[hep-th\]](#).
- [44] H.Itoyama, A.Mironov, A.Morozov, and And.Morozov *JHEP* **131:7** (2012) , [arXiv:1204.4785 \[hep-th\]](#).
- [45] H.Itoyama, A.Mironov, A.Morozov, and And.Morozov *Int. J. of Mod. Phys. A***28** (2013) 1340009, [arXiv:1209.6304 \[hep-th\]](#).
- [46] H. J. Jie Gu [arXiv:1407.5643 \[hep-th\]](#).
- [47] M. Jimbo *Commun. Math. Phys.* **102** (1986) 537–547.
- [48] J.M.F.Labastida *AIP Conf. Proc.* **484** (1-40) 1999, [arXiv:9905057 \[hep-th\]](#).
- [49] J.M.F.Labastida and E.Pèrez *J. Math. Phys.* **39** (1998) 5183–5198, [arXiv:9710176 \[hep-th\]](#).
- [50] V. F. R. Jones *Bull. Amer. Math. Soc.* **12** (1985) 103–111.
- [51] V. F. R. Jones *Bull. Am. Math. Soc.* **12:1** (1985) 103–111.
- [52] V. F. R. Jones *Ann. Math.* **126** (1989) 335–388.
- [53] L. Kauffman *Topology* **26** (1987) 395–407.
- [54] L. H. Kauffman, *The Interface of Knots and Physics*. Ams. Math. Soc., 1996.
- [55] R. K. Kaul *Commun.Math.Phys.* **162** (1994) 289–320, [arXiv:9305032 \[hep-th\]](#).
- [56] R. K. Kaul [arXiv:9804122 \[hep-th\]](#).
- [57] M. Khovanov *Duke Math. J.* **101** (2000) 359–426.
- [58] A. N. Kirillov and N. Y. Reshtikhin *Leningrad Branch of Steklov Mathematical Institute preprint* .
- [59] A. Y. Kitaev, A. Shen, and M. N. Vyalyi, *Classical and Quantum Computation*. American Mathematical Soc., 2002.
- [60] A. Klimyk and K. Schmüdgen, *Quantum Groups and Their Representations*. Springer Science & Business Media, 2012.
- [61] V. G. Knizhnik and A. B. Zamolodchikov *Nucl. Phys.* **B247** (1984) 83–103.
- [62] M. Kontsevich *Advances in Soviet Math.* **16:2** (1993) 137–150.
- [63] B.-H. Kwon [arXiv:1309.5052 \[hep-th\]](#).
- [64] L. D. Landau and L. M. Lifshitz, *Course of theoretical physics. Vol. 3*. Butterworth-Heinemann. Series: Quantum Mechanics, 1976.
- [65] L. D. Landau and L. M. Lifshitz, *Course of theoretical physics. Vol. 5*. Butterworth-Heinemann, 1987.
- [66] Q. C. Lin Chen *Pacific Journ. of Math.* **257** (2012) 267318, [arXiv:1007.1656 \[math.QA\]](#).

- [67] M.Alvarez and J.M.F.Labastida *Nucl. Phys.* **B395** (1993) 198–238, arXiv:9110069 [hep-th].
- [68] A. Mironov, A. Morozov, and A. Morozov *Mod. Phys. Lett.* **A29** (2014) 1450183, arXiv:1408.3076 [hep-th].
- [69] A. Mironov, A. Morozov, A. Morozov, P. Ramadevi, and V. K. Singh arXiv:1504.00371 [hep-th].
- [70] A. Morozov and A. Rosly (1991) .
- [71] A. Morozov and A. Smirnov *Nucl. Phys.* **B835** (2010) 284–313, arXiv:1001.2003 [hep-th].
- [72] H. R. Morton and H. J. Ryder *Geom. Topol. Monogr.* **1** (1998) 365–381, arXiv:9810197 [math].
- [73] M. Peskin and D. Schroeder, *An Introduction to Quantum Field Theory*. Addison-Wesley Publishing, 1995.
- [74] A. Polyakov, *Gauge Fields and Strings*. CRC Press, 1987.
- [75] P.Ramadevi, T.R.Govindarajan, and R.K.Kaul *Nucl.Phys* **B402** (1993) 548–566, arXiv:9212110 [hep-th].
- [76] J. H. Przytycki and P. Traczyk *Kobe J. Math.* **4** (1988) 115–139.
- [77] E. P.V. and K. V.D., *Quantum Mechanics*. Nauka (in Russian), 1974.
- [78] P. Ramadevi, T. Govindarajan, and R. Kaul *Nucl.Phys* **B422** (1994) 291–306, arXiv:9312215 [hep-th].
- [79] N. Y. Reshetikhin and V. G. Turaev *Commun. Math. Phys.* **127** (1990) 1–26.
- [80] R.K.Kaul and T.R.Govindarajan *Nucl.Phys* **B380** (1992) 293–336, arXiv:9111063 [hep-th].
- [81] V. Rubakov, *Classical Theory of Gauge Fields*. Princeton University Press, 2009.
- [82] A. Salakh, “To appear.”.
- [83] V. K. S. Satoshi Nawata, P. Ramadevi arXiv:1504.00364 [hep-th].
- [84] A. S. Schwarz in *Baku International Topological Conference Abstracts, Vol. 2*. 1987.
- [85] B. V. Shabat, *Introduction to complex analysis*. Providence, R.I., AMS, 1990.
- [86] S.Nawata, P.Ramadevi, and Zodinmawia arXiv:1302.5144 [hep-th].
- [87] S.Nawata, P.Ramadevi, and Zodinmawia arXiv:1302.5143 [hep-th].
- [88] P. V. Spencer Bloch *Journal of Number Theory* **148** (2015) 328364, arXiv:1309.5865 [hep-ph].
- [89] A. Stern *Ann. of Phys.* **323** (2008) 204–249.
- [90] V. G. Turaev *Invent. Math.* **92** (1988) 527–533.
- [91] A. G. I. V. E. Korepin, N. M. Bogoliubov, *Quantum Inverse Scattering Method and Correlation Functions*. Cambridge University Press, 1997.
- [92] V.Dolotin and A.Morozov *Nucl. Phys.* **B878** (2014) 12–81, arXiv:1308.5759 [hep-th].

- [93] M. B. Voloshin and K. Ter-Martirosyan, *The Theory of Gauge Interactions of Elementary Particles*. Energoatomizdat, Moscow (in Russian), 1984.
- [94] V. Prasolov and A. Sosinski, *Knots, links, braids, and 3-manifolds*. Amer. Math. Soc. Publ. Providence, 1996.
- [95] E. Witten *Comm. Math. Phys.* **121** (1989) 351–399.
- [96] Y. Zhang¹, Y.-W. Tan, H. L. Stormer, and P. Kim *Nature* **438** (2005) 201–204.
- [97] Zodinmawia and P. Ramadevi *Nucl. Phys.* , [arXiv:1209.1346](#) [hep-th].
- [98] Zodinmawia and P. Ramadevi *Nucl. Phys.* **870** (2013) 205–242, [arXiv:1107.3918](#) [hep-th].

A Obtaining of a non-trivial solution of classical equations for the $SU(2)$ Chern-Simons

Here we explain how explicit form (4.26) of a classical $SU(2)$ Chern-Simons field with a line-like singularity can be obtained.

The simplest non-trivial solution for the classical $SU(2)$ Chern-Simons equations can be obtained with help of the fact the three-dimensional sphere is the group variety of the $SU(2)$ group. Because the three-dimensional sphere is obtained from the three-dimensional flat space by adding the infinitely distant point, and because the $SU(2)$ group is a double covering of the rotation group, this fact can be presented visually. Namely, a point $\vec{r} = (x, y, z)$ in the flat three-dimensional space corresponds to the rotation around the unity vector $\vec{n} = \frac{\vec{r}}{r}$ on the angle $\psi = 4 \arctan \frac{r}{a}$, a being an arbitrary parameter; the pair of points $(-\vec{r}, \vec{r})$ corresponds to the same rotation, and the point $\vec{r} = (0, 0, 0)$ together with the infinitely distant point correspond to the unity transformation. In turn, a rotation around a unity vector \vec{n} on the angle ψ can be related to the $SU(2)$ matrix

$$\begin{aligned} \Omega \left(\vec{n} = \frac{\vec{r}}{r}, \psi = \arctan \frac{a}{r} \right) &= \begin{pmatrix} \cos t + in_z \sin t & (n_x + in_i) \sin t \\ (n_x - in_y) \sin t & \cos t - in_z \sin t \end{pmatrix} = \\ &= \frac{1}{r\sqrt{r^2 + a^2}} \begin{pmatrix} r^2 + ia z & a(ix + y) \\ a(ix - y) & r^2 - ia z \end{pmatrix}, \quad \vec{r} \equiv (x, y, z), \end{aligned} \quad (\text{A.1})$$

composition of two rotations corresponding then to the product of the matrices (this correspondence is known as the quaternionic representation of the rotation group), and an $SU(2)$ matrix corresponds to a rotation, since it is a generic $SU(2)$ matrix standing in (A.1).

The described one to one correspondence is even excessive for our purposes. We will use (A.1) just as an explicit example of a non-trivial, regular everywhere but the coordinate origin, distribution of the unitary matrices Ω in the three-dimensional space. The corresponding components of the Chern-Simons field are

$$\begin{aligned} A_x &= \Omega^{-1} \partial_x \Omega = \frac{a}{r^2 (r^2 + a^2)} \begin{pmatrix} -i(ay + 2xz) & i(-x^2 + y^2 + z^2) + (az - 2xy) \\ i(-x^2 + y^2 + z^2) - (az - 2xy) & i(ay + 2xz) \end{pmatrix}, \\ A_y &= \Omega^{-1} \partial_y \Omega = \frac{a}{r^2 (r^2 + a^2)} \begin{pmatrix} i(ax - 2yz) & -i(az + xy) + (x^2 - y^2 + z^2) \\ -i(az + xy) - (x^2 - y^2 + z^2) & -i(ax - 2yz) \end{pmatrix}, \\ A_z &= \Omega^{-1} \partial_z \Omega = \frac{a}{r^2 (r^2 + a^2)} \begin{pmatrix} i(x^2 + y^2 - z^2) & (ix + y)(ia - 2z) \\ (ix - y)(ia + 2z) & -i(x^2 + y^2 - z^2) \end{pmatrix} \end{aligned} \quad (\text{A.2})$$

Solution (4.26) with a line-like singularity is obtained from (A.1) as

$$\tilde{\Omega} = \Omega(x, y, z = 0) = \frac{1}{\sqrt{r^2 + a^2}} \begin{pmatrix} a & ix + y \\ ix - y & a \end{pmatrix}, \quad (\text{A.3})$$

the components of the Chern-Simons fields being obtained then as

$$\tilde{A}_x = A_x(x, y, z = 0), \quad \tilde{A}_y = A_y(x, y, z = 0), \quad \tilde{A}_z = 0. \quad (\text{A.4})$$

B On the form of the Green functions for the abelian Chern-Simons theory in Lorenz and holomorphic gauges.

Here we clarify some subtleties of deriving the explicit expressions for the Chern-Simons Green functions in the Lorenz and holomorphic gauge.

Lorenz gauge. First, we derive the expression for the Green function for the Euclidian Chern-Simons in the covariant Lorenz gauge $\partial_k A_k = 0$, which we used when discussing the QFT interpretation of the linking number in sec.4.3. First, let us notice that the Green function by definition appears in the integral form of the classical equations of motions,

$$\epsilon^{kji} \partial_j A_i(x) = 4\pi J^k(x) + \text{boundary conditions} \quad (\text{B.1})$$

\Downarrow

$$A_i(x) = \int d^3y G_{ij}(x-y) J^j(y) = \int d^3y J^j(y) G_{ji}(y-x). \quad (\text{B.2})$$

The gauge and boundary conditions hold for $A_i(x)$, if $G_{ij}(x-y)$ satisfy similar conditions, i.e., $\partial^i G_{ij}(x-y) = \partial^j G_{ij}(x-y) = 0$, and G_{ij} is regular in the whole space but the field sources and vanishes at the infinity. One can rewrite then (B.1) as $\partial_i A_j - \partial_j A_i = 4\pi \epsilon_{ijk} J^k$ and take the divergency of both parts to obtain $\partial^2 A_i = 4\pi \epsilon_{ijk} \partial^j J^k$ provided that $\partial_i A^i = 0$. The same follows from (B.2) if the Green function satisfy $\partial^2 G_{ij}(x-y) = 4\pi \epsilon_{ijk} \partial^k \delta(x-y)$ ($J^k(y)$ is unaffected by ∂^2 since $\partial \equiv \frac{d}{dx}$). The latter condition together with the gauge and boundary conditions define $G_{ij}(x-y)$ unambiguously, hence the solution

$$G_{ij}(x-y) = 4\pi \epsilon_{ijk} \partial^k \frac{1}{|\vec{x} - \vec{y}|}, \quad (\text{B.3})$$

which satisfies all those conditions, should satisfy (B.2) as well. Note that the Green function is *not* required to be a solution of the classical equation with the delta-function in the r.h.s.; definition (B.2) requires only that

$$\epsilon^{kji} \partial_j G_{il}(x-y) = 4\pi \delta_l^k \delta(x-y) + \partial^k f_l \quad (\text{B.4})$$

for a function f_l vanishing fast enough, since $\partial_k J^k = 0$ due to the classical equations of motion.

Holomorphic gauge. Now demonstrate how one can verify that each factor in the kernel of Kontsevich integral (4.59,4.60) is indeed the Green function of the classical equation of motions for Chern-Simons action in the holomorphic gauge (D.12). Namely, one may can either imply the definition

$$\partial_z f(z, \bar{z}) \equiv \lim_{|C| \rightarrow 0} \frac{1}{|C|} \oint_{z \in C} f(z, \bar{z}) dz, \quad (\text{B.5})$$

or pass to the real vector fields:

$$\begin{aligned} \partial_z u &\equiv (\partial_x + i\partial_y)(u_x - iu_y) = \mathbf{div} \vec{u} + i \mathbf{rot} \vec{u}, \\ \frac{1}{z} &= \frac{\bar{z}}{|z|^2} = \frac{x - iy}{x^2 + y^2} = \frac{\vec{r}}{r^2} \\ \Gamma_{\partial G} \frac{\vec{r}}{r^2} &= 0, \quad \Phi_{\partial G} \frac{\vec{r}}{r^2} = \delta_{0 \in G}. \end{aligned} \quad (\text{B.6})$$

C Plat representation of knot and presenting Kontsevich integral as a contraction of the “elementary contribution” operators

Here we outline the Wilson average with the knot as a contour, defined as the Gaussian average w.r.t. the Chern-Simons action in the holomorphic gauge, can be reduced to the Kontsevich integral presented as a contraction of certain elementary constituents.

Structure of the Kontsevich integral. A knot, which is by definition a curve embedded in the three-dimensional space, is cut into layers by the horizontal, i.e., normal to the selected direction (the t axes) with the planes tangent to the curve at its various critical points. Each layer contains several (even number) disconnected pieces of the original curve. The Kontsevich integral is given then by an infinite series of integrals of the increasing multiplicity. A term with a certain multiplicity is, in turn, a sum of integrals with a certain distribution of the integration variables over the layers. Finally, each summand is a product of “elementary factors” with all the variables running in the same segment for each factor.

Plat representation of knot. To match the Wilson average with the Kontsevich integral, one has to bring a knot to a special form, performing the proper continuous deformation. This form of a knot is called a *plat* representation of knot [54] and may be described as follows.

A knot is by definition a closed curve embedded into the three-dimensional space. If one selects a space direction, the contours have critical points. Select then two horizontal planes normal to the selected direction, so that no critical points are contained between the planes. If the t axis passes in the selected direction, the plains are given by the equations $t = t_0$ and $t = t_n > t_0$, and we will refer them to as the lower one and the upper one, respectively. The curve crosses the upper plane in $2m$ points, which are pairwise connected above the plane by m arcs of the contour. One should then continuously transform the curve arranging all the arcs in m mutually parallel vertical planes, all maximum points having the same height $t = t_{max}$. The arcs of the contour below the lower plane (section III in fig.16) should be arranged similarly, the height of the minimum points being $t = t_{min}$. The arcs of the contours between the selected planes have no critical points. Therefore, one can arrange vertically each one, but generally not all of them are the same time. For instance, if two arcs intertwine (section I in fig.16), at least one of them can not be everywhere vertical. Apart from that, one arc may first intertwine with an other arc and with one more arc (section II in fig.16); the first arc can not be then vertical in the intermediate region. It turns out that all “non-trivial events” are exhausted by these two cases [27]. One can complete then the procedure by selecting $n - 1$ more horizontal planes $t = t_i$ with $i = \overline{1, n - 1}$ and $t_0 \leq t_1 \leq \dots \leq t_2 \leq t_n$ such that no more than one elementary event happens between any two neighboring planes, i.e. all but no more than three arcs are vertical in each layer $t_i \leq t \leq t_{i+1}$, $i = \overline{1, n}$.

Elementary segments of the integration contour and elementary constituent of the integral. After the knot is brought to a plat representation, it is split into a collection of subsequent segments,

$$\gamma = \bigcup_{i=1}^m \bar{\gamma}_{2i-1} \gamma_{2i-1} \bar{\gamma}_{2i} \gamma_{2i}, \quad (\text{C.1})$$

where γ_{2i-1} and γ_{2i} for $i = \overline{1, m}$ are, respectively, ascending and descending arcs with $t_1 \leq t \leq t_2$, while $\bar{\gamma}_{2i-1}$ and $\bar{\gamma}_{2i}$ with $i = \overline{1, m}$ are, respectively, upper and lower closing arcs with $t_n \leq t$ and $t \leq t_0$.

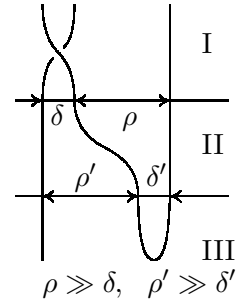


Figure 16: “Non-trivial events” in a plat representation of knot.

Composition property of the path exponential (4.35) enables to write then

$$\text{Pexp} \oint dx^\mu A_\mu = \prod_i \text{Pexp} \int_{\gamma_i} \prod_j dx^\mu A_\mu \text{Pexp} \int_{\gamma_{i,j}} dx^\mu A_\mu. \quad (\text{C.2})$$

Taking the trace and introducing the operators

$$S(\gamma_{i,j}) = \bigoplus_{i=1}^k \text{Pexp} \int_{\gamma_{i,j}} dx^\mu A_\mu, \\ Q(\bar{\gamma}_1, \bar{\gamma}_3, \dots) = \bigoplus_{i=0}^m \text{Pexp} \int_{\bar{\gamma}_{2i+1}} dx^\mu A_\mu, \quad \tilde{Q}(\bar{\gamma}_2, \bar{\gamma}_4, \dots) = \bigoplus_{i=0}^m \text{Pexp} \int_{\bar{\gamma}_{2i}} dx^\mu A_\mu, \quad (\text{C.3})$$

one can identically rewrite the same decomposition as

$$\text{Tr Pexp} \oint dx^\mu A_\mu = Q^{k_1^0 \dots k_{2m}^0}(\bar{\gamma}_1, \bar{\gamma}_3, \dots) \tilde{Q}_{k_1^{n+1} \dots k_{2m}^{n+1}}(\bar{\gamma}_2, \bar{\gamma}_4, \dots) \prod_j S_{k_1^{j+1} \dots k_{2m}^{j+1}}^j(\gamma_{i,j}) \quad (\text{C.4})$$

Due to the presence of the delta-function $\delta(t - t')$ in the Green function, the pairing, and hence all Gaussian correlators vanish for the fields taken at the points lying in different layers, so that coordinates of the points satisfy $t < t_i < t'$ at least for one i . Therefore, properties (4.49) hold for the selected splitting of the contour, and decomposition (4.49) still takes place after taking the average. One writes,

$$\langle \text{Tr Pexp} \oint dx^\mu A_\mu \rangle = \quad (\text{C.5})$$

$$= \text{Tr} \left\{ \left\langle Q^{k_1^0 \dots k_{2m}^0}(\bar{\gamma}_1, \bar{\gamma}_3, \dots) \right\rangle \left\langle \tilde{Q}_{k_1^{n+1} \dots k_{2m}^{n+1}}(\bar{\gamma}_2, \bar{\gamma}_4, \dots) \right\rangle \prod_j \left\langle S_{k_1^{j+1} \dots k_{2m}^{j+1}}^j(\gamma_{i,j}) \right\rangle \right\}, \quad (\text{C.6})$$

Further observation concerns the arcs placed in the same layer. First, the Green function being the decreasing function of the distance between arcs, and the value of the integral being independent of the arcs positions in the space, a contribution that contains the pairing of fields from the points in different arcs from the same layer must vanish if the arcs can be separated in the layer, i.e., if they do not intertwine neither in this layer nor in the two neighboring ones. In this case,

$$\langle S(\gamma_1, \gamma_2) \rangle \equiv \left\langle \text{Pexp} \int_{\gamma_1} dx^\mu A_\mu \otimes \text{Pexp} \int_{\gamma_2} dx^\mu A_\mu \right\rangle = \left\langle \text{Pexp} \int_{\gamma_1} dx^\mu A_\mu \right\rangle \otimes \left\langle \text{Pexp} \int_{\gamma_2} dx^\mu A_\mu \right\rangle \equiv (\text{C.7}) \\ \equiv \langle S(\gamma_1) \rangle \otimes \langle S(\gamma_2) \rangle, \text{ if } \gamma_1 \text{ is separated from } \gamma_2.$$

D Examples of calculating the elementary non-trivial contributions to the Kontsevich integral

In the above section, we sketched the prove of the Kontsevich integral taking form of the tensor contraction of the operators associated with the specially selected parts of the integration contour (which is the knot). To complete our discussion on properties of the Kontsevich integral, we enumerate the distinct elementary operators, discussing their properties and calculating explicitly the lowest order contributions to each one.

Trivial contributions Due to the form of the Green function, all integrals over the vertical arcs vanish. Integrals over the closing arcs (section III in fig.16) vanish as well, since the points of any two arcs can be pairwise matched by the horizontal segments. Hence, the corresponding elementary operators contain only the zero-order term of the perturbative series, being equal

$$S_{\gamma_1, \dots, \gamma_l} = \underbrace{\mathbb{1} \otimes \dots \otimes \mathbb{1}}_{l \text{ factors}}, \quad \text{if } \dot{z}(t) = 0 \text{ for } (t, z, \bar{z}) \in \gamma_k \text{ with } k = \overline{1, l}, \quad (\text{D.1})$$

and

$$Q = \tilde{Q} = \underbrace{\mathbf{1} \otimes \dots \otimes \mathbf{1}}_{m \text{ factors}}, \quad (\text{D.2})$$

respectively.

Crossing point contributions First of the two non-trivial operators corresponds to an intertwining of two arcs, which contains a crossing point when projected on a plane (section I in fig.16). This operator can be evaluated explicitly and takes a rather simple form,

$$R \equiv \left\langle \text{Pexp} \int_{\gamma} dx^{\mu} A_{\mu}(x) \otimes \text{Pexp} \int_{\gamma'} dx'^{\nu} A_{\nu}(x') \right\rangle = q^{T_a \otimes T_a} \quad (\text{D.3})$$

The last term of the equality contains a somewhat symbolic notation for the result, and the exact sense of which is clarified below.

We recall that modulo discussion in sec.4.5, only pairings of the fields at the points from different arcs should be left in the Wick theorem, for instance, up to the fourth order one writes,

$$\begin{aligned} & \left\langle \left(\mathbf{1} + \int_{\gamma} dx^{\mu} A^{\mu}(x) + \int_{\gamma} dx^{\mu} \int_0^x dy^{\nu} A_{\mu}(x) A_{\nu}(y) + \dots \right) \otimes \left(\mathbf{1} + \int_{\gamma'} dx'^{\mu} A_{\mu}(x') + \int_{\gamma'} dx'^{\mu} \int_0^{x'} dy'^{\nu} A_{\mu}(x') A_{\nu}(y') + \dots \right) \right\rangle \\ & = \mathbf{1} \otimes \mathbf{1} + \\ & + \int_{\gamma} dx'^{\mu} \int_{\gamma'} dx^{\mu} \langle A_{\mu}^a(x) A_{\nu}^b(x') \rangle T^a \otimes T^a + \int_{\gamma} dx^{\mu} \int_0^x dy^{\nu} \int_{\gamma'} dx'^{\mu} \int_0^{x'} dy'^{\nu} \left\langle A_{\mu}^a(x) A_{\rho}^c(x') \right\rangle \left\langle A_{\nu}^b(y) A_{\sigma}^d(y') \right\rangle + \\ & + \left\langle A_{\nu}^b(y) A_{\rho}^c(x') \right\rangle \left\langle A_{\mu}^a(x) A_{\sigma}^d(y') \right\rangle \left\langle A_{\mu}^a(x) A_{\sigma}^d(y') \right\rangle T^a T^b \otimes T^c T^d + \dots \end{aligned} \quad (\text{D.4})$$

Now, it is important that the Green function decomposes into the product of the group factor and coordinate dependent scalar factor,

$$\langle A_{\mu}^a(x) A_{\rho}^c(x') \rangle = t^{ac} g_{\mu\rho}(x - x'), \quad (\text{D.5})$$

in particular, $\frac{A_{\mu}^1(x) A_{\rho}^2(x')}{A_{\mu}^2(x) A_{\rho}^3(x')} = \text{const}$ and $\frac{A_{\mu}^1(x) A_{\rho}^2(x')}{A_{\nu}^1(y) A_{\rho}^2(y')} = \frac{A_{\mu}^2(x) A_{\rho}^3(x')}{A_{\nu}^2(y) A_{\rho}^3(y')}$. As a result, all terms with the same distribution of the Green function arguments over the contour arcs have assemble into the sum over various parings of the group generators multiplied on the common coordinate dependent factor, e.g., the second order term takes form

$$, \quad (\text{D.6})$$

while the forth order term becomes

$$\int_{\gamma} dx^{\mu} \int_0^x dy^{\nu} \int_{\gamma'} dx'^{\mu} \int_0^{x'} dy'^{\nu} g_{\mu\rho}(x - x') g_{\nu\sigma}(y - y') \left\{ \tau^{ac} \tau^{bd} + \tau^{ad} \tau^{bc} \right\} T^a T^b \otimes T^c T^d, \quad (\text{D.7})$$

where four out of six possible parings remained, after the self-interaction contributions were excluded. Generally, one can demonstrate that the group factor in a k order term has the form

$$R^{(k)} = \sum_{\sigma \in \text{perm}(k)} T_{a_1 \dots a_k} \otimes T_{\sigma(a_1 \dots a_k)}, \quad (\text{D.8})$$

where the sum is over all permutation of k elements. Moreover, the scalar coefficients, which arise as the integrals of the coordinate dependent factors, turn out to be proportional to the subsequent powers of the same quantity for the subsequent terms of the expansion. Finally, each term enters the

sum with a numeric factor of $\frac{1}{k!}$. These three observations are concentrated in the notation for the crossing operator used in (D.3).

Let us now take the integrals of the coordinate dependent factors explicitly. We use not plain and prime variables for one and the arcs,

$$\gamma : x = x(t) \equiv (t, z(t), \bar{z}(t)), \quad \gamma' : x' = x'(t)(t, z'(t), \bar{z}'(t)), \quad (\text{D.9})$$

and we recall that the coordinate factor in the Green function is equal to $g_{0z}(x(t) - x'(t')) = \frac{\delta(t-t')}{z(t)-z'(t)}$. The fourth order coordinate factor is then

$$\begin{aligned} & \int_0^1 dt \int_0^t ds \int_0^1 dt' \int_0^t ds' \dot{x}^\mu(t) \dot{x}'^\rho(t') g_{\mu\rho}(x(t) - x'(t')) \dot{y}^\nu(s) y'^\sigma(s') g_{\nu\sigma}(y(s) - y'(s')) = \\ & = \int_0^1 dt \int_0^t ds h_{\mu\rho} \dot{x}^\mu(t) \dot{x}'^\rho(t) f(x(t) - x'(t)) h_{\nu\sigma} \dot{y}^\nu(s) y'^\sigma(s) f(y(s) - y'(s)) = \\ & \int_0^1 dt \int_0^t ds \frac{(\dot{z}(t) - \dot{z}'(t))(\dot{z}(s) - \dot{z}'(s))}{(z(t) - z'(t))(z(s) - z'(s))} = \frac{1}{2} \log^2 \frac{z(0) - z'(0)}{z(1) - z'(1)}, \end{aligned} \quad (\text{D.10})$$

where log stands for the multi-valued function $\log \vartheta(t) \equiv \int_0^1 dt \frac{\dot{\vartheta}(t)}{\vartheta(t)}$. Higher order factors are evaluated similarly,

$$\begin{aligned} & \int_\gamma dx_1^{\mu_1} \int_0^{x_1} dx_2^{\mu_2} \dots \int_0^{x_{k-1}} dx_k^{\mu_k} \int_{\gamma'} dx_1^{\nu_1} \int_0^{x_1'} dx_2^{\nu_2} \dots \int_0^{x_{k-1}'} dx_k^{\nu_k} g_{\mu_1\nu_{m_1}}(x_1 - x_1') g_{\mu_2\nu_{m_2}}(x_2 - x_2') \dots g_{\mu_k\nu_{m_k}}(x_k - x_k') \\ & = \int_0^1 dt_1 \int_0^{t_1} dt_2 \dots \int_0^{t_{k-1}} dt_k \frac{(\dot{z}(t_1) - \dot{z}'(t_1))(\dot{z}(t_2) - \dot{z}'(t_2)) \dots (\dot{z}(t_k) - \dot{z}'(t_k))}{(z(t_1) - z'(t_1))(z(t_2) - z'(t_2)) \dots (z(t_k) - z'(t_k))} = \frac{1}{k!} \log^k \frac{z(0) - z'(0)}{z(1) - z'(1)}. \end{aligned}$$

Finally, the answer is

$$R = e^{\hbar T_a \otimes T^a} \equiv \mathbb{1} + \sum_{k=1}^{\infty} \frac{\hbar^k}{k!} \sum_{\sigma \in \text{perm}_k} T_{a_1 \dots a_k} \otimes T_{\sigma(a_1 \dots a_k)}. \quad (\text{D.11})$$

Associators The second non-trivial elementary contribution operator is known under the name of *Drinfeld associator*. It involves already three arcs placed as in sec.II in fig.16,

$$\Phi \equiv \left\langle \text{Pexp} \int_\gamma dx^\mu A_\mu(x) \otimes \text{Pexp} \int_{\gamma'} dx'^\nu A_\nu(x') \otimes \text{Pexp} \int_{\gamma''} dx''^\rho A_\rho(x'') \right\rangle, \quad (\text{D.12})$$

and it has a much more involved structure than the crossing point operator. To demonstrate the difference between the two operators, we calculate one of the fourth order contributions to the Drinfeld associator explicitly.

Namely, we consider the contribution arising from the pairing

$$\int_\gamma dx^\mu \int_0^x dy^\nu \int_{\gamma'} dx'^\mu \int_{\gamma''} dy'^\nu \left\langle A_\mu^a(x) A_\rho^c(x') \right\rangle \left\langle A_\nu^b(y) A_\sigma^d(y') \right\rangle T^a \otimes T^b T^c \otimes T^d, \quad (\text{D.13})$$

which, in turn, arises from the term

$$\left(\int_\gamma dx^\mu A_\mu(x) \right) \otimes \left(\int_{\gamma'} dx'^\nu \int_0^{x'} dy'^\rho A_\nu(x') A_\rho(y') \right) \otimes \left(\int_{\gamma''} dx''^\sigma A_\sigma(y) \right) \quad (\text{D.14})$$

in the expansion of (D.12). Selecting the variables on the connection components as

$$\gamma : x = x(t) = (t, z(t), \bar{z}(t)), \quad \gamma' : x = x(t) = (t, z'(t), \bar{z}'(t)), \quad \gamma'' : x = x(t) = (t, z''(t), \bar{z}''(t)), \quad (\text{D.15})$$

we obtain that the integral of the coordinate dependent factor of the considered contribution takes the explicit form

$$\int_0^1 \int_0^t ds dt \frac{(\dot{z}(t) - \dot{z}'(t))(\dot{z}'(s) - \dot{z}''(s))}{(z(t) - z'(t))(z'(s) - z''(s))}. \quad (\text{D.16})$$

Taking into account that the first and the last arcs being vertical and supposing that

$$z''(t) = 1 + z(t), \quad (\text{D.17})$$

one can present the result in the form

$$\begin{aligned} \int_0^1 \int_0^t ds dt \frac{(\dot{z}(t) - \dot{z}'(t))(\dot{z}(s) - \dot{z}'(s))}{(z(t) - z'(t))(1 + z(s) - z'(s))} &= \int_0^1 dt \frac{\dot{z}(t) - \dot{z}'(t)}{z(t) - z'(t)} \log \frac{1 + z(t) - z'(t)}{1 + z(0) - z'(0)} = \\ &= \text{Li}_2(z'(0) - z(0)) - \text{Li}_2(z'(1) - z(1)) - \log(1 + z(0) - z'(0)) \log \frac{z(1) - z'(1)}{z(0) - z'(0)}, \end{aligned} \quad (\text{D.18})$$

where the dilogarithm function is by definition

$$\text{Li}_2(x) \equiv - \int_0^x \frac{dy}{y} \log(1 - y) = \int_0^x \sum_{k=0}^{\infty} \frac{y^{k-1}}{k} = \sum_{k=0}^{\infty} \frac{y^k}{k^2} \quad (\text{D.19})$$

One usually suppose that the second contour is infinitely close to the first one on the upper boundary of the selected area, becoming infinitely close the third one on the lower boundary. Expression (D.18) then notably simplifies,

$$\boxed{z'(0) \rightarrow z(0), \quad z'(1) \rightarrow z''(1), \quad \Rightarrow \quad \text{the answer} \rightarrow \zeta(2) = \frac{\pi^2}{6}}, \quad (\text{D.20})$$

where we used that $\text{Li}_2(0) = 0$, $\text{Li}_2(1) = \zeta(2)$, and the Riemann zeta-function is defined as the series $\zeta(m) \equiv \sum_{k=0}^{\infty} \frac{1}{k^m}$ and can be evaluated explicitly with help of the expansion by definition

$$\frac{\sin(\pi x)}{\pi x} = \prod_{n=1}^{\infty} \left(1 - \frac{x^2}{n^2}\right) = 1 - \zeta(2)x^2 + \dots \quad (\text{D.21})$$

A remarkable property of the Drinfeld associator is that it can be obtained from a solution of the Knizhnik-Zamolodchikov equation for the WZW conformal blocks [61]. This property gives a link between the Kontsevich integral, with is associated with perturbative expansion for the Chern-Simons Wilson average, and the axiomatic definition of the exact Wilson average, which we briefly outlined in sec.4.1.